Eddy currents in aluminum framed ships: a development and application of model techniques for the determination of magnetic effects of eddy currents in AMc 143 and class minesweepers moving in the earth's magnetic field

Kusters, N. L.; Epp, E. R.; Morris, R. M.; Rackow, A. D.

Report (National Research Council Canada. Radio and Electrical Engineering Division : ERA); no. ERA-228, 1953-06

ERA-228

SECRET

NATIONAL RESEARCH COUNCIL OF CANADA

RADIO AND ELECTRICAL ENGINEERING DIVISION

EDDY CURRENTS IN ALUMINUM FRAMED SHIPS

A DEVELOPMENT AND APPLICATION OF MODEL TECHNIQUES FOR THE DETERMINATION OF MAGNETIC EFFECTS OF EDDY CURRENTS IN AMc 143 AND CLASS MINESWEEPERS MOVING IN THE EARTH'S MAGNETIC FIELD.

N. L. KUSTERS R. M. MORRIS A. D. RACKOW E. R. EPP

OTTAWA

JUNE 1953

ABSTRACT

An experimental investigation of the magnetic field produced by eddy currents created in the aluminum structure of the AMc. 143 and class minesweeper when rolling in the earth's magnetic field has been carried out. Model techniques have been developed for this purpose. A reduced scale model of the minesweeper was rotated at a constant angular velocity in the earth's magnetic field and the induced eddy current field distribution was extensively explored by means of a flux-gate magnetometer. The angular velocity of rotation was made to correspond to the peak angular velocity attained by the full-scale ship during a sinusoidal rolling motion. The results obtained have been compared with full-scale trial measurements. There is reasonable agreement between the results of model and full-scale tests.

A theoretical investigation of the external eddy current field produced by an infinitely long rolling cylinder is presented. It is shown, that in the midship region, the ship may be represented by an equivalent cylinder. The cylinder analogy is used also in explaining other features of the experimental results.

An estimate is made of the eddy current field due to pitching of the class AMc. 143 ship.

CONTENTS

TEXT

TABLE OF SYMBOLS

Symbol	Description
$\vec{H}_i$	Vector eddy-current field at (r,θ) (oersteds)
r	Magnitude of radius vector $\vec{r}$ (cm)
θ	Angle (degrees) measured in the direction of rotation from the direction of uniform exciting field H_e to the radius vector $\vec{r}$
$\vec{\mu}_r$	Unit vector in the radial direction
$\vec{\mu}_\theta$	Unit vector in the tangential direction
H_e	Intensity of uniform exciting field (oersteds)
b	Cylinder radius (cm)
a	Cylinder wall thickness (cm)
ρ	Resistivity of cylinder material (ohm-cm)
ω	Angular velocity of rotation (rad/sec)
ϕ	Angle between direction of uniform exciting field H_e and the axis of maximum current in the cylinder wall (rad)
H_v	Vertical component of exciting field or Component of earth's field vertical to ship's deck
H_h	Horizontal component of exciting field or Component of earth's field athwartship.
h_1	Horizontal component of eddy-current field induced by H_v
h_2	Horizontal component of eddy-current field induced by H_h
v_1	Vertical component of eddy-current field induced by H_h

TABLE OF SYMBOLS

Symbol	Description
v_2	Vertical component of eddy-current field induced by H_v
$H_{p\ max}$	Maximum value of radial component of induced magnetic field at cylinder wall (oersteds)
*H_s, H_m	Eddy current field of ship and model at corresponding points (oersteds)
dl	Element of length (cm)
k	Linear scale factor of model
γ	Angle between element of conductor length and a radius vector r
I_s, I_m	Currents in corresponding ship and model members (amperes)
E_s, E_m	Voltages induced in corresponding ship and model members (volts)
R_s, R_m	Resistances of corresponding ship and model members (ohms)
B_s, B_m	Uniform exciting field flux density (gauss)
v_s, v_m	Effective linear velocity (cm/sec) of conductor across field B_s, B_m
ω_s, ω_m	Maximum angular velocity (rad/sec)
b_s, b_m	Radius of rotation (cm)
ρ_s, ρ_m	Resistivity of conductor material (ohm-cm)
A_s, A_m	Cross sectional area of conductors (cm^2)
t	Time
τ	Time constant
α, p	Roll and pitch angles at time t

*Note: The subscripts "s" and "m" refer to ship and model, respectively.

TABLE OF SYMBOLS

Symbol	Description
a_o, p_o	Maximum angle of roll or pitch.
T_a, T_p	Period of roll or pitch (seconds)
σ_s, σ_m	Conductivity of conductor material mhos/cm
ω_r, ω_p	Maximum angular velocity in roll or pitch
H	Horizontal component of earth's total field.
Z	Vertical component of earth's total field.
Φ	Magnetic heading of ship measured east from north.
v	Total vertical component of eddy-current field.
h	Total horizontal component of eddy-current field transverse to the ship's axis.
ℓ	Longitudinal component of eddy-current field normal to the plane containing "h" and "v".

EDDY CURRENTS IN ALUMINUM FRAMED SHIPS

I - INTRODUCTION

A. OBJECT OF THE WORK

The AMc. 143 and class minesweeper has a wooden hull reinforced by an internal framework of fabricated aluminum. This framework forms a three dimensional network of electrical conductors of high conductivity. When it oscillates—owing to rolling and pitching of the ship—in the earth's magnetic field, eddy currents are generated in the conducting circuits. Such currents create an associated oscillating magnetic field in the vicinity of the ship, which could possibly actuate a magnetic mine. The object of the work reported here is to determine the magnitude and distribution of the magnetic field caused by eddy currents in an AMc. 143 and class ship.

B. BACKGROUND

Two methods of construction of minesweepers have been proposed where aluminum is used as a substitute for wood or ferromagnetic material. The first proposed method would employ an internal aluminum framework reinforcing an aluminum shell which forms the hull. To our knowledge no ships have been constructed by this method. The second method employs an internal aluminum framework reinforcing a wooden shell which forms the hull. This second method of construction is used in the AMc. 143 and class ships. Two types of these are built, one type having aluminum decks and the other having wooden decks.

The eddy-current magnetic field created by the all-aluminum hull has been estimated at N.R.C.[1]* by computing the eddy-current field of a rotating cylinder equivalent in dimensions to an AMc. 143 and class ship. This calculation shows that the all-aluminum hull could create magnetic disturbances, when the ship rolls or pitches, which are large compared with the known sensitivities of magnetic mines. The cylinder calculation was later checked by experiments [2] on a scale-model cylinder after the necessary similitude relationships and experimental techniques had been developed.

The eddy-current field of aluminum-framed, wooden-hull ships has already been investigated to a limited extent. The field at a few points under a full-scale ship of the type having aluminum decks

* Superscripts refer to numbered items in the Bibliography

has been measured by NRC [3] . The field due to a type similar to that having wooden decks has been calculated by the British Admiralty Research Laboratory [4] at four depths amidships under the keel.

C. OUTLINE OF PROCEDURE

The methods of investigation already used [3,4] on aluminum-framed wooden-hull ships are unsuitable when detailed information about the field distribution in the space surrounding the ship is required. To obtain such information, a scale model has been constructed and field measurements have been made in its vicinity.

The theory of scaling of this model was developed from the theory of the rotating cylinder which has been reported previously [1,2] and from similitude relationships between an element of conductor on the ship and the equivalent element on a model. The cylinder theory has been introduced, not only to assist in determining model scaling, but also to indicate the general form of the eddy-current field of a ship and to demonstrate the manner in which the inductance of the ship framework members influences the field form.

The scaling relations developed by the methods indicated above show that the angular velocity of the model must increase as the size of the model decreases. For a model of convenient size the required angular velocity becomes so large that it cannot be produced easily by an oscillation which simulates that of the ship. It has been necessary, therefore, to rotate the model continuously in order to produce the required angular velocity. It is not possible, using this technique, to simulate the field effects of eddy currents in an oscillating ship exactly, but the field effects may be obtained, to an approximation which is discussed later, when the continuous rotational velocity of the model is scaled to the maximum angular velocity occurring during a sinusoidal oscillation of the ship.

A model, designed according to the proper scaling factors, was constructed in three stages, where each stage represented a possible ship structure as follows:-

Stage 1 - The model of a framework, considered by the RCN to be the minimum useful framework for this type of construction, was fabricated.

Stage 2 - Members representing decks were added to the Stage 1 structure.

Stage 3 - Additional members were added to the Stage 2 structure to complete the full representation, except for superstructure, of the framework of an AMc.143 and class ship with aluminum decks.

At each stage of construction the eddy-current field produced when the model rotated in a known exciting field was measured.

D. EXTERNAL FIELD OF AN INFINITELY-LONG HOLLOW ROTATING CYLINDER

The rotating cylinder theory indicates to an approximation the form of the eddy-current field produced by an oscillating ship. The analysis of the infinite rotating cylinder has already been carried out,[1,2] but the results of previous work will be re-stated here, and put into a form which will permit easy comparison with the test results obtained from the ship model.

It is shown in Report ERA-211[2] that the induced field $\vec{H}_i$ at any point (r,θ) external to an infinitely-long hollow cylinder rotating in a uniform field, is given by the following equation:-

$$\vec{H}_i = \frac{H_e C_2}{\sqrt{1 + C_2^2}} \left[\vec{\mu}_r \frac{b^2}{r^2} \sin(\theta - \phi) - \vec{\mu}_\theta \frac{b^2}{r^2} \cos(\theta - \phi) \right] \text{ oersteds,} \quad (1)$$

where

$$C_2 = \frac{0.2\pi ab\omega}{10^8 \rho} \quad \text{and} \quad \phi = \tan^{-1} C_2 ,$$

r = magnitude of radius vector $\vec{r}$ (cm),
θ = angle (degrees) measured in the direction of rotation from the direction of uniform exciting field H_e,
$\vec{\mu}_r$ = unit vector in the positive radial direction,
$\vec{\mu}_\theta$ = unit vector in the positive tangential direction,
H_e = Intensity of uniform exciting field (oersteds),
b = cylinder radius (cm),
a = cylinder wall thickness (cm),
ρ = resistivity of cylinder material (ohm-cm),
ω = angular velocity of rotation (rad/sec),
ϕ = angle between the direction of uniform exciting flux H_e and the axis of maximum current in the cylinder wall (rad).

As demonstrated in Appendix I, the equation of the flux lines created by the rotating cylinder is given by:

$$r = nb \cos(\theta - \phi), \quad \text{where } n > 1. \quad (2)$$

The plot of Equation (2) is a family of circles passing through a common point at the center of the cylinder, and having their centers on a line making an angle ϕ with the direction of the exciting field. A plot of these flux lines is given in Fig. 1.

Since measurements of the fields due to ships are usually made in a rectangular co-ordinate system it is useful to convert the field expressed by Equation (1) into its horizontal and vertical components. As shown in Appendix 2, with the sign convention given there, these components at any point on a horizontal line transverse to the axis of the cylinder and at a depth nb below the center of the cylinder rotating in the clockwise direction are:-

$$h_1 = -KH_v \cos^2\theta \cos(2\theta - \phi) \quad (3)$$

$$v_2 = KH_v \cos^2\theta \sin(2\theta - \phi) \quad (4)$$

$$v_1 = -KH_h \cos^2\theta \cos(2\theta - \phi) \quad (5)$$

$$h_2 = -KH_h \cos^2\theta \sin(2\theta - \phi) \quad (6)$$

where $K = \frac{1}{n^2} \frac{C_2}{\sqrt{1 + C_2^2}}$, and $n > 1$.

H_v and H_h are the vertical and horizontal exciting fields shown in Figs. 2 and 3,

h_1 and v_2 are horizontal and vertical eddy-current field components induced by H_v,

v_1 and h_2 are vertical and horizontal eddy-current field components induced by H_h.

In Fig. 2, the components h_1 and v_2 are plotted as percentages of the maximum value of h_1. In Fig. 3, the components v_1 and h_2 are plotted as percentages of the maximum value of v_1. The cases for both directions of rotation are shown, with an assumed value for ϕ of 10°. The zeros, principal maxima and minima of the functions $\cos^2\theta \cos(2\theta - \phi)$ and $\cos^2\theta \sin(2\theta - \phi)$, are determined in Appendix II and are summarized in the following table:-

TABLE I

Function	Angles at which Zeros occur	Angles at which Maxima and Minima occur
$\cos^2\theta \cos(2\theta - \phi)$	$\theta = \frac{\phi}{2} \pm 45°$	$\theta = \frac{\phi}{3}$, $\theta = \frac{\phi}{3} \pm 60°$
$\cos^2\theta \sin(2\theta - \phi)$	$\theta = \frac{\phi}{2}$	$\theta = \frac{\phi}{3} \pm 30°$

If, from a given cylinder of known dimensions and angular velocity, a set of curves such as those of Figs. 2 and 3 are obtained experimentally, it is possible to determine the angle ϕ (and the time constant of the cylinder as will be shown later) by two methods:-

1. By substituting the values of the zeros, maxima and minima of the curves and solving the above values of the equations for the angle ϕ

2. By substituting $\theta = 0$ into Equations (3) and (4), or (5) and (6) above.

Then:

$$\left|\frac{v_2}{h_1}\right| = \tan \phi \text{ , and } \phi = \tan^{-1} \left|\frac{v_2}{h_1}\right| \qquad (7)$$

$$\left|\frac{h_2}{v_1}\right| = \tan \phi \text{ , and } \phi = \tan^{-1} \left|\frac{h_2}{v_1}\right| \qquad (8)$$

The angle ϕ is thus obtainable from the ratio of the intercepts of the curves with the vertical line through the center of the cylinder.

II - MODEL SCALING TECHNIQUES

A. STATEMENT OF THE PROBLEM

The problem of model scaling is to determine the proper scale factors of a model which, when made to oscillate in a similar manner to that in which the ship oscillates, will produce, in a known exciting field, a measurable eddy-current field whose magnitude and phase are related in a known manner to the eddy-current field of the ship. During a sinusoidal oscillation, the angular velocity of a ship varies in a sinusoidal manner between zero and a maximum value. Because of this angular velocity variation and the inductance of the ship's framework, currents in the framework will vary with time in a complicated manner. For this reason it would be necessary, in a true model system, to oscillate the model in order to obtain a true representation of the field of the ship. However, it has been found impractical to attempt to obtain the necessary angular velocities by oscillation, so a method involving continuous rotation of a model has been developed. An estimate of the approximation so introduced will be dealt with in Section E(b). To this approximation it is possible to reproduce the eddy-current field of an oscillating ship by that of a model rotating at a constant angular velocity scaled to the peak angular velocity of the ship oscillation.

B. SCALING OF AN INFINITELY LONG HOLLOW ROTATING CYLINDER

The theory of scaling of the rotating model is based in part upon a modification of the analyses presented in Reports ERA-195[1] and ERA-211[2]. In these reports, the eddy-current field produced by a hollow cylinder of infinite length rotating about its central longitudinal axis was derived. It was demonstrated that the magnitude and direction of this field was influenced by an effect termed "feedback". This "feedback" effect is the effect of the inductance of the cylinder. The analysis presented in Report ERA-195 applies exactly to a cylinder rotating continuously at constant angular velocity, but does not apply exactly to a cylinder oscillating in a sinusoidal manner.

With the modification that the analysis applies to a rotating rather than to an oscillating cylinder, Report ERA-195 shows the following:

a) The uniform exciting field can be considered as a radial field sinusoidally distributed around the circumfrence of the cylinder. The maximum of this radial field is equal to and acts in the direction of the uniform field.

b) The radial component of the eddy-current field is also sinusoidally distributed around the circumference of the cylinder. Its maximum, H_{pmax}, and the direction $(90° + \phi)$ in which it acts relative to the constant exciting field may be determined by rearrangement of the formulae of Report ERA-195 into the following forms:-

$$H_{pmax} = \frac{\left(\frac{0.2\pi ab}{10^8 \rho}\right)\omega}{\sqrt{1 + \left[\left(\frac{0.2\pi ab}{10^8 \rho}\right)\omega\right]^2}} H_e \,. \qquad (9)$$

This maximum is displaced by an angle of (90° + ϕ) in the direction of rotation with respect to H_e.

The various symbols are defined as follows:

$$\phi = \tan^{-1}\left(\frac{0.2\pi ab}{10^8\rho}\right) \cdot \omega \qquad (10)$$

H_{pmax} = Maximum value (oersteds) of radial component of eddy-current magnetic field at the cylinder wall

H_e = Intensity of uniform exciting field (oersteds)

ϕ = Angle between direction of uniform exciting flux H_e and the axis of maximum current in the cylinder wall

a = Cylinder wall thickness (cm.)

b = Cylinder radius (cm.)

ω = Angular velocity of rotation (rad/sec.)

ρ = Resistivity of cylinder material (ohm-cm.)

c) In the case of a hollow cylinder rotating at a constant angular velocity ω the vectors representing H_{pmax} and H_e are fixed in space and the angle between them is (90° + ϕ).

d) As shown in Section 8 of Report ERA-195[1], the relationship between induced field and exciting field may be represented in terms of feedback theory. This representation provides a useful means for determining the requirements for model scaling. Using this approach, Equations (9) and (10) above may be expressed in terms of a standard type of transfer function[6] in the form of the following single equation which shows both magnitude and phase relationships:-

$$\frac{H_{pmax}}{H_e} = \frac{j\omega\tau}{1 + j\omega\tau} \qquad (11)$$

where τ and ω are defined as follows:

τ is the time constant of the system, and is given by

$$\tau = \frac{0.2\pi ab}{10^8\rho} \qquad (12)$$

ω is the angular velocity of rotation.

The plot of Equation (11) on a log magnitude and angle graph is given in Fig. 4.

From the above analysis, and from an inspection of Fig. 4, the following requirement for correct scaling of a model rotating cylinder may be derived:-

Provided the same exciting field is used for both model and cylinder, the product "$\omega\tau$" must be the same in the model as in the full-scale cylinder if the magnitude and phase relationships are to be the same in both cases. This is equivalent to the statement in Report ERA-211 that the factors $\frac{\rho}{a^2}$ must be the same for models of all scales. This requirement leads to the scaling equations:-

$$\omega_m \tau_m = \omega_s \tau_s , \tag{13}$$

$$\text{or} \quad \frac{a_m^2 b_m \omega_m}{\rho_m} = \frac{a_s^2 b_s \omega_s}{\rho_s} , \tag{14}$$

where "m" and "s" refer to the model and the full-scale cylinder, respectively.

It should be noted that when the requirement is fulfilled, the model will produce the same field in magnitude and direction, at a scale distance, as the full-scale cylinder.

C. SCALING OF THE SHIP MODEL

By the cylinder method it has been demonstrated that when the proper scaling factors are introduced, a model cylinder should produce the same field in magnitude and direction at a scale distance as does the full-scale cylinder. The proper scaling factors are determined by use of Equation (14). That a similar scaling requirement to Equation (14) exists for the model of a framed ship will now be shown:-

Suppose that H_s is the field produced by eddy currents in the ship at a given external point and that H_m is the field produced by eddy currents in the model at a corresponding point in the model system. The desired relationship between these two fields, as indicated by cylinder theory, is that $H_m = H_s$ for all external points.

Consider an element of circuit length in the ship dl centimeters long and an equivalent element of length in the model kdl ($k < 1$ and is the scaling factor for linear dimensions). The magnetic intensity dH_s at a point r centimeters from dl, when dl carries a current of I_s amperes, and when Υ is the angle between the current element and the vector r, is given by:-

$$dH_s = \frac{I_s \sin \Upsilon \, dl}{10r^2} \text{ oersteds.} \tag{15}$$

Similarly, the magnetic intensity dH_m at scale distance from the model is

$$dH_m = \frac{I_m \sin \Upsilon \, kdl}{10(kr)^2} \text{ oersteds,} \tag{16}$$

where I_m is the current carried by an element kdl in the model. The angle γ is the same in both systems. For the two fields to be the same, it follows from Equations (15) and (16) that:

$$I_m = kI_s \,. \tag{17}$$

Using Ohm's law this becomes

$$\frac{E_m}{R_m} = \frac{k\,E_s}{R_s} \,, \tag{18}$$

where E_s and E_m are voltages (in volts) induced in elements dl and kdl, respectively, because of their motion in the magnetic field, and R_s and R_m are resistances (in ohms) of these elements.

The voltage induced in an element dl is given by

$$E_s = 10^{-8}\, B_s dl\, \nu_s \text{ volts}, \tag{19}$$

where B_s is a uniform exciting field flux density in gauss (in air B= H), and ν_s is the component of velocity (in cm/sec) of element dl perpendicular to the direction of field B_s.

Similarly the voltage induced in an element kdl in the model system is given by

$$E_m = 10^{-8}\, B_s kdl\, \nu_m \,. \tag{19(a)}$$

If the ship-model and ship are moving in the same exciting field B about corresponding axes, then at corresponding instants in their motions it follows that

$$\frac{kdl\ \nu_s}{R_s} = \frac{kdl\ \nu_m}{R_m} \,. \tag{20}$$

But in general $\nu = \omega b$,

where ω is the angular velocity (in rad/sec) of an element about the axis of rotation and b is the radius of rotation.

$$\therefore \frac{\omega_s b_s}{R_s} = \frac{\omega_m b_m}{R_m} = \frac{k\,\omega_m b_s}{R_m} \tag{21}$$

But since, in general, the resistance is given by $R = \rho \frac{dl}{A}$,

then

$$\frac{\omega_s A_s}{\rho_s} = \frac{\omega_m A_m}{\rho_m} \quad ; \tag{22}$$

where ρ_s and ρ_m are resistivities (in ohm-cm) of the materials in ship and model frameworks respectively, and A_s and A_m are cross sections of corresponding members of ship and model.

Equation(22)gives the required relationship for model scaling. It is analogous to the scaling requirement for the cylinder, which is

$$\frac{a_m b_m \omega_m}{\rho_m} = \frac{a_s b_s \omega_s}{\rho_s} \quad . \tag{23}$$

III - DESIGN AND CONSTRUCTION OF MODEL

A. CALCULATION OF SCALING FACTORS

Although it is desirable to make a small model, for convenience in construction and handling, there are several reasons why the model must be made as large as is feasible. For instance, the scaling condition given by Equation(22)shows that the angular velocity must vary inversely as k^2 ($k < 1$ and is the scale factor of linear dimensions). Thus, because there is a limit to the amount by which the angular velocity may be increased, there is also a limit to the amount by which the model dimensions may be decreased. A second consideration exists because the detecting element of the measuring instrument must be reduced in size as "k" decreases, in order that the measurement may approximate a "point" measurement. This results in a reduction in the sensitivity of the detecting element which is inherent in this type of detection.

After a preliminary consideration of the above factors, it was decided to represent the ship (length 150 feet) by a model about 6 feet in length. The factor k was therefore set at:-

$$k = \frac{1}{24} . \qquad (24)$$

If a true scale model (aluminum frame with $k = 1/24$) were constructed, the scaling equation (#22) re-arranged in the following form

$$\frac{\omega_m}{\omega_s} = \frac{A_s}{A_m}\frac{\rho_m}{\rho_s} \qquad (25)$$

shows that

$$\frac{\omega_m}{\omega_s} = \frac{A_s}{A_m} = \frac{1}{k^2} = 576. \qquad (26)$$

The estimated maximum angular velocity of the ship occurs during a ± 30-degree 8-second roll. Considering this roll as a simple harmonic motion governed by the equation, $\alpha = \alpha_o \sin \frac{2\pi t}{T_\alpha}$ the maximum angular velocity is:

$$\omega_s = \left(\frac{d\alpha}{dt}\right)_{max} = \alpha_o \frac{2\pi}{T\alpha} = \frac{2\pi 30}{8} = 23.6 \text{ deg/sec}, \qquad (27)$$

where α = roll angle at time "t", α_o = maximum roll angle, T_α is period of roll.

$$\omega_m = 23.6 \times 576 = 13{,}600 \text{ deg/sec, or about 2300 r p m} \qquad (28)$$

Thus for a model of true geometric similarity, a prohibitively high angular velocity would be required. It is necessary to distort some of

the scaling factors to reduce the angular velocity requirement. This has been done in two ways:-

1. The cross sections of the conducting model framework members were reproduced to a scale of 1/12 x 1/12 ($4k^2$) and applied to the wooden hull which is made to a scale of 1/24.

$$\therefore \frac{A_s}{A_m} = 144 \qquad (29)$$

2. The model framework members were made of copper of 100% IACS (International Annealed Copper Standard) conductivity to represent the ship's structural aluminum alloy of 40% IACS conductivity.

$$\therefore \frac{\sigma_s}{\sigma_m} = \frac{\rho_m}{\rho_s} = 0.4 \ , \qquad (30)$$

where σ is the conductivity in mhos/cm.

By these means, ω_m was reduced by a factor of about 10, to

$\omega_m = 12 \times 12 \times .4 \times 23.6 = 1360$ deg/sec, or to 227 rpm.

If this velocity were to be obtained as a maximum of a sinusoidal oscillatory motion of amplitude 30°, the period would be

$$T_\alpha = \frac{30 \times 2\pi}{1360} = 0.14 \text{ seconds.}$$

A large irregularly-shaped model structure would be difficult to oscillate at 30° amplitude in .14 seconds per oscillation. However, it can easily be rotated continuously at 1360 deg/sec (227 rpm). It was, therefore, decided to make the model field measurements during such a continuous rotation. The approximations introduced by this method and the measuring technique will be described later.

The method of ship model scaling may be summarized as follows: a copper framework of members whose cross sectional areas are 1/144 of the areas of corresponding ship members, attached to a wooden model of the ship's hull of scale 1/24 and rotated at a continuous angular velocity of 227 rpm in a given exciting field should give, at scale distances (1/24), an effect equal to the maximum produced by the full-scale ship in the same exciting field during a ± 30-degree 8-second roll.

B. MAIN ASSUMPTIONS

The aluminum frame structure of the AMc.143 and class minesweeper is shown in Davie Shipbuilding Co. Plan No. 589-H-2. The copper framework of the model was designed from this structure by using the scale factors derived above.

The following assumptions were necessary to the design:

1. Since the copper framework was attached to the surface of a solid wooden model hull, the assumption was made that internal members on the ship could be represented adequately by equivalent conductors on the surface of the hull. The methods of representation are described below.

2. The conductivity of the structural aluminum is 40% IACS, and the riveted joints in the structural aluminum may be disregarded. The validity of these assumptions has been verified by a separate investigation.[6]

3. The distortion in scale of the cross sections of the framework (these cross sections have a linear scale of 1/12 as compared with the ship-shell scale of 1/24) will cause little misrepresentation by the model field at distances which are large compared with the linear dimensions of the sections.

C. REPRESENTATION OF INTERNAL MEMBERS

Internal framework members (those not on the contours of the outer shell of the ship) constitute about 20% of the total structure. They therefore contribute about 20% of the magnetic disturbance. Their effects are represented on the model by members producing the same fields, but placed on the surface of the model hull. The calculation for equivalent members at the surface is as follows:-

(a) Deck Beams and Decks

Consider two circuit elements each of length dl centimeters, disposed symmetrically about a rotational axis and moving with an instantaneous angular velocity ω. These two elements rotate about an axis Y_1 in their plane in the presence of an exciting field H_e oersteds, as shown in section in Fig. 5. A field will be produced at P whose component normal to H_e and in the plane of the paper is

$$dH_1 = 2\left(\frac{I_1 dl}{10 d_1^{\,2}}\right)\sin\delta_1 \text{ oersteds.} \qquad (32)$$

Substitute the following four equations into Equation 32:

$$I_1 = \frac{E_1}{R_1} = \frac{10^{-8} B dl \omega b_1}{\rho \frac{dl}{A_1}} \text{ amperes ,} \qquad (33)$$

$$B = H_e, \qquad (34)$$

$$d_1 = \sqrt{h^2 + b_1^{\,2}} \text{ , and} \qquad (35)$$

$$\sin \delta = \frac{b_1}{\sqrt{b_1^2 + h^2}} \quad . \tag{36}$$

The result is

$$dH_1 \propto \frac{b_1^2 A_1}{(b_1^2 + h^2)^{3/2}} \quad . \tag{37}$$

If these current elements of cross sectional area A_1 are replaced by a pair of elements dl each of cross sectional area A_2 at radius b_2 and rotated with the same angular velocity ω in the same field H_e as before, then:

$$dH_2 \propto \frac{b_2^2 A_2}{(b_2^2 + h^2)^{3/2}} \quad . \tag{38}$$

For the condition that $dH_1 = dH_2$ the following holds:

$$\frac{A_2 b_2^2}{(b_2^2 + h^2)^{3/2}} = \frac{A_1 b_2^2}{(b_1^2 + h^2)^{3/2}} \quad , \tag{39}$$

and when h is large compared with b_1 and b_2, this reduces approximately to

$$A_2 b_2^2 = A_1 b_1^2 \quad . \tag{40}$$

If rotation occurs about the axis Y_2 (Fig. 5) rather than Y_1, the instantaneous motion can be considered as a combination of a translation in the direction of the field and rotation about the axis Y_1. Translation in the direction of the field induces no voltage, so the total effect may be considered to be due to rotation of the pair of elements about a central axis in their own plane.

The product Ab^2 (Eq. 40) is the expression for the moment of inertia of an area A about a rotational axis a distance b away. A pair of members (A_2) which are attached to the surface of the ship must have, therefore, cross sectional areas with the same moment of inertia about a central axis in their own plane as a pair of internal members (A_1) which they represent. This applies, not only to members in the same horizontal plane as the axis of rotation of the ship, but also to other members in

the structure. As shown above, the "moment of inertia" representation involves some approximation, but its accuracy does not need to be great since only about 20% of the eddy current field is due to internal members.

This method of representation has been applied to two types of internal sections:

1. Sections of longitudinal beams - Here Equation (40) was applied as follows:

$$A_2 = \left(\frac{b_1}{b_2}\right)^2 A_1 , \qquad (41)$$

where A_2 = sectional area of external member attached at the same level as the beam, and

A_1 = sectional area of longitudinal beam.

2. Sections of internal decks. As can be shown from Fig. 6, in the case of internal decks,

$$b_2^2 A_2 = t\int_0^{b_2} b_1^2 \, d(b_1) = \left[\frac{b_1^3}{3} t\right] = \frac{b_2^3}{3} t \quad .$$

$$\therefore A_2 = b_2 \frac{t}{3} \qquad (42)$$

where A_2 = sectional area of external member representing half the deck sectional area,

b_2 = half deck width,

t = thickness of deck.

In both cases the calculated area A_2 was then multiplied by 1/144 to obtain the cross section of the model member.

(b) Bulkheads, Transverse Beams, and Pillars

During rolling these are not voltage generating members. However, they contribute their conductance to the network formed by the ship's frame. Hence they must be represented in the model framework.

Bulkheads were represented by transverse bands on the surface of the model. These bands were calculated approximately by taking the average cross-sectional area of the bulkhead when looking from deck to keel, multiplying this by 1/144 to convert to the model, and then by 1/2, since there are two band sections joining the deck to the keel.

Transverse Beams and Pillars were represented by increasing the cross-section of the nearest section of transverse frame or bulkhead band by an amount equal to 1/144 of the section of the beam or pillar.

D. CONSTRUCTION OF MODEL

A wooden model of 1/24 scale was obtained from the Royal Canadian Navy. Two views of this are shown in Figs. 7 and 8. The three-stage procedure outlined in Section I (C) was then followed in applying the framework to this model. Table II gives the dimensions of all the members used in the construction at each of the three stages.

Stage 1. - A minimum structure was applied to the wooden hull. Two views of this are given as Figs. 9 and 10. Field measurements (to be described later) were made on this structure.

Stage 2 - Members representing the aluminum decks were added. These additional members and the method of representation are listed in Table II. Field measurements were made on the new structure.

Stage 3 - Additional members were added to complete the structure of the AMc.143 and class with aluminum decks. Two views of the complete structure are given as Figs. 11 and 12. Additional members also listed in Table II have been added for this stage. Field measurements were again repeated.

All copper members were precut, formed on the wooden hull and drilled to take the copper nails which fastened them to the hull. Intersecting members were soldered together at the intersections.

Brass stub shafts were inserted into sockets in the ends of the wooden hull. These shafts were arranged so that the extended line through their axes passed through the center of gravity of the model and was parallel to the plane through the water line. The water line corresponding to the estimated deep draft condition of the ship was marked on the model. Drafts of the ship estimated by the RCN were: stern 7'5-1/2", midship 7'0", bow 6'6-1/2". All depths reported here are measured below this water line.

DATA ON MODEL MEMBERS

(All members are copper. Cross sections are 1/144 cross sections of the corresponding members on the prototype.)

TABLE II A

TRANSVERSE FRAMES AND BULKHEADS

(Identified according to Davie Shipbuilding and Repairing Company drawing no. 589-H-2).

Frame No.	Cross section (sq in.)	Thickness (in.)	Width (in.)	Length (approx.) (in.)
Transom	0.0125	0.036	0.350	23-3/4
96	0.0363	0.1875	0.190	23-1/4
95	0.0363	0.1875	0.190	24-7/8
94	0.0363	0.1875	0.190	25-1/8
93	0.0363	0.1875	0.190	25-1/2
92	0.0535	0.1875	0.285	27
91 (Bulkhead)	0.208	0.1875	1.10	27
90	0.0535	0.1875	0.285	27
89	0.0363	0.1875	0.190	27-7/8
88	0.0363	0.1875	0.190	28-1/2
87	0.0363	0.1875	0.190	29
86	0.0363	0.1875	0.190	29-3/8
85	0.0363	0.1875	0.190	29-7/8
84	0.0363	0.1875	0.190	31-7/8
83	0.0363	0.1875	0.190	32-7/8
82 (Bulkhead)	0.271	0.1875	1.20	34-1/4
81	0.0437	0.1875	0.233	33-1/2
80	0.0437	0.1875	0.233	33-7/8
79	0.0437	0.1875	0.233	34-1/8
78	0.0437	0.1875	0.233	34-7/8
77	0.0437	0.1875	0.233	35-1/8
76	0.0437	0.1875	0.233	35-5/8
75	0.0437	0.1875	0.233	36
74	0.0437	0.1875	0.233	36-1/2
73 (Bulkhead)	0.314	0.1875	1.68	37-7/8
72	0.0437	0.1875	0.233	37-1/4
71	0.0437	0.1875	0.233	37-1/2
70	0.0437	0.1875	0.233	37-7/8
69	0.0437	0.1875	0.233	38-1/4
68 (Upper Half Bulkhead)	0.255	0.1875	1.36	38-1/2
(Lower Half)	0.0539	0.1875	0.288	
67	0.0539	0.1875	0.288	38-3/4

Frame No.	Cross section (sq. in.)	Thickness (in.)	Width (in.)	Length (approx.) (in.)
66	0.0539	0.1875	0.288	39-1/4
65	0.0539	0.1875	0.288	39-3/8
64	0.0539	0.1875	0.288	39-5/8
63	0.0539	0.1875	0.288	39-7/8
62	0.0539	0.1875	0.288	40
61	0.0539	0.1875	0.288	40-1/4
60	0.0539	0.1875	0.288	40-1/2
59	0.0539	0.1875	0.288	40-5/8
58	0.0539	0.1875	0.288	40-3/4
57	0.0539	0.1875	0.288	40-7/8
56	0.0539	0.1875	0.288	41-1/8
55	0.0539	0.1875	0.288	41-1/4
54	0.0539	0.1875	0.288	41-7/8
53	0.0539	0.1875	0.288	42-5/8
52	0.0539	0.1875	0.288	43-3/8
51 (Bulkhead)	0.449	0.1875	2.40	45-1/2
50	0.0539	0.1875	0.288	45
49	0.0539	0.1875	0.288	45-3/4
48	0.0539	0.1875	0.288	46-1/2
47	0.0539	0.1875	0.288	47-1/8
46	0.0539	0.1875	0.288	47-3/4
45 (Upper Half Bulkhead	0.329	0.1875	1.75	49-1/4
(Lower Half)	0.0437	0.1875	0.233	
44	0.0437	0.1875	0.233	48-3/8
43	0.0437	0.1875	0.233	48-1/2
42	0.0437	0.1875	0.233	48-1/2
41	0.0437	0.1875	0.233	48-1/4
40	0.0437	0.1875	0.233	48-1/8
39	0.0437	0.1875	0.233	48
38	0.0437	0.1875	0.233	47-7/8
37	0.0437	0.1875	0.233	47-3/4
36	0.0437	0.1875	0.233	47-5/8
35 (Bulkhead)	0.342	0.1875	1.82	48-3/4
34	0.0437	0.1875	0.233	47-3/8
33	0.0437	0.1875	0.233	47
32	0.0437	0.1875	0.233	46-7/8
31	0.0437	0.1875	0.233	46-5/8
30	0.0437	0.1875	0.233	46-1/2
29	0.0437	0.1875	0.233	46-3/8
28 (Bulkhead)	0.316	0.1875	1.68	47-1/8
27	0.0435	0.1875	0.232	45-7/8
26	0.0435	0.1875	0.232	45-5/8
25	0.0435	0.1875	0.232	45-3/8

Frame No.	Cross section (sq. in.)	Thickness (in.)	Width in.	Length (approx.) (in.)
24	0.0435	0.1875	0.232	45
23	0.0435	0.1875	0.232	44-3/4
22 (Lower Half Bulkhead)	0.219	0.1875	1.17	44-5/8
(Upper Half)	0.0435	0.1875	0.232	
21	0.0435	0.1875	0.232	44-1/4
20	0.0435	0.1875	0.232	43-3/4
19	0.0435	0.1875	0.232	43-1/2
18	0.0435	0.1875	0.232	43-3/8
17	0.0435	0.1875	0.232	42-7/8
16	0.0435	0.1875	0.232	42-1/4
15 (Middle section Bulkhead)	0.211	0.1875	1.12	42
(Remainder)	0.0435	0.1875	0.232	
14	0.0435	0.1875	0.232	41-7/8
13	0.0435	0.1875	0.232	41-3/8
12	0.0435	0.1875	0.232	41
11 (Bulkhead)	0.173	0.1875	0.92	40-7/8
10	0.0435	0.1875	0.232	40-1/8
9	0.0435	0.1875	0.232	39-3/8
8	0.0435	0.1875	0.232	38-3/4
7	0.0435	0.1875	0.232	38-3/8
6 (Bulkhead)	0.150	0.1875	0.80	37-7/8
5	0.0435	0.1875	0.232	36
4	0.0435	0.1875	0.232	34-1/2

TABLE II B

LONGITUDINAL MEMBERS

(Identified according to Davie Shipbuilding and Repairing Company drawing no. 589-H-2).

(1): Members in minimum structure (Stage I).

Name of Member	Cross section (sq.in.)	Thickness (in.)	Width (in.)
Keel	0.314	0.375	0.84
#1 Bottom Long. Girder			
Stern to frame 66	0.0344	0.1875	0.184
Frame 66 to frame 51	0.091	0.1875	0.486
Frame 51 to bow	0.060	0.1875	0.320
#2 Bottom Long. Girder			
Stern to frame 73	0.023	0.102	0.226
Frame 73 to frame 51	0.064	0.1875	0.341
Frame 51 to frame 35	0.038	0.1875	0.203
Frame 35 to frame 11	0.023	0.102	0.226
#3 Bottom Long. Girder	0.018	0.102	0.176
Lower Deck Stringer	0.0349	0.1875	0.186
Bilge Stringer	0.0349	0.1875	0.186
Upper Surface Deck Beams	0.0375	0.1875	0.199
Exterior equivalent of upper deck interior longitudinal members			
Frame 45 to frame 25	(0.0108 at Fr. 45 to (0.0138 at Fr. 25	0.060	0.18 at Fr 45 to 0.23 at Fr 25
Frame 25 to bow	0.0264	0.060	0.44
Exterior equivalent of lower deck interior longitudinal members			
Frame 91 to frame 68	0.0116	0.040	0.29
Frame 28 to frame 11	0.0044	0.040	0.11

(2): Decking (Added for Intermediate Structure, Stage II).

Name of Member	Cross section (sq. in)	Thickness (in.)	Width (in.)
* Exterior equivalent of forward part of upper deck:			
At frame 45	0.095	0.1875	0.5
At frame 28	0.092	0.1875	0.5
At frame 15	0.071	0.1875	0.375
At frame 6	0.0365	0.1875	0.2
*Exterior equivalent of aft part of lower deck:			
At frame 91	0.0365	0.1875	0.2
At frame 68	0.065	0.1875	0.35
*Exterior equivalent of forward part of lower deck:			
At frame 28	0.065	0.1875	0.35
At frame 6	0.018	0.1875	0.1

Upper surface of model is decked with copper plate 0.045" thick to represent decks. This is 1/6 actual deck thickness, and since the model dimensions are 1/24 those of its prototype, the section ratio is brought down to 1:144.

(3): Strakes (Added for Complete Structure, Stage III).

Name of Member	Cross section (sq.in.)	Thickness (in.)	Width (in.)
Foc'sle deck sheer strake	0.0632	0.045	1.40
Upper deck sheer strake	0.0625	0.045	1.40
Intermediate strake	0.0172	0.040	0.43
Lower deck strake	0.0313	0.040	0.78
Bilge strake	0.0382	0.040	0.95

* See Section III - ERA-228.

IV - MEASUREMENT TECHNIQUES

A. CO-ORDINATE SYSTEMS

(a) Exciting Field. If the horizontal and vertical components of the earth's total field are H and Z, the exciting fields along the principal axes of the ship in the even keel position with respect to the horizontal plane, are shown in Fig. 13. It is convenient, however, to give exciting fields in terms of a set of rectangular co-ordinates which are fixed with respect to the ship. In such a system let the exciting field be defined as follows:

H_v - Component vertical to ship's deck - Positive when directed from deck to keel

H_h - Component athwarthship - Positive when directed from starboard to port

H_ℓ - Component parallel to the keel - Positive when directed from stern to bow

For the even keel position the relationships between these and the earth's field are:

$$H_v = Z \tag{43}$$

$$H_h = H \sin \Phi \tag{44}$$

$$H_\ell = H \cos \Phi \, , \tag{45}$$

where Φ is the magnetic heading of the strip measured East from North (degrees).

For other than even keel the components H_v, H_h and H_ℓ are functions of the angles of roll and pitch.

(b) Eddy-Current Field. The eddy-current field co-ordinate system chosen here is fixed with respect to the earth and has the following components at a point M below the ship (see Fig. 13):-

v —vertical component of the eddy-current field with reference to the earth's horizontal plane - Positive downwards.

h — horizontal component transverse to the ship's axis and in the earth's horizontal plane. Positive from starboard to port.

ℓ — longitudinal component normal to the plane containing h and v. Positive from stern to bow

B. SEPARATION OF H_v AND H_h COMPONENTS

The earth's field was used as the exciting field of the model. Rolling experiments were designed so that the effect of H_v and H_h could be determined separately. (H_ℓ is ineffective in producing eddy-current fields during rolling).

Fig. 14 illustrates the method of determining the eddy-current field due to H_v. Here the longitudinal axis of the ship model was aligned in the north-south direction and measurements were made with the model rotating at the instant when the model was in the attitude, with respect to the exciting field Z, shown in Fig. 14. Eddy-current field components at a point M are denoted by h_1, and v_2.

Fig. 15 illustrates the method of determining the eddy-current field due to H_h. The same exciting field Z was used and the measurements were made at the same point M with respect to the ship's water line. However, the measurement was now made at the attitude with respect to the exciting field Z shown in Fig. 15. The eddy-current field components are denoted by v_1 and h_2 at the point M.

The eddy-current field which would occur if the ship rolls in an exciting field $H_v = Z$ and $H_h = Z$ could then be determined as v_1+v_2; h_1+h_2 To determine the effects of other exciting field conditions the following relationships may be used:-

h_1 and v_2 vary directly as H_v (46)

v_1 and h_2 vary directly as H_h. (47)

C. APPARATUS

(a) Supporting Frame, Model Drive, and Measuring Boards. The stub shafts of the ship model were supported in bearings attached to the wooden structure shown in Fig. 16. An aluminum pulley was fixed to one shaft (see Fig. 11). A long V-belt extended over this pulley to the pulley of a 1/2 hp d-c motor placed eleven feet from the axis of the model. A thyratron, adjustable, constant-speed control was used to set and hold the speed of the motor. A Hasler, type A, high speed tachometer (0-20,000 rpm) was used to measure the rotational velocity of the ship model. The motor and control were sufficiently distant from the field measuring device that negligible disturbance to the eddy-current field measurement was caused by their electromagnetic fields.

Two plywood boards, used to position the detecting element of the magnetometer, were supported by the framework in a plane normal to the rotational axis of the model. These two boards are shown in Fig. 17. Holes were drilled in the boards in known positions with respect to the

water line of the ship model. These holes were drilled identically in both boards so that any position relative to the ship model's water line on the lower measuring board could be duplicated on the side measuring board. The detecting element could be fastened to either board by an attached supporting rod, which could be inserted through any hole and clamped with a knurled nut. By this means the detecting element could be positioned accurately at predetermined points. A protractor was fastened to the detector enabling it to be set at any required angle. The measuring boards could be moved to any position along the longitudinall axis of the ship model and set transverse to the axis.

The lower measuring board was used in measuring the eddy-current field components due to an exciting field vertical to the ship's deck. The side measuring board was used in measuring components due to an exciting field parallel to the ship's decks. The use of the two measuring boards described, enabled the earth's vertical field to act as the exciting field in both cases in the manner shown in Figs. 14 and 15.

(b) Triggering Contactor. A triggering contactor assembly, shown in Fig. 16 is used to indicate when the rotating ship's model is in a predetermined position with respect to the exciting field. This structure supports two contacts which are closed once per revolution by a wiper attached to an extension of the model shaft. The two contacts can be set at any angle on a circle in such a way that they can be closed by the wiper at any predetermined angle of the ship relative to the keel-down position shown in Fig. 14. The contacts close for a period of time corresponding to 8.5° of each revolution. The contactor is used to trigger the oscilloscope of the field-measuring device.

(c) Exciting Field Magnetometer. The exciting fields in which the model rotated were measured by a U.S. Navy Magnetometer. This is a Mark 5, Model 5, two-core, flux-gate type instrument manufactured by the Leeds and Northrup Company for the U.S. Naval Ordnance Laboratory.

(d) Eddy-Current Field Magnetometer. A separate magnetometer was used to measure the eddy-current fields. The detecting element of this is visible in Fig. 17. This detector could be set at any angle in any one of the mounting holes in the measuring board (Fig. 17). The magnetometer was a slightly modified form of the type described by Rose and Bloom.[7] Fig. 18 is a block diagram of the apparatus.

The output from the 1000-cycle oscillator is filtered and fed into the exciting coil of the detector element. If this element is in an external magnetic field, harmonics are generated in the 1000-cycle wave form. In this particular instrument, the second harmonic (2000-cycle) is used as a measure of the external magnetic field in which the

detector is located. The output connections parallel the input, but the signal is fed through a band pass filter which passes only the 2000-cycle harmonic. The signal out of the 2000-cycle filter is amplified and applied directly to the input of an oscilloscope. A change in the magnetic field at the detector may thus be observed as a variation in amplitude of the 2000-cycle oscilloscope signal.

A feedback coil (see Ref. 7), in the form of an outer solenoid surrounding the sensitive element is used to make the magnetometer a "null" instrument. The battery-supplied current (A_1, Fig. 18), to the feedback coil is varied by adjusting a potentiometer manually until the oscilloscope signal is a minimum. The magnetic field at the detector element can then be calculated as the product of the nulling current, A_1, and the feedback coil constant. The feedback coil constant was measured by the use of a set of Helmholtz coils as 98 mg/ma.

The sensitive element in the detector consists of a tube of mu-metal of wall thickness 0.006", length 1-3/4", and outside diameter 3/16". The exciting coil surrounding the mu-metal strip was wound to give the correct impedance (1000 ohms at 1000 cycles) to match the impedances of the filters.

When the detector is in a strong field, such as the earth's vertical component, it is necessary to buck out this unwanted field. This is accomplished by a third, battery-supplied solenoid wound over the feedback coil. This coil had a coil constant of 85 mg/ma.

(c) The Oscilloscope. The oscilloscope shown in Fig. 18 was a Cossor, Model 1049. It has an electrical beam trigger which enabled the 2000-cycle signal to be viewed only during the time (8.5° of the rotation) when the triggering contactor shown in Fig. 16 was closed. Since this contactor is adjustable in a circle, the eddy-current field set up by the rotating ship can be measured at any time during a revolution.

D. PROCEDURE

(a) Determination of Eddy-Current Field Due to Vertical Component of Exciting Field

The procedure for determining the components h_1 and v_2, which are those due to the H_v component of the exciting field, was the following:

(1) The rotational axis of the model was aligned in the North-South direction (with the bow North) by the use of a magnetic compass. Only the earth's vertical component was then effective in producing eddy-currents in the rotating model. The model field then simulated the field produced by the ship when rolling in the vertical component alone of the earth's total field.

(2) The triggering contactor (initiating the oscilloscope sweep) was set to close in the deck-horizontal position as shown in Fig.14.

(3) The detector element was set horizontally in one of the holes in the lower measuring board, (Fig. 17), which was placed in the midship position. The detector was now in the earth's zero field.

(4) The model was rotated at 227 rpm and the d-c current required in the feedback coil to null the magnetometer signal as observed on the oscilloscope was recorded. Since the magnetometer signal appeared on the oscilloscope only during the time the triggering contactor was closed, the measured field corresponded to the field produced when the model was in the keel-down position. The product of the feed-back current (ma) and coil constant (mg/ma) then gave the h_1 component in milligauss.

(5) The rotation was stopped.

(6) The detector was then turned through 90° (Fig. 17).

(7) The magnetometer signal due to the vertical component of the earth's field was balanced out by means of the earth balancing coil.

(8) The model was again rotated at 227 rpm and the resulting signal again balanced out by the feedback coil current when the model was in the keel-down position. This measurement gave the v_2 component.

(9) The above procedure was carried out with the detector in each of the plug-in measuring holes of the mounting board shown in Figs. 16 and 17.

(10) The measuring board was then moved in turn to the quarter-fore and quarter-aft positions and the measurements repeated.

(b) Determination of Eddy-Current Field due to Horizontal Component of Exciting Field

The procedure for determining v_1 and h_2 which are those components due to the H_h component of the exciting field was the following:-

(1) The triggering contactor was set to close for the deck-vertical position shown in Fig. 15.

(2) Similar measurements to those for the H_h component of the exciting field were made at each of the plug-in holes in the side measuring board. These holes were placed at positions with respect to the ship's keel corresponding to those in the lower measuring board, as shown in Figs. 16 and 17.

(c) Determination of Eddy-Current Fields for Other than Keel-Down Positions

(1) With the longitudinal axis of the model in the North-South direction a measurement of component h_1 was made as in Part (a) above. The contactor was then set at other angles, as shown in Fig. 37, and the measurement of h_1 repeated at each angle. The method is indicated and the results shown in Fig. 37.

(2) The same method was used in measuring the variation in components v_1, h_2 and v_2 with contactor angle. The results are shown in Figs. 38, 39 and 40.

E. CALIBRATION AND ACCURACY

Three principal factors influence the accuracy with which the ship's field may be determined by model techniques. These are:

(a) The accuracy of representation of the ship's structure.

(b) The approximation introduced by rotating rather than oscillating the model.

(c) The accuracy of the measurements of the eddy-current field of the model.

(a) Accuracy of Representation Although the model was designed to produce an eddy-current field as closely similar to that of the ship as possible, four main approximations were introduced into its design.

The surface of the wooden hull shown in Figs. 7 and 8 was constructed to represent the outer surface of the wooden planking of the ship's hull. The model copper framework should be internal to this surface for a precise representation of the ship. However, this framework was fastened over the surface of the wooden hull and thus was displaced outward from its proper position. Such displacement of the framework will introduce an approximation into the representation. The keel of the model, however, was designed so that its lower surface represented accurately the proper position of the base line of the ship relative to the other parts of the ship. This special care was taken in the representation of the keel because it is one of the most important field producing members, being large in cross section and close to the point of measurement.

A second approximation in representation is that of the effect of internal members. This approximation is explained in detail in Section III (B).

A third approximation in representation is introduced by the fact that the aluminum superstructure of the ship is not represented in the model.

A fourth approximation is introduced by the dilation of the scales of the cross sections of the framework members (see Section III).

(b) Approximation Introduced by Rotating Rather Than Oscillating the Model

In all model test results, the model was continuously rotated at a constant angular velocity scaled to the peak angular velocity attained by the ship during a sinusoidal rolling motion. If the model were oscillated to simulate the rolling action of the full-scale ship, its angular velocity would vary continuously with time. Because of the inductance of the model framework, it would be expected that the eddy-current field created when the model reaches its peak angular velocity would differ from that created when the model rotates continuously at this peak angular velocity. An estimate of this difference may be obtained from equivalent cylinder theory.

A theory of the eddy-current field produced external to a thin, hollow, infinitely long, conducting cylinder oscillating in a uniform magnetic field is developed and discussed in Appendix IV. This theory is compared with that for the same cylinder rotating continuously in the same magnetic field. Those results of the analysis which allow an estimate of the approximation introduced by rotation rather than oscillation of the model will now be given.

Fig. 19 gives graphical comparison between the horizontal field produced by a cylinder when rotating and that produced by the same cylinder when oscillating, in a vertical exciting field. The constant angular velocity of the rotating motion is equal to the maximum angular velocity attained during the oscillating motion. These curves are calculated for a cylinder having constants only approximately equal to those of the ship's equivalent cylinder - which is described in Appendix III - and are therefore used only to estimate the probable error in the representation.

Curve A, Fig. 19, calculated by the methods of Section I (D), is a plot of the horizontal component on a normalized scale of the eddy-current field, produced by cylinder rotation. The values given are those along a horizontal line transverse to the axis and below the cylinder. The usual shift in space, previously observed in Fig. 2, is present. For Curve A the space phase shift is 14°.

Curve B, Fig. 19, is a plot of the normalized horizontal component of the field produced by cylinder oscillation. The amplitude of the oscillation is about $\pm$ 30° and the period lies within the range of

ship rolling periods. Curve B was calculated by employing the results of the analysis given in Appendix IV. The field distribution is calculated at the instant when the angular velocity of the oscillating cylinder is maximum. At this position ($\theta = 0$) the magnitude of the normalized horizontal field for the cylinder when rotating is 18% higher than the magnitude for the cylinder when oscillating.

Curve C, Fig. 19, shows the normalized horizontal field distribution for the oscillating cylinder at a later time than Curve B when, although the angular velocity is no longer maximum, the field is maximum. This effect is due to the inductance of the cylinder. At the $\theta = 0$ position the magnitude of the normalized horizontal field for the cylinder when rotating is now only 8% higher than the magnitude for the cylinder when oscillating.

Although these results are not directly applicable to the case of the model ship technique they do indicate that the results obtained for the ship model for maximum field conditions under the keel are somewhat high. The results also indicate that the ship model results represent the maximum field produced by a ship during its rolling cycle more closely than they represent the field produced at the instant when the ship has attained maximum angular velocity.

Fig. 20 is a graph of the normalized horizontal component of the field as a function of time at the $\theta = 0$, $\theta = 22.5°$, $\theta = 45°$ positions for the cylinder when oscillating. At the $\theta = 0$ position the field is essentially a sinusoidal function of time and lags the angular velocity of the cylinder nearly by the angle $\tan^{-1} \omega\tau$, where τ is the time constant of the cylinder and $\omega = \frac{2\pi}{\tau a}$. At this position the second harmonic effect discussed in Appendix IV is very small. The horizontal field magnitude reaches a maximum value at a time later than that at which the peak of angular velocity occurs. This condition was also shown in Fig. 19. At the $\theta = 22.5°$ position the eddy current field is no longer sinusoidal in time but shows considerable distortion. This is due to the increased importance of the second harmonic effect discussed in Appendix IV. At the $\theta = 45°$ position the field is due entirely to the second harmonic effect. Here the field is unidirectional at all times and is of double frequency.

These effects are discussed in detail in Appendix IV.

(c) Accuracy of the Measurements of Exciting and Eddy-Current Field.

(1) The Earth's Field as the Exciting Field

In all eddy-current field measurements, the vertical component of the earth's magnetic field was used as the exciting field.

The magnitude of the eddy-current field is proportional to the magnitude of the exciting field in which the model rotates. It is

therefore necessary that accurate measurements of the exciting field be made during the model tests. Further, if the exciting field is not uniform in space and constant in time, errors will be introduced into the eddy-current field measurements. Non-uniformity in space would mean that different conducting members in the model would be moving in different exciting fields. This would not simulate the conditions normally encountered by the ship. Non-constancy in time, besides affecting the measurement of the earth's field, would be particularly serious in the eddy-current field measurement. This is due to the fact that a small variation in the component of the earth's field along the axis of the detector will superimpose directly on the component of eddy-current being measured and thereby may cause a large error in the measurement.

Eddy-current field measurements were made at two different sites. The first site was in a steel framed building, the second in a wooden building having no ferromagnetic material. Magnetometer surveys of the exciting field were made at each of these sites. These surveys showed both spatial non-uniformities and time variations of the exciting field, necessitating certain precautions in the eddy-current field measurements. The results of the surveys and the methods of compensating for variations are given in the following paragraphs.

The magnitude of the earth's vertical field was measured with a Mark 5 Model 5 U.S. Navy Magnetometer. This instrument is accurate to ± 5 mg.

Model experiments were performed in the steel framed building after stages 1 and 2 of the model construction. Space variations of the field were measured with the Navy Magnetometer placed in the vertical position at various points in the space about the model. These measurements were made when the earth's field was particularly constant in time. Eight such measurements were taken and the highest and lowest fields obtained were 370 mg and 358 mg, respectively. The average of the measurements was 366 mg which was taken at the exciting field. Thus the largest deviations from this value are about 2%.

Measurements on the completed model (after stage 3 of the construction) were made in the building free of ferromagnetic material. A field survey made at ten points in the space around the model showed a mean vertical field of 555 mg, the highest field being 562 mg and the lowest 544 mg (the observatory value of the earth's vertical field at Ottawa is 562 mg). Again the largest deviations from the average are about 2%.

During the course of the model tests it was found that time variations of the earth's magnetic field may affect the eddy-current measurements seriously unless certain precautions are taken. Measurements taken in the steel framed building showed that during the course of an eddy-current field measurement the component of the earth's field

along the axis of the detector could vary by as much as 2 mg. Thus if the detector is to measure eddy current fields in the range 0 - 30 mg, precautions must be taken for time variations in the earth's field in order that large percentage errors in the model results be avoided. The precautionary measures consisted of nulling the earth's field along the axis of the detector immediately before and after each eddy-current field measurement by means of the earth-balancing coil described in Section IV. (p. 25). The average of any difference was applied as a correction to the eddy-current field reading. Time variations in the building free of ferromagnetic material were found to be of the same order as those observed in the steel framed building and the same precautions were taken.

The exciting field base was chosen as 560 mg. All eddy-current field measurements were referred to this base by linear extrapolation.

(2) Eddy-Current Field For the null method of using the eddy-current field magnetometer described in Section IV C(d) the magnetic field is given by the formula[8] :-

$$B = MI_f + K_1 + K_2,$$

where

B is the component of the field under measurement (mg)
M is the solenoid constant of the feedback coil (mg/ma)
I_f is the nulling current in the feedback coil (ma)
K_1 is an additive constant which is independent of the field (mg)
K_2 is an additive constant due to the misalignment between the detector and the field to be measured (mg).

Accurate measurement of an eddy-current field requires that M I_f and K_2 be known accurately, and that the two constants M and K_1 do not change appreciably during the time of the measurement. These requirements were examined for the case of the eddy-current field magnetometer with the following results:-

By the use of a set of Helmholtz coils the solenoid constant M was measured and tested over a range of fields extending from +560 mg to -560 mg and found to be 98 mg/ma ± 1% over this range. Variations in M are probably not greater than published values for other instruments of this type whose variations are reported to be less than 0.1% [8].

The additive constant K_1 varies slightly with operating conditions, such as a-c voltage, frequency, temperature and magnetic treatment of the detector [8]. Sufficiently controlled conditions were not available for making accurate measurements of variations in K_1.

However, precautions were taken to minimize such variations by operating the magnetometer unit from a Sorenson regulator, by taking each single measurement in as short a period as possible (about 45 seconds) and by subjecting the magnetic core to as small magnetic field variation as possible during a measurement. Several experimental checks were made by one of the designers of this instrument under these conditions. They indicated that the value of K_1 is less than 0.5 mg and that variations are less than this value.

The system was arranged so that the earth's field with the model at rest could be balanced out by means of the earth-balancing coil while the feedback coil current "I_f" was set at zero. Then, with the model rotating at constant angular velocity, the current "I_f" was increased until a null condition was observed on the oscilloscope. The nulling current meter was a standard 3-1/2" panel meter with an accuracy of 2% of full scale, except in the case of stage 3 measurements where a 1/4% meter was used. Meters of appropriate ranges were inserted into the circuit in order to keep the reading within the upper two-thirds of the meter scale.

The spread in the measurements of the maximum values of h_1 and v_1 after stage 3 was checked by measuring the same eddy-current field a number of times. The following table shows the results of six measurements of each of the quantities h_1 and v_1 at each of three depths under the keel at midship

TABLE III

	19' Under Water Line midship (Stage 3)		24' Under Water Line midship (Stage 3)		29' Under Water Line midship (Stage 3)	
	h_1	v_1	h_1	v_1	h_1	v_1
Max.	29.5	31.4	19.9	23.4	13.4	17.1
Min.	27.8	29.2	16.9	20.3	11.6	14.9
Mean	28.3	31.0	18.3	21.6	12.4	15.9
Spread	(+1.2 mg (-.5	(+.4 mg (-.8	(+1.6 (-1.4	(+1.8 (-1.3	(+1.0 (-.8	(+1.2 (-1.0

The uncertainty in any single measurement due to variations in the exciting field and because of the instrumentation is within the range of ± 2 mg. Uncertainties in the measurements of the values of h_2 and v_2 are of the same order.

The constant K_2 is normally added to allow for misalignment of the detecting element within the detector mounting, and for misalignment of the mounting with respect to the component of eddy-current field to be measured[8]. In the case of the measurements of h_1 and v_1 the detector was rotated into zero field before the measurement, by varying the position of the detector until the oscilloscope signal was a minimum. An eddy current field measurement was then made for this position of the detector. This process was repeated for each position of the magnetometer on the measuring boards. In this method, the constant K_2 becomes dependent on the uniformity of the exciting field as well as on the accuracy of the model set-up and is not reliably known. However, for the measurement of the maximum values of h_1 and v_1 (nearly under the keel), the angle of the magnetic axis is not critical since the measurements were made at the peak of the sine curve shown in Fig. 39. In the case of the stage 3 measurements the exciting field was uniform and therefore the errors due to the detector alignment were small. In the measurements of h_2 and v_2, the constant K_2 may introduce slightly larger errors because the angle at which those components are measured is determined by setting the detector element in static zero field and then turning 90° into the vertical direction before making the eddy current field measurement.

A further possibility of error lies in the statement of the position of the detector element with respect to the model. The positioning of the center of the detector is within 1/16" of the position stated with respect to the water line in the model system.

It is difficult to evaluate the effects of all these approximations on the accuracy of the measurement of the field of a rolling ship by the model techniques developed here. However, during the course of the investigation, it was possible to measure the field at a few points under a full-scale AMc 143 minesweeper with aluminum decks. Model measurements were compared with these measurements to give an estimate of the effectiveness of the technique. This comparison (given in Section VII below) shows that the model produces an eddy current field which is on the average about 15% lower in magnitude than that of the full-scale ship.

V - TEST RESULTS

a) Figs. 21 to 36 inclusive give the results of measurements of components h_1 and v_2 brought to a common exciting field base of $H_h = 560$ mg, and of v_1 and h_2 brought to a common exciting field base of $H_h = 560$ mg.

b) Figs. 37 to 40, inclusive, show the variations in signal from the detector, because of the shape of the ship, when the contactor is set to make the measurement at any attitude of the ship with respect to the exciting field.

c) Fig. 41 shows the effect of rotating the detector at a fixed measuring point with the contactor set to measure the field at the keel-down position.

d) Figs. 42 and 43 inclusive (Experimental Curves), show the eddy-current field as a function of angular velocity of roll. A comparison is given in these figures with similar functions (Theoretical Curves) calculated from the case of an infinite rotating cylinder. The calculations and comparisons are described in Section VI.

e) Figs. 44 and 45 give complete transverse profiles of the field of the model at midship taken at high angular velocity and for both directions of rotation. These tests were made to determine the time constant of the ship's framework as accurately as possible. The method of determining time constants is given in Section VI.

VI - ANALYSIS OF RESULTS

A. EDDY-CURRENT FIELD AS A FUNCTION OF EXCITING FIELD

All test results have been presented for exciting fields of 560 mg. In Fig. 46 a combination of exciting fields, which is approximately that existing at Ottawa, Canada, when the ship is heading east and west has been chosen. The eddy-current field has been derived for this condition from Figs. 29 and 30 by using the relationships given by Equations (46) and (47.) The eddy-current fields caused by any exciting field conditions may be derived in this way.

B. EDDY-CURRENT FIELD AS A FUNCTION OF DEPTH

Data are replotted from other figures, and some new data are also plotted in Figs. 47 and 48 to show the variation of field strength with depth. These curves show that the field strength varies approximately as the inverse square of the depth below the water line.

C. EDDY-CURRENT FIELD COMPARED WITH FIELD OF AN EQUIVALENT CYLINDER

In the introduction, a cylinder analogy was used to show the approximate form of the eddy-current field of the ship's framework. The experimental work on the ship model has produced field forms which are remarkably similar in form to those of the cylinder. It seemed reasonable to assume that the ship's field, under the midship section where end effects are small, could be closely represented by that of an infinite cylinder of appropriate dimensions. A logical basis for choosing both appropriate dimensions and the position of the cylinder relative to the ship has been attempted in Appendix III. A comparison of the characteristics of this cylinder with those of the ship, as determined experimentally from the model, follows:-

(a) Field Forms

Transverse profiles of the field under the midship of the model and the cylinder as determined by the method of Appendix III, are compared in Figs. 49 and 50. For the conditions assumed, there is good agreement in the case of the eddy-current field due to H_v. The H_h field agrees well in form, but the magnitude of the cylinder field is smaller than that of the ship probably because in this direction, the ship circuits are greater than the cylinder circuits.

(b) Variation with Angular Velocity

In Fig. 51 the horizontal and vertical components of H_1 for a cylinder have been derived from Equation (1) and plotted on a semi-log plot as a function of $\frac{a\nu}{\rho}$ for the point $r = b$, $\theta = 0$. These

functions are again plotted over a limited range in Fig. 52 where it is shown clearly that the vertical component is not linear with angular velocity whereas the horizontal component is nearly linear over a certain range.

In Figs. 42 and 43 the particular conditions for the cylinder described in Appendix III were substituted and the results as a function of angular velocity were compared with data obtained from the ship model. Notice that conversion from values at the cylinder wall to the 19'depth has been carried out using the inverse square law. Here again the H_v field agreement is good, but the H_h field would obviously require a larger cylinder for good agreement.

(c) Time Constants

It is demonstrated above that the ship's field is very similar to that of the cylinder chosen in Appendix III. For the case of a cylinder the angle ϕ may be determined from the field plots by the use of Equations (7) and (8). The time constant of the cylinder (given by $\tau = \frac{0.2\pi ab}{10^8 \rho}$) may then be obtained from the relationship

$$\tau = \frac{\tan \phi}{\omega} = \frac{\left|\frac{v_2}{h_1}\right|_{\theta = 0}}{\omega} = \frac{\left|\frac{h_2}{v_1}\right|_{\theta = \frac{\pi}{2}}}{\omega} . \qquad (49)$$

Because of the agreement between midship model field and cylinder field it is reasonable to expect that an estimate of the time constants of the ship's circuits may be obtained from an equation of the above form when v_2, h_1, h_2 and v_1 are taken from ship model field profiles. Because of the differences between the H_v and H_h excited fields, two "lumped" time constants are involved and these are given by:-

$$\tau_{H_v} = \frac{\left|\frac{v_2}{h_1}\right|_{\theta = 0}}{\omega} , \text{ and} \qquad (50)$$

$$\tau_{H_h} = \frac{\left|\frac{h_2}{v_1}\right|_{\theta = \frac{\pi}{2}}}{\omega} . \qquad (51)$$

In order to obtain reasonably accurate values for v_2 at $\theta = 0$ and h_2 at $\theta = \frac{\pi}{2}$, a set of measurements was taken at an increased angular velocity, and for both directions of rotation. The higher angular velocity seemed to give a more favorable ratio of v_2 and h_2 to the background field. The results are given in Figs. 44 and

45, and Equations(50)and(51)applied to these curves provide the following time constants for the stage 3 structure:

$$\tau_{H_v} = \frac{\frac{7}{26}}{6.62 \times \frac{2\pi}{60}} = .4 \text{ sec. (from Fig. 44)} \qquad (52)$$

$$\tau_{H_h} = \frac{\frac{15}{36}}{6.62 \times \frac{2\pi}{60}} = .6 \text{ sec. (from Fig. 45).} \qquad (53)$$

Equations(7)and(8)applied to all test results indicate that the time constants have been determined with about the following accuracy:

$$\tau_{H_v} = .4 \pm .1 \text{ sec.,}$$
$$\tau_{H_h} = .6 \pm .1 \text{ sec.}$$

The cylinder equivalent to the AMc. and Class ship (Appendix III) has a phase shift $\phi = 10°$ for an angular velocity equivalent to the maximum obtained by the ship. This yields a time constant of 0.5 seconds, as shown in Appendix III.

(d) Conclusion

On the basis of the case of the single ship described here it appears that a good estimate of the magnitude and space distribution of the eddy-current fields under the midship section and the time constants of the ship's circuits may be obtained by the equivalent cylinder method.

VII - COMPARISON WITH FULL-SCALE TESTS

The horizontal components of the eddy-current field of a full-scale AMc.143 and Class ship with aluminum decks has been measured at a few points [3]. The stage 3 structure of the model described in the present report was designed to produce the same eddy-current field as this ship. A comparison of equivalent eddy-current field measurements is given in Table IV. In this table the results of tests on the full-scale ship are given. The comparison is made by converting the model test results to the conditions under which the full-scale ship results were obtained. The conversion of model results is discussed in detail in Appendix V.

Table IV shows that full-scale ship measurements are, on the average, about 15% higher in magnitude than model measurements. The difference occurs because of the effects discussed in Section IV(E) above. It is probable that a major part of the difference exists because the aluminum superstructure of the ship is not represented on the model. There is also the possibility that the ice protection belt may form a conducting loop. It is not clearly known by the authors whether the ice protection belt forms part of the conducting structure of the ship since it may or may not be insulated from the other members by the wooden hull. The fact that full-scale results are consistently higher than model resultssupports the belief that these structures may contribute to the eddy-current field.

TABLE IV

COMPARISON OF TEST RESULTS FROM FULL SCALE AND MODEL SHIPS
FOR AN EXCITING FIELD OF H_v = 542 mg, H_h = 113 mg

Location	Depth Under Keel	Depth Under Water Line (Deep Condition)	SHIP TESTS (ERA-231) "COWICHAN"			MODEL TESTS (ERA-228 Stage 3 (Complete Structure)		Deviation of Model Tests From Ship Tests (%)
			Magnetic Disturbance (mg/deg/sec)	Avg. Single Amp. of Velocity (deg/sec)	Magnetic Signal (mg)	Angular Velocity (deg/sec)	Magnetic Signal $h_1' + h_2'$ (mg)	
Midship	18'	25'	.83	4.9	4.1	4.9	3.6	-12%
	23'9"	30'9"	.55	5.7	3.1	5.7	3.0	-3%
Quarter Ship	18'	24'9"	.88	5.2	4.6	5.2	3.7	-20%
Fore	23'9"	30'6"	.56	5.5	3.1	5.5	2.8	-10%
Quarter Ship	16'	23'3"	.71	4.9	3.5	4.9	2.5	-29%
Aft	21'9"	29'	.45	6.1	2.7	6.1	2.2	-19%

VIII - ESTIMATE OF FIELD DUE TO PITCHING

The model tests were not extended to measure the eddy-current fields due to the effect of pitching. However, estimates based upon the rolling experiments and upon indirect measurements were made.

Two types of framework circuits are effective in producing magnetic fields during pitching. These are: (a) Horizontal Circuits, such as those formed by longitudinals and beams - the field of these may be derived from roll measurements - and (b) Transverse Vertical Circuits, such as those formed by transverse frames - an approximate method of estimating their field is given here.

A. HORIZONTAL CIRCUITS

These circuits oscillating in the horizontal component of the earth's field will have eddy-currents which produce vertical fields under the keel. The effect will be a maximum when the ship is on a N-S heading, and a sinusoidally varying field will then be produced which has a maximum approximately at the time when the circuit is passing through the horizontal plane.

As we have shown previously, horizontal circuits contribute to the field caused by roll and their effects due to roll have been measured. It is possible by simply adjusting for the difference in angular velocity between pitch and roll motions to derive the pitching field from roll measurements to a first approximation.

Consider one of these horizontal loops of area S having a pitch oscillation of period T_p and maximum angle P_o. A sinusoidal current will be generated with a maximum given by

$$I_p = \frac{E_p}{R} \propto \frac{P_o}{T_p} \quad \frac{H_\ell S}{R} , \tag{54}$$

when E_p is the emf induced and R is the resistance of the loop.

The same loop moving with a roll oscillation at period T_α and a maximum angle α_o in the same field will have a sinusoidal current of maximum value

$$I_\alpha \propto \frac{\alpha_o}{T_\alpha} \quad \frac{H_h S}{R} . \tag{55}$$

The pitch effect H_{i_p} from horizontal circuits can thus be derived from the roll effect H_{i_α} by the use of formula:

$$H_{i_p} = \left(\frac{P_o T_\alpha}{\alpha_o T_p}\right) H_{i_\alpha} \quad . \qquad (56)$$

When the maximum roll and pitch conditions are:- Roll ±30° in 8 seconds; Pitch ±8° in 4.5 seconds, the multiplier $\left(\frac{P_o T_\alpha}{\alpha_o T_p}\right)$ is .475. The vertical effects due to rolling when the ship is E-W are shown in Figs. 22, 24, 26, 28, 30, 32, 34, 36 for an exciting field of 560 mg. The effects at points amidships under the keel, of pitch of horizontal circuits in a 142 mg. field are derived from these as shown in Table V. Pitch effects may be derived similarly from roll effects at any other point.

TABLE V

Position - Depth Under Water Line	Vertical Effect at Midship Due to a Pitch of ±8° in 4.5 sec. of Hor. Circuits for a N-S Heading at Ottawa (H_h = 142 mg)		
	Stage 1	Stage 2	Stage 3
19'	.475 x 3.7 = 1.8 mg.	2.9 mg.	3.8 mg.
24'	.475 x 2.7 = 1.3 mg.	-	2.5 mg.
29'	.475 x 1.2 = 0.6 mg.	1.3 mg.	1.9 mg.

B. TRANSVERSE VERTICAL CIRCUITS

When the ship is on any heading, its transverse vertical circuits are moving in the vertical component of the earth's field when the ship pitches. The principal circuits are the transverse frames which make up a solenoid-like structure of conductors. To determine the eddy-current field of this structure, the current was estimated by calculation and the field was measured experimentally by a model technique.

(a) Calculation of Current

A mean frame was considered to bound an area S sq. cm. equal to the mean of areas of frames 16 and 40 (see Davie Dwg. 589-H-2). The resistance R around the periphery of a mean frame is about 315 microhms. The maximum current in the frame was calculated from the following formula

$$I_p = \frac{2\pi \times 2\pi}{360} \frac{P_o}{T_p} \frac{S}{R} \times 10^{-8} H_v , \qquad (57)$$

where P_o is the maximum pitch angle in degrees, T_p is the period of pitch in seconds and H_v is vertical component of the exciting field in oersteds.

When $P_o = 8°$, $T_p = 4.5$ secs, R = 315 microhms, and S = 420,000 sq cm. (mean of areas bounded by frames 16 and 40),

$$I_p = 2\pi \times \frac{2\pi \times 8}{360} \times \frac{1}{4.5} \times \frac{420{,}000}{315 \times 10^{-8}} \times 10^{-8} H_v ,$$

$$= 2.6\ H_v \qquad (58)$$

(b) Measurement of External Field

Because of the shape of the structure, a calculation of its external field could not be made by using the formulas for solenoids of ordinary shapes. The external field was therefore determined experimentally by a model technique.

An insulated wire was wound transversely on the structure of the model shown in Figs. 11 and 12 to form a solenoid with a turn for each single frame. At the bulkheads a number of turns were close wound to represent a decreased resistance due to the large cross section. The number of turns at the bulkheads was determined by the ratio of cross section of bulkhead to frame of the model.

$$n_b = \frac{A_b}{A_f} , \qquad (59)$$

where n is number of turns, A is area of cross section and subscripts indicate bulkheads.

The field in the vicinity of the resulting solenoid was explored approximately by means of the U.S. Navy Mark 5, Model 5 magnetometer. The results are shown in Fig. 53 for the case where the current in the model solenoid is

$$i = 2.6\ H_v\ k = 2.6 \times .560 \times \frac{1}{24} = .060 \text{ amperes},$$

where $k = \frac{1}{24}$ linear scale factor of model,

and $H_v = .560$ = vertical component of exciting field.

BIBLIOGRAPHY

1. "A Calculation of the Magnetic Field Produced by the Rolling Motion of a Non-Magnetic Conducting Ship's Hull in the Earth's Field", National Research Council, Radio and Electrical Engineering Divisional Report No. ERA-195.

2. "Measurement of the Magnetic Field Disturbance Caused by a Rotating Non-Magnetic Conducting Hollow Cylinder", National Research Council, Radio and Electrical Engineering Divisional Report No. ERA-211.

3. "Eddy-Current Magnetic Field Measurements on Class AMc. 143 Aluminum-Framed Minesweeper HMCS "Cowichan", National Research Council, Radio and Electrical Engineering Divisional Report No. ERA-231.

4. "Eddy Currents in Aluminum-Framed Minesweepers", Admiralty Research Laboratories Report ARL/R1/Maths 4.27.

5. "Servomechanisms", Chapter 8, Brown and Campbell, John Wiley and Sons.

6. "Electrical Resistance Measurements of Riveted Joints in Aluminum Plates as used in the Class AMc. 143 Minesweeper", National Research Council, Radio and Electrical Engineering Divisional Report No. ERB-285.

7. "A Saturated Core Recording Magnetometer", D.C. Rose and J.N. Bloom, Canadian Journal of Research A-28, pp. 153-156.

8. "Calibration of and Errors in Magnetometers of the G.E. Type", U.S. Bureau of Ordnance - NAVORD OD7938.

9. "Static and Dynamic Electricity", W.R. Smythe, McGraw-Hill Book Co.

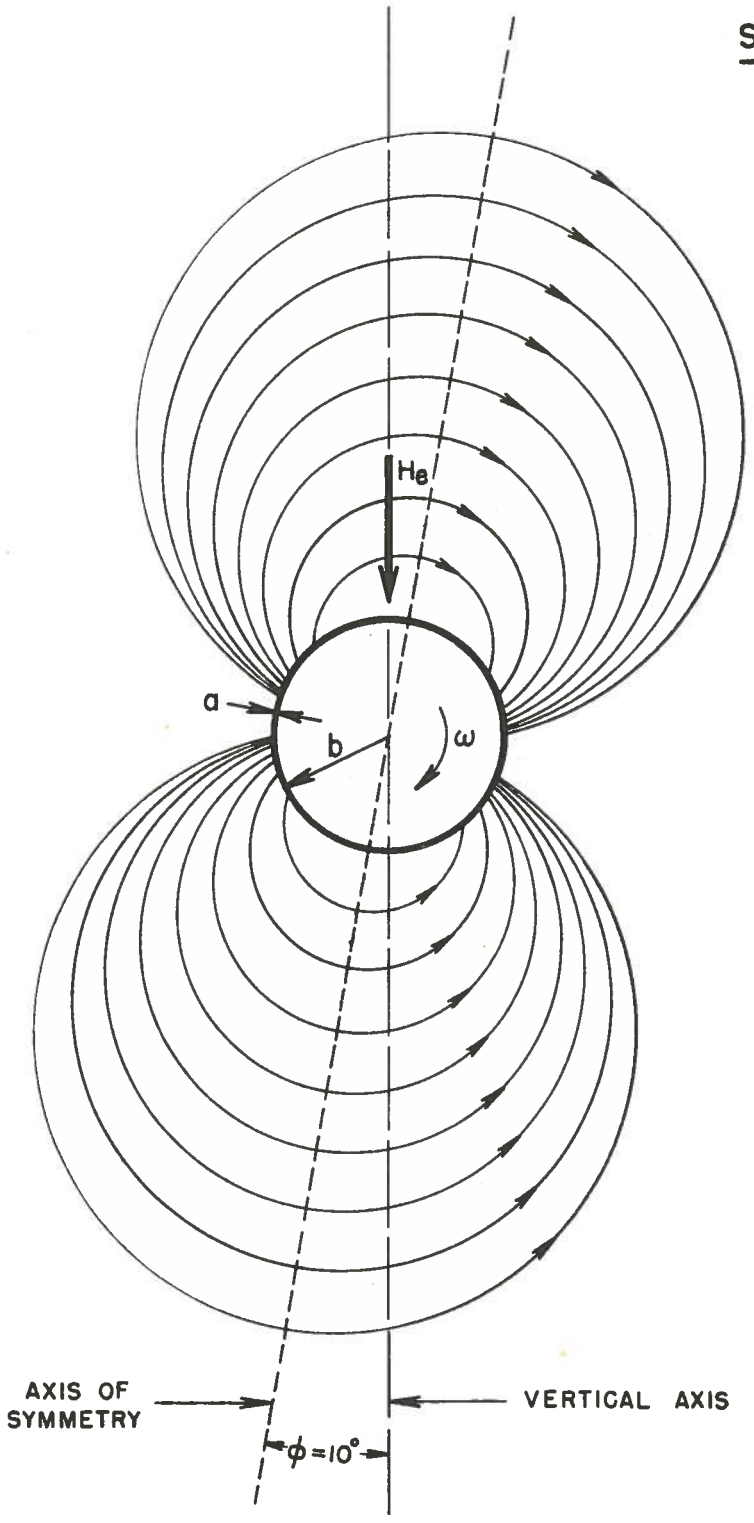

FLUX LINES CREATED BY A THIN CYLINDER ROTATING IN A UNIFORM MAGNETIC FIELD

FIG. 1

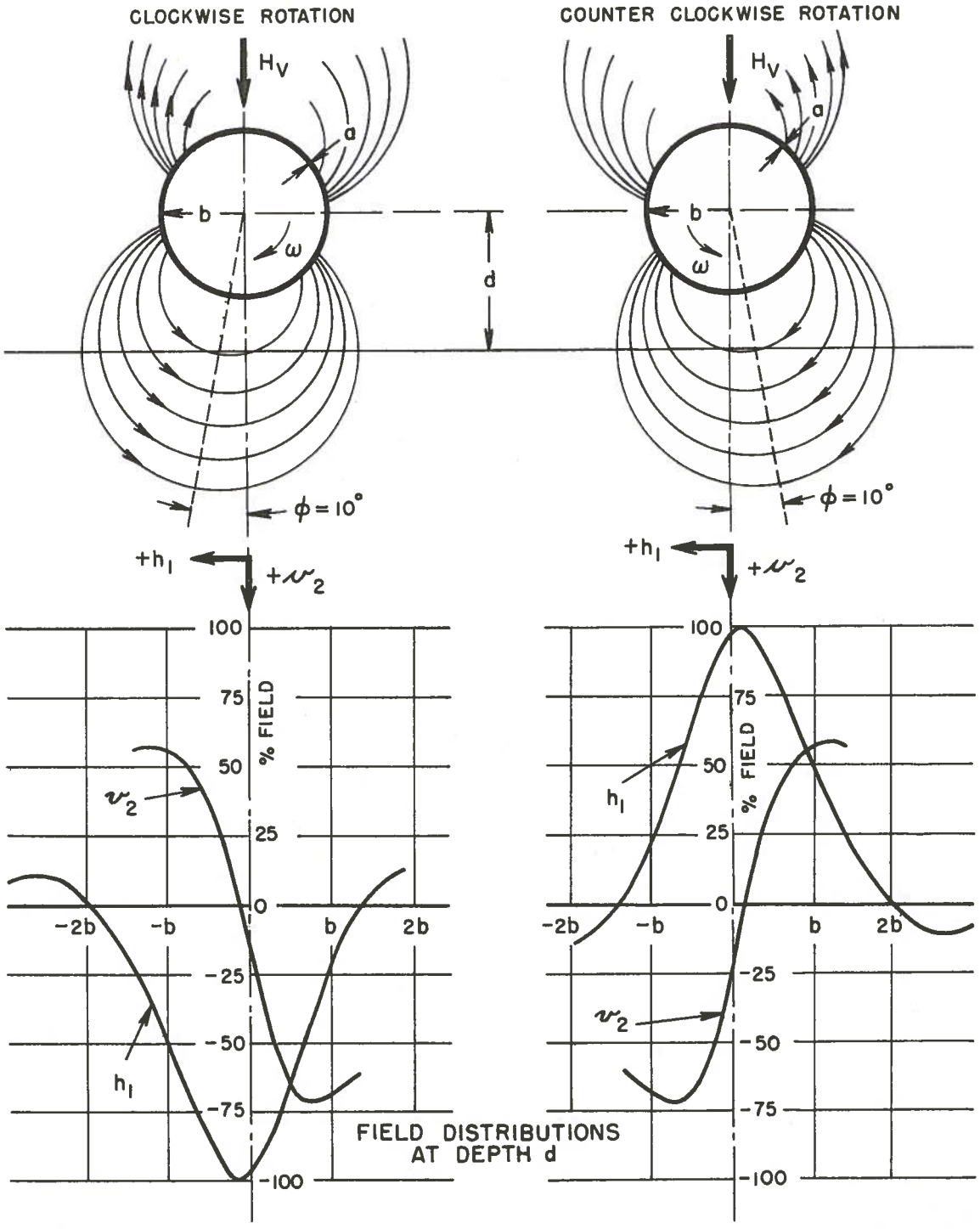
CLOCKWISE ROTATION
COUNTER CLOCKWISE ROTATION
H_V
a
b
ω
d
$\phi = 10°$
$+h_1$
$+v_2$
100
75
50
25
0
-25
-50
-75
-100
% FIELD
v_2
h_1
-2b
-b
b
2b
FIELD DISTRIBUTIONS
AT DEPTH d

SECRET

FIG. 2

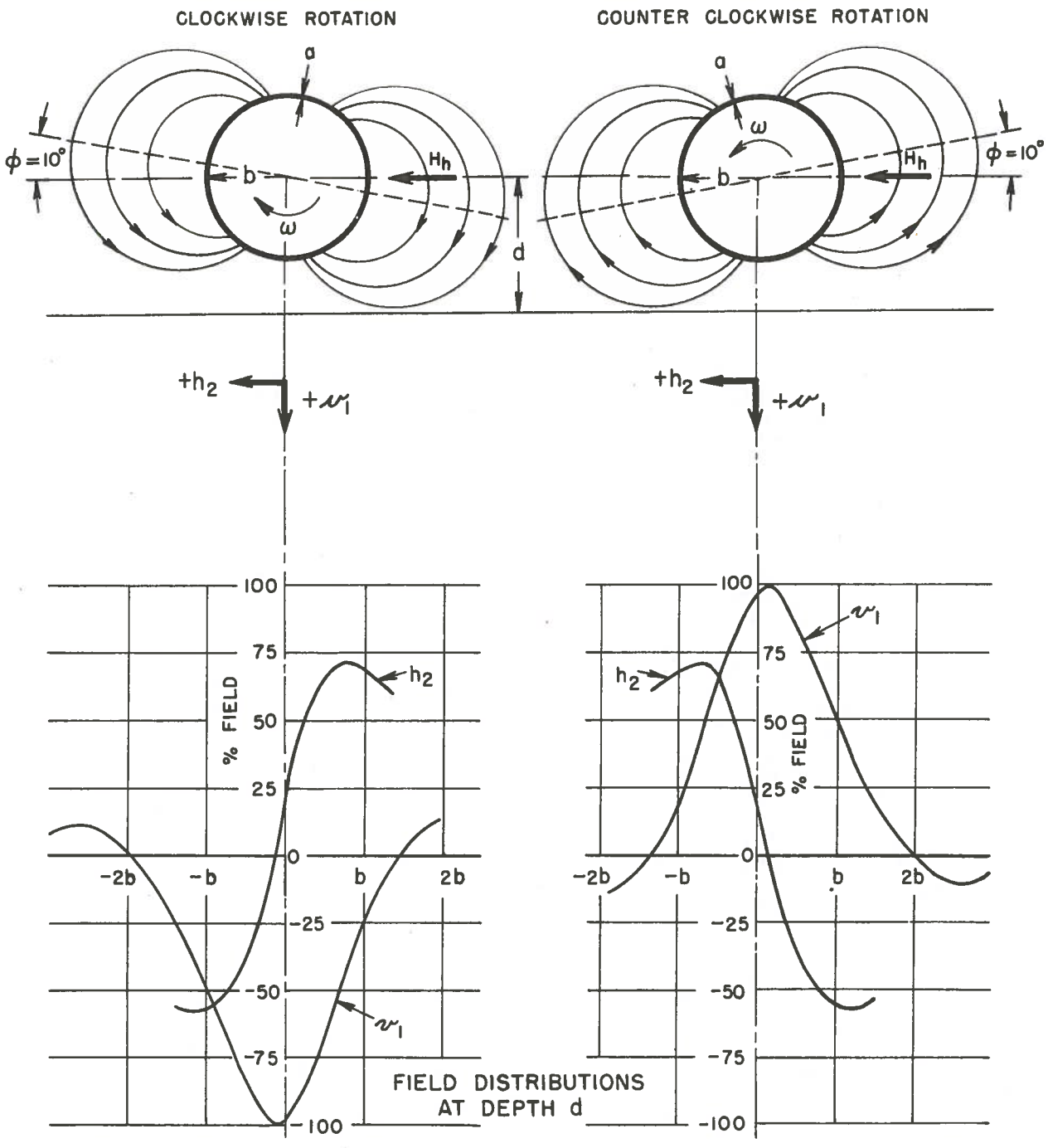
CLOCKWISE ROTATION
COUNTER CLOCKWISE ROTATION
a
b
ω
Hh
ϕ=10°
d
+h2
+ν1
100
75
50
25
0
-25
-50
-75
-100
-2b
-b
b
2b
% FIELD
h2
ν1
FIELD DISTRIBUTIONS
AT DEPTH d

SECRET

FIG. 3

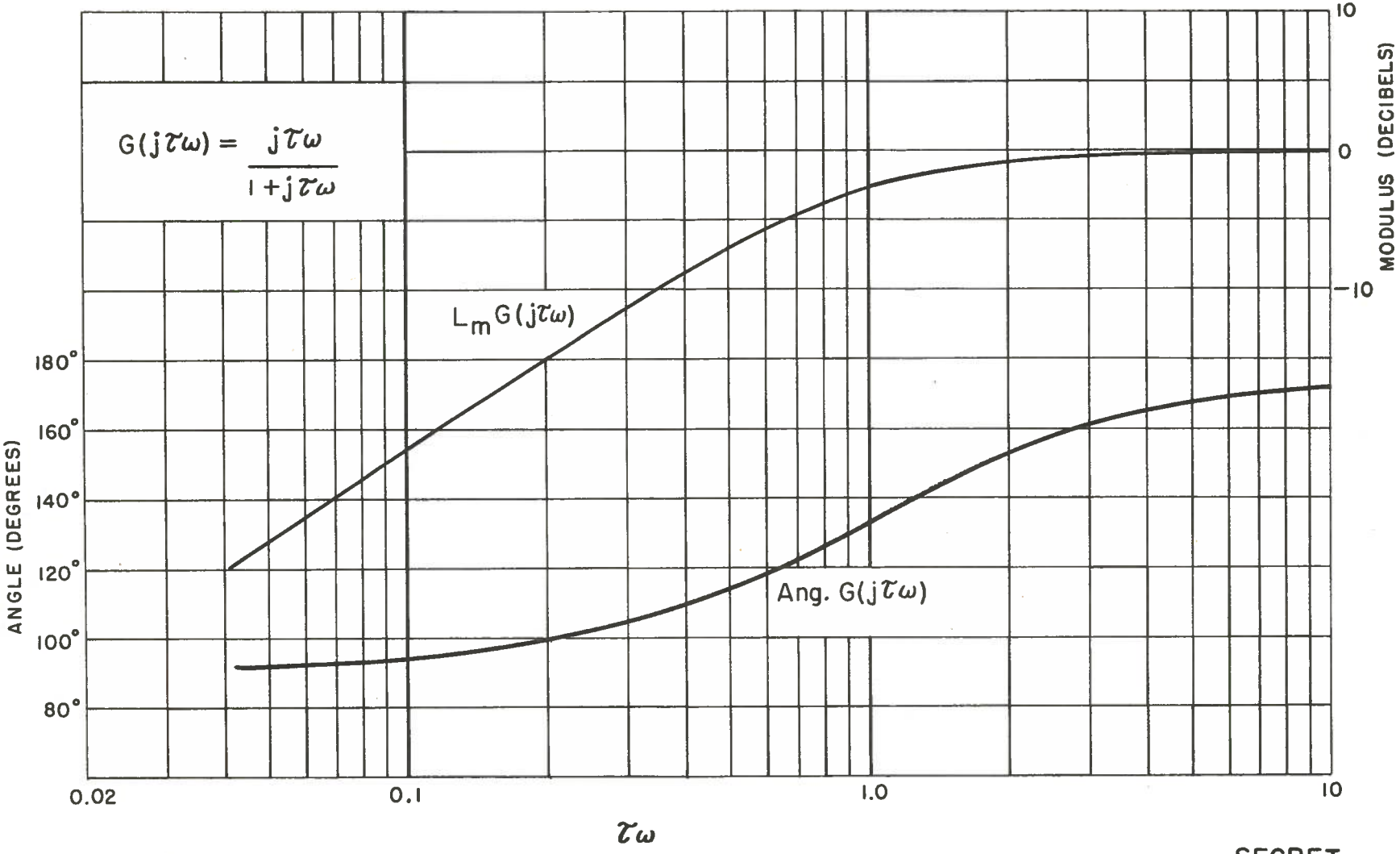
$G(j\tau\omega) = \frac{j\tau\omega}{1+j\tau\omega}$
$L_m G(j\tau\omega)$
Ang. $G(j\tau\omega)$
ANGLE (DEGREES)
180°
160°
140°
120°
100°
80°
MODULUS (DECIBELS)
10
0
−10
0.02
0.1
1.0
10
$\tau\omega$

SECRET

FIG. 4

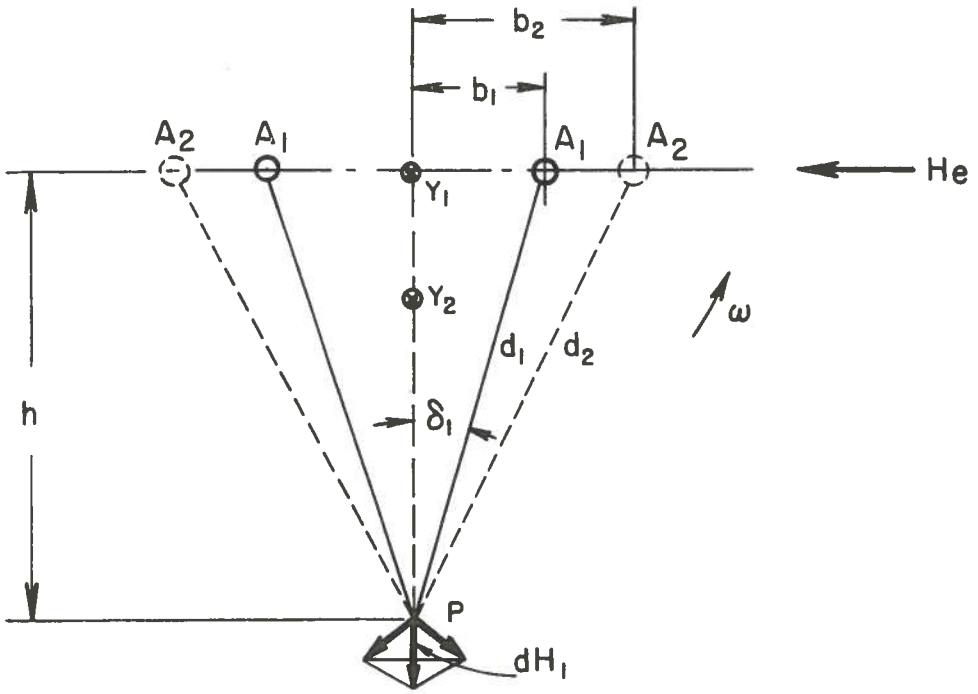

FIG. 5

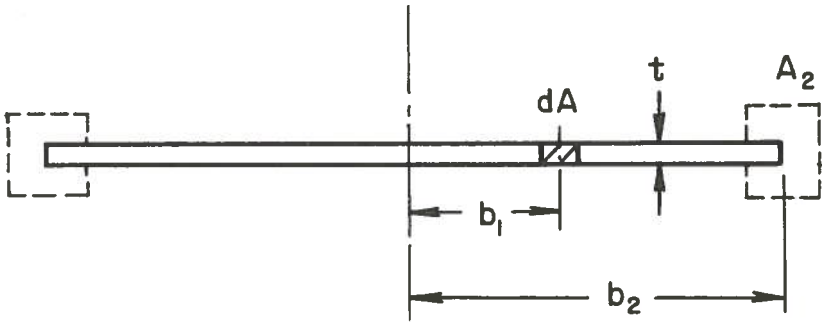

FIG. 6

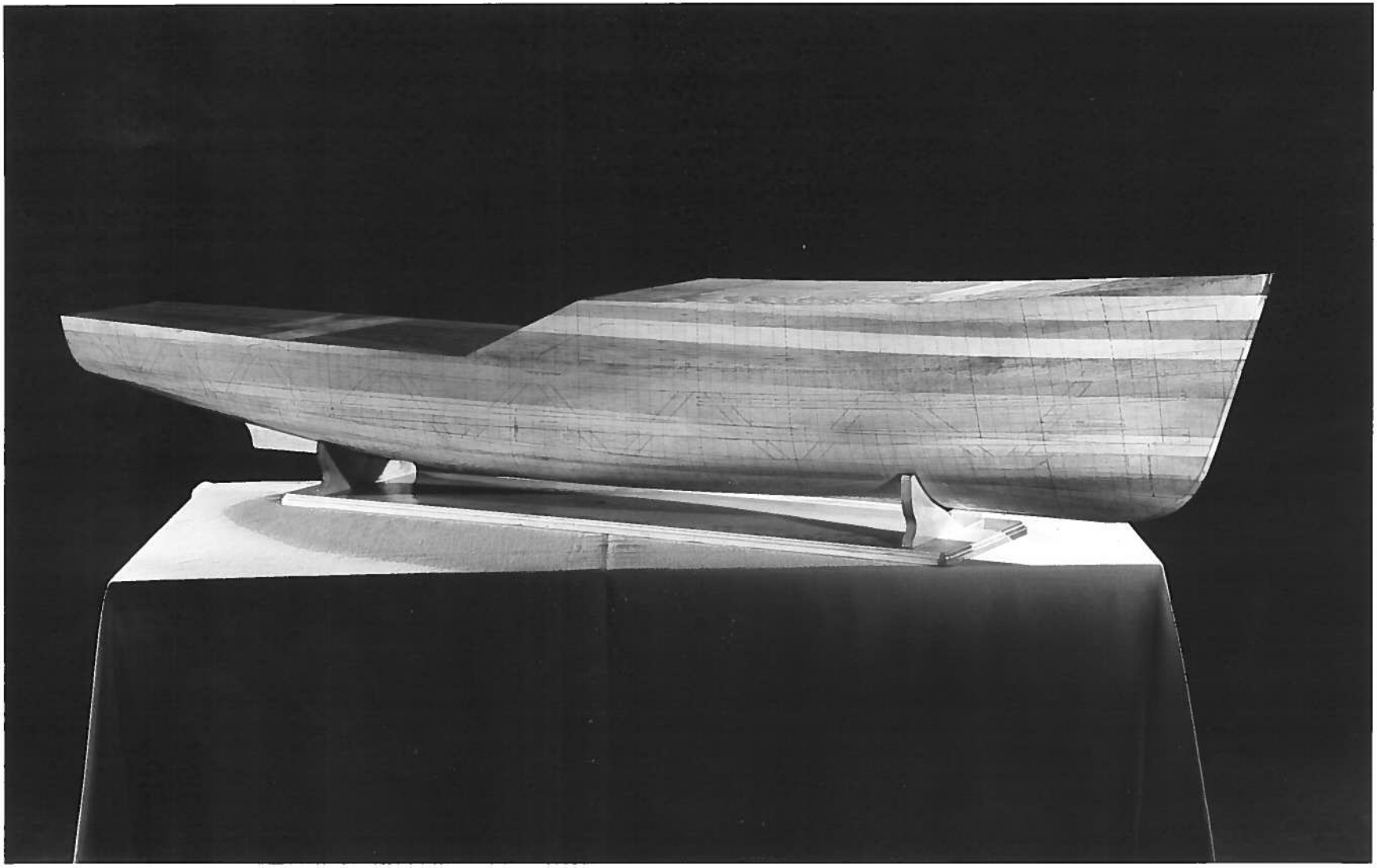

SECRET

FIG. 7
STARBOARD VIEW OF WOODEN MODEL

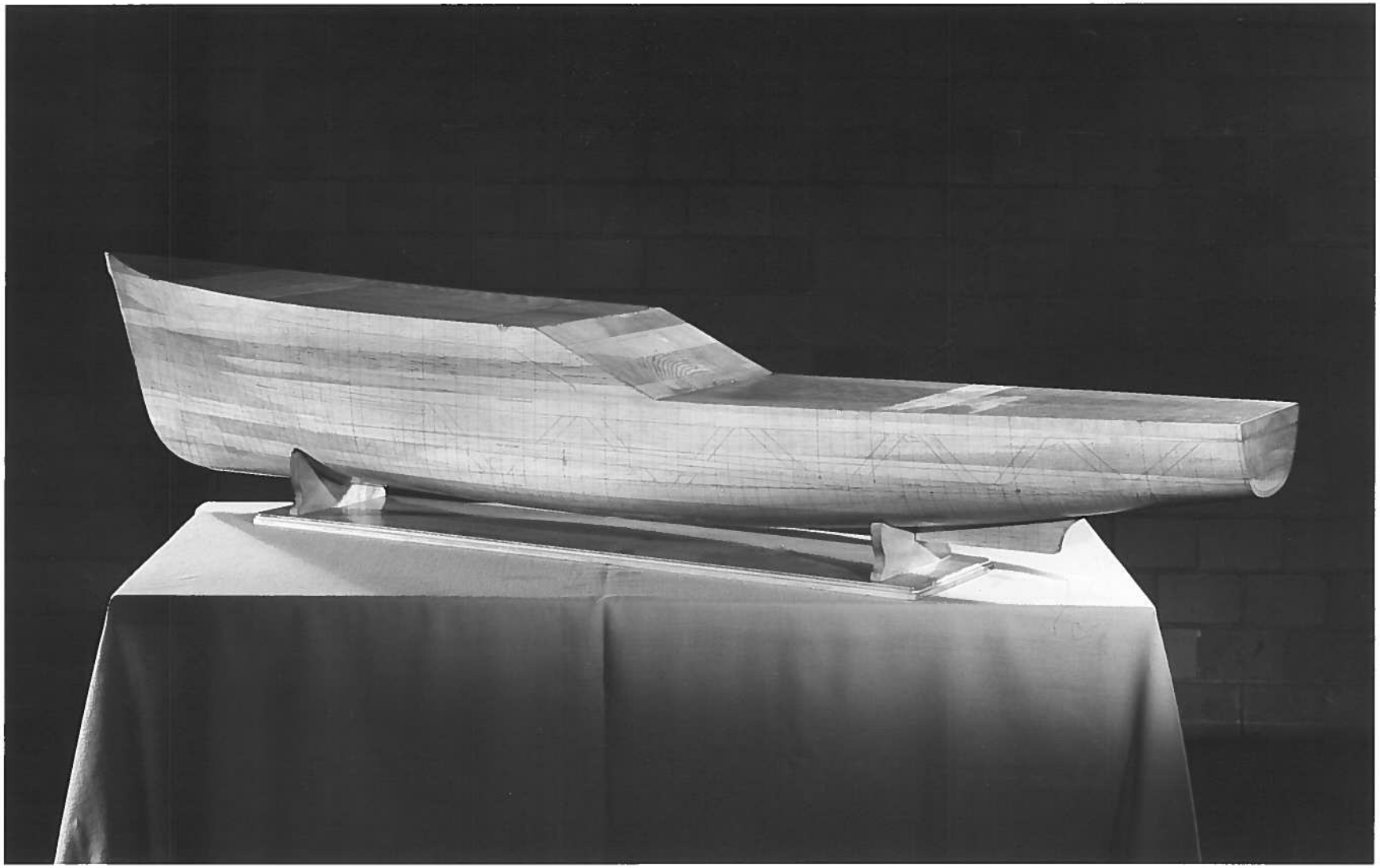

SECRET

FIG. 8
PORT VIEW OF WOODEN MODEL

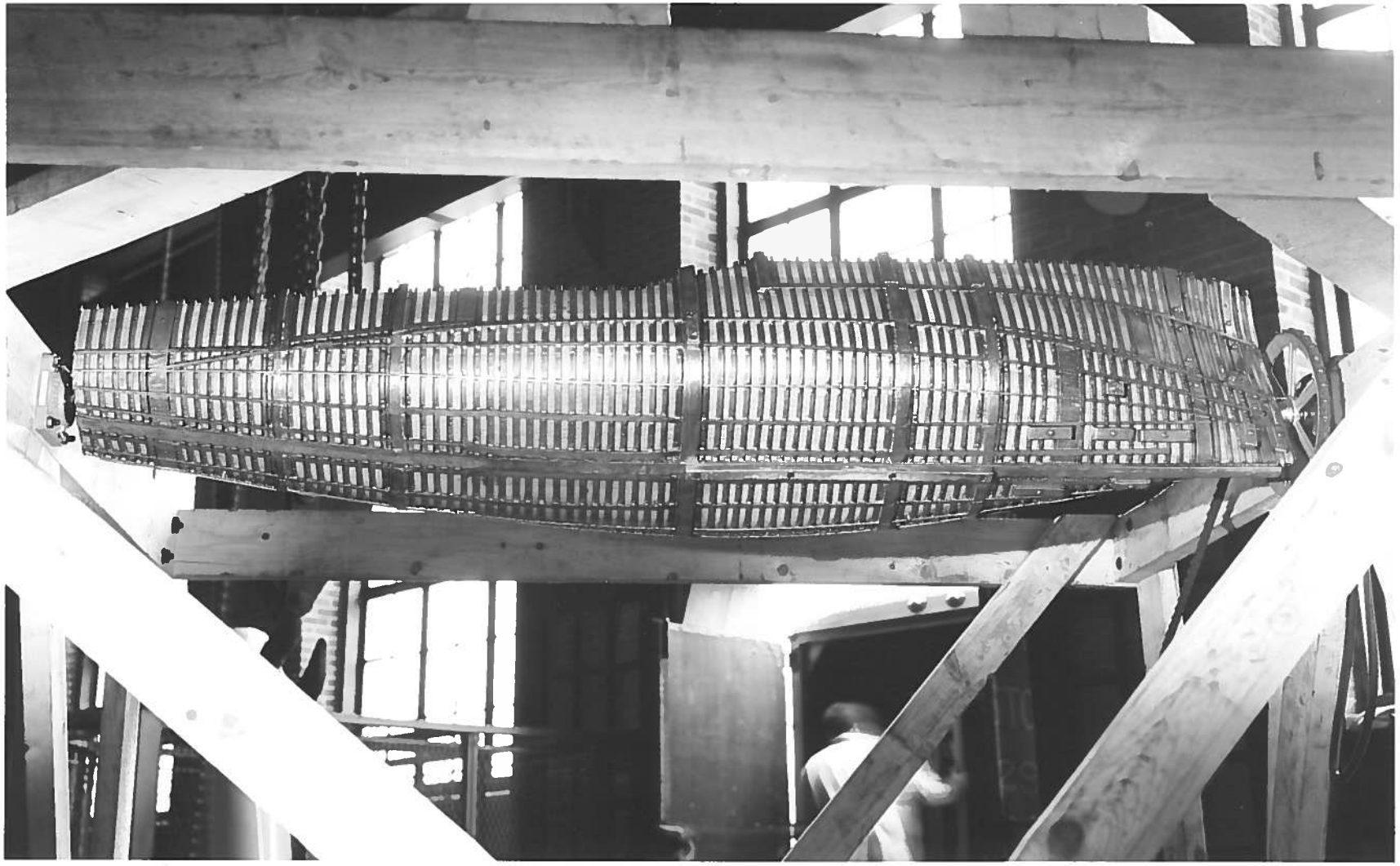

FIG. 9
BOTTOM VIEW OF STAGE 1 FRAMEWORK

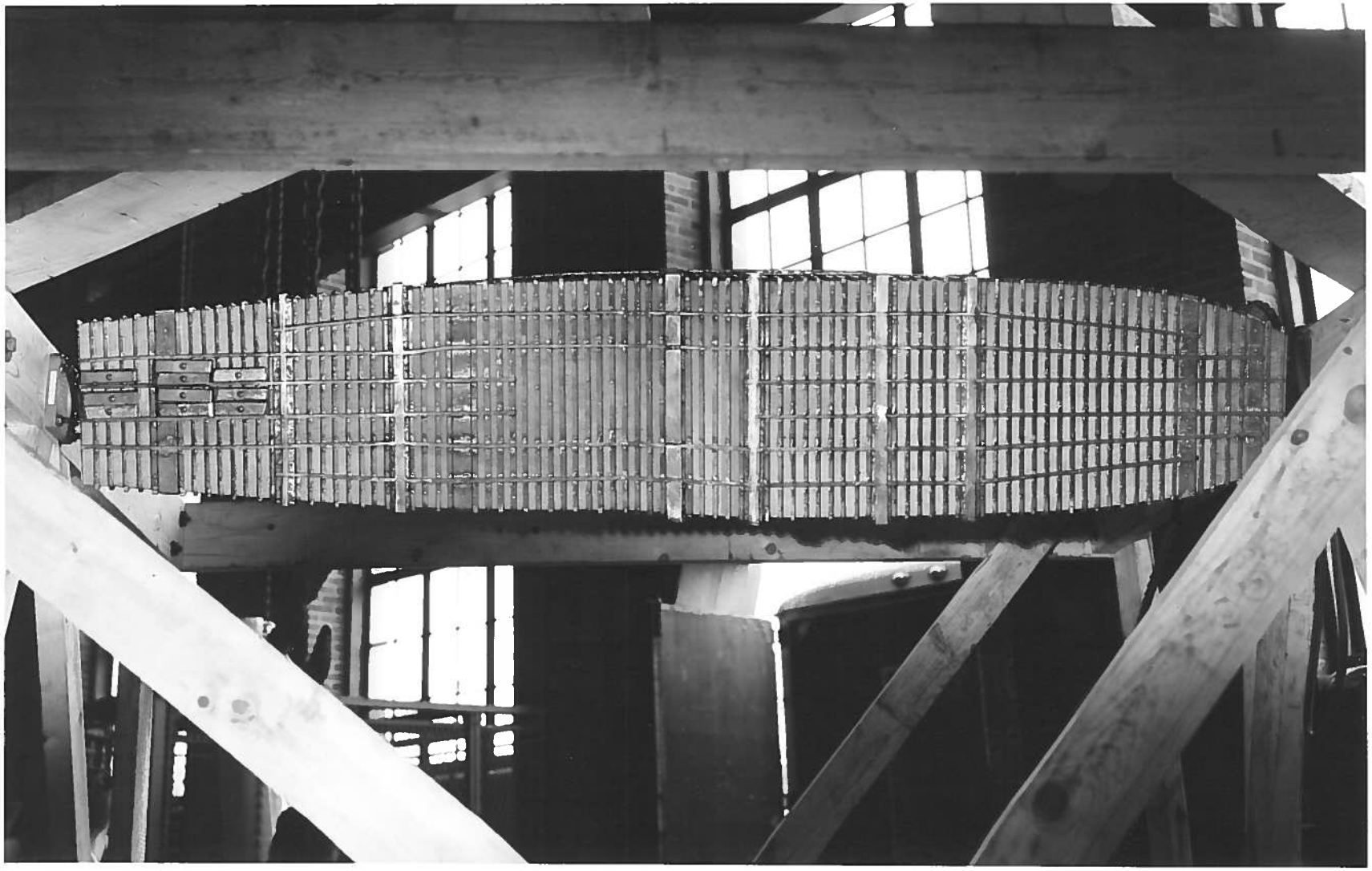

SECRET

FIG. 10
TOP VIEW OF STAGE 1 FRAMEWORK

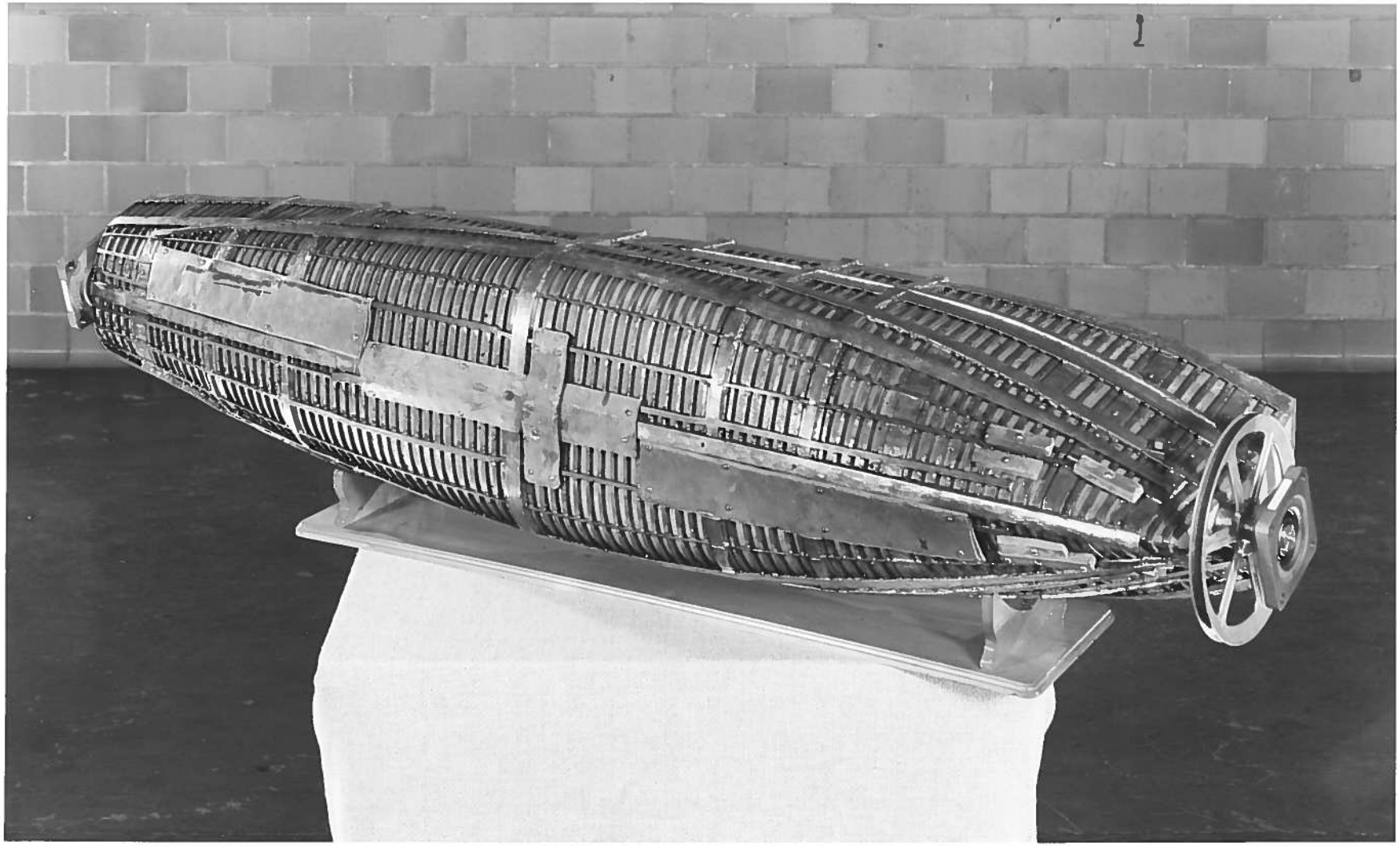

SECRET

FIG. II
BOTTOM VIEW OF STAGE 3 FRAMEWORK

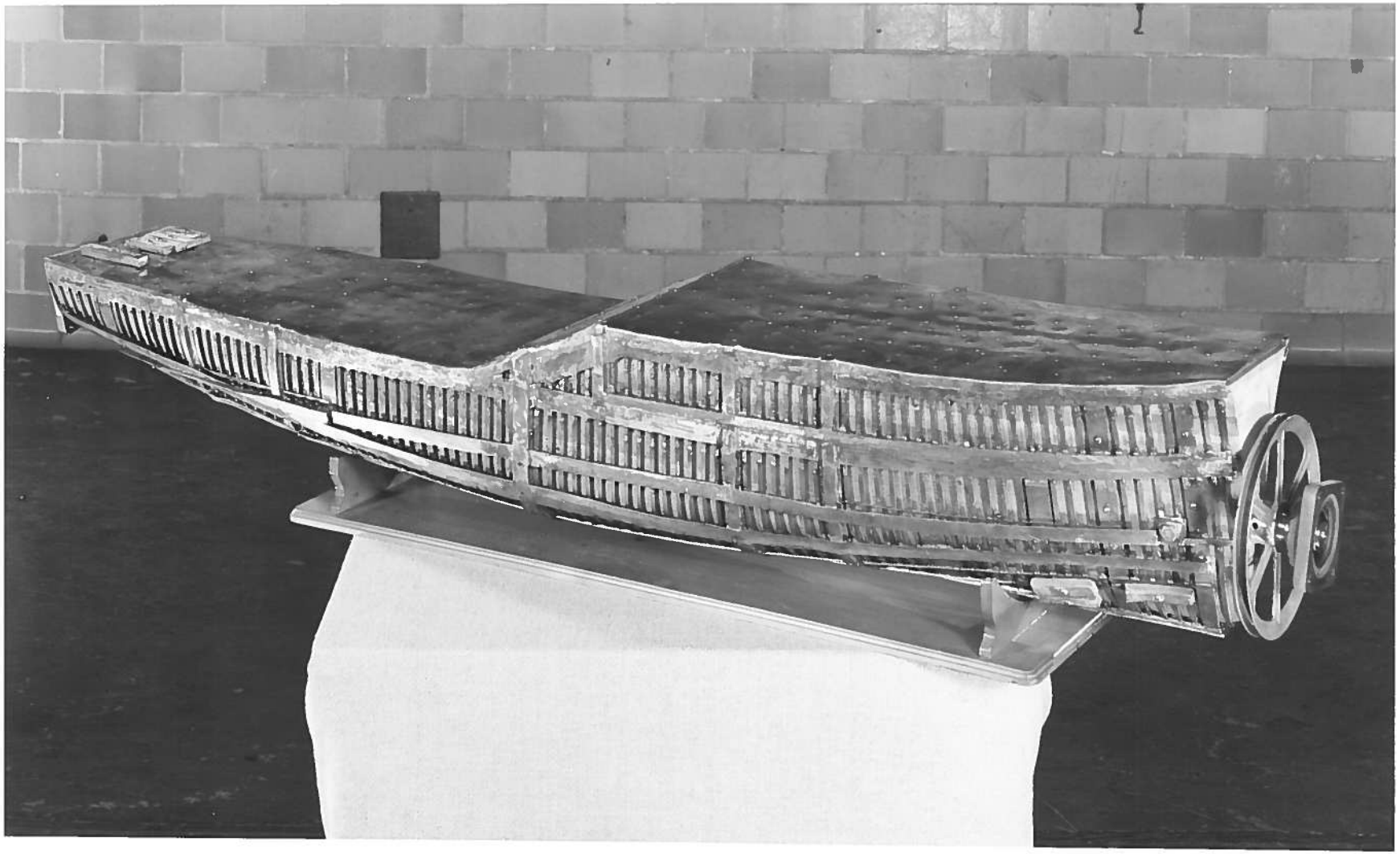

SECRET

FIG. 12
TOP VIEW OF STAGE 3 FRAMEWORK

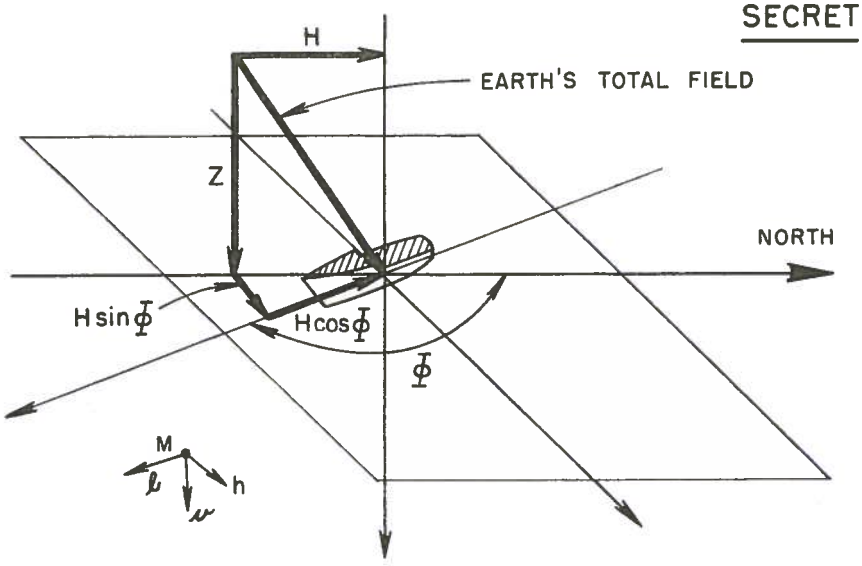

FIG. 13

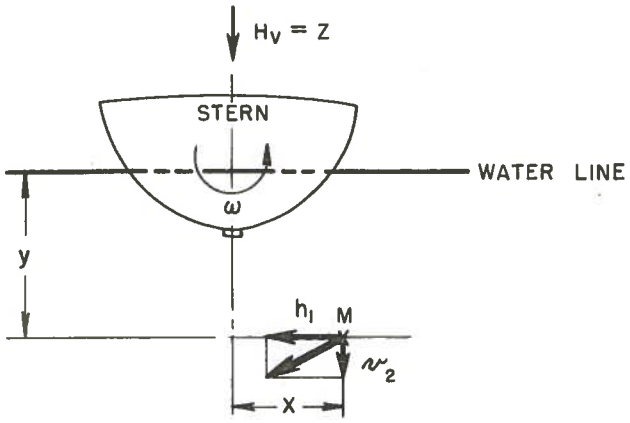

FIG. 14

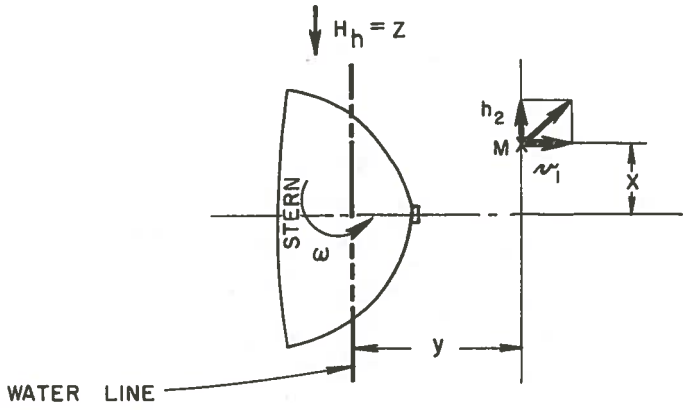

FIG. 15

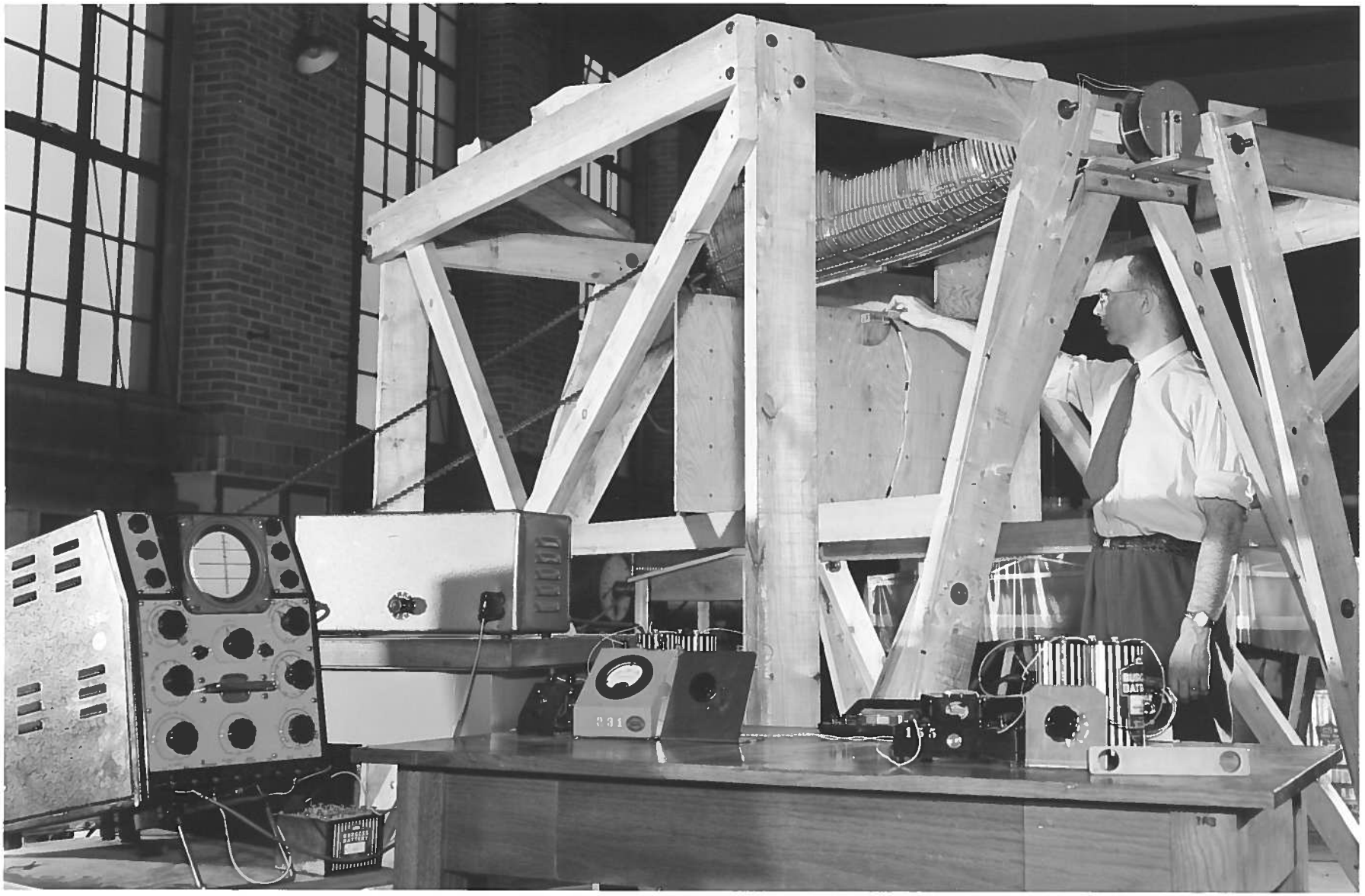

FIG. 16
APPARATUS USED FOR MEASUREMENT OF EDDY-CURRENT FIELDS

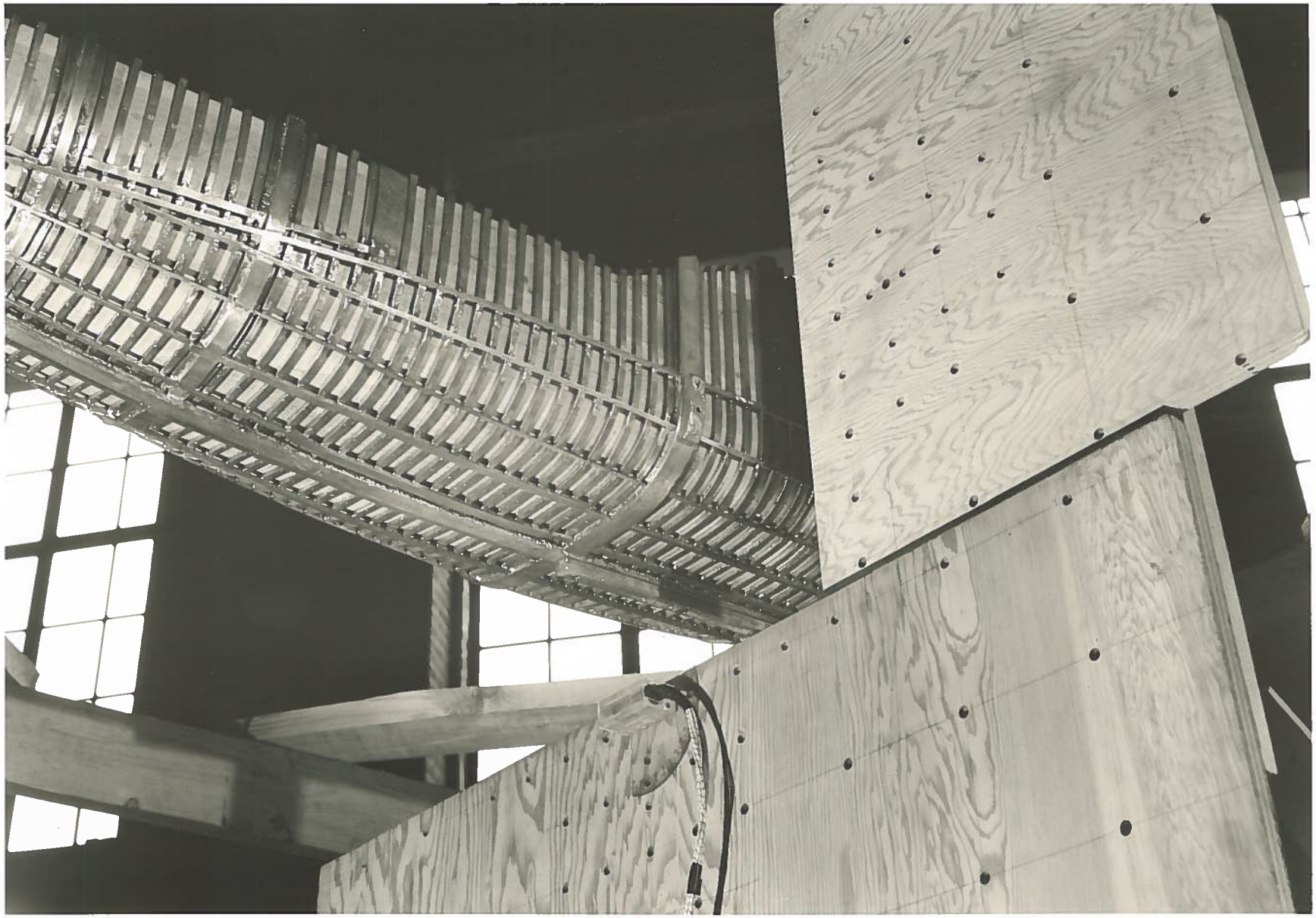

FIG. 17
MAGNETOMETER DETECTING ELEMENT IN POSITION

SECRET

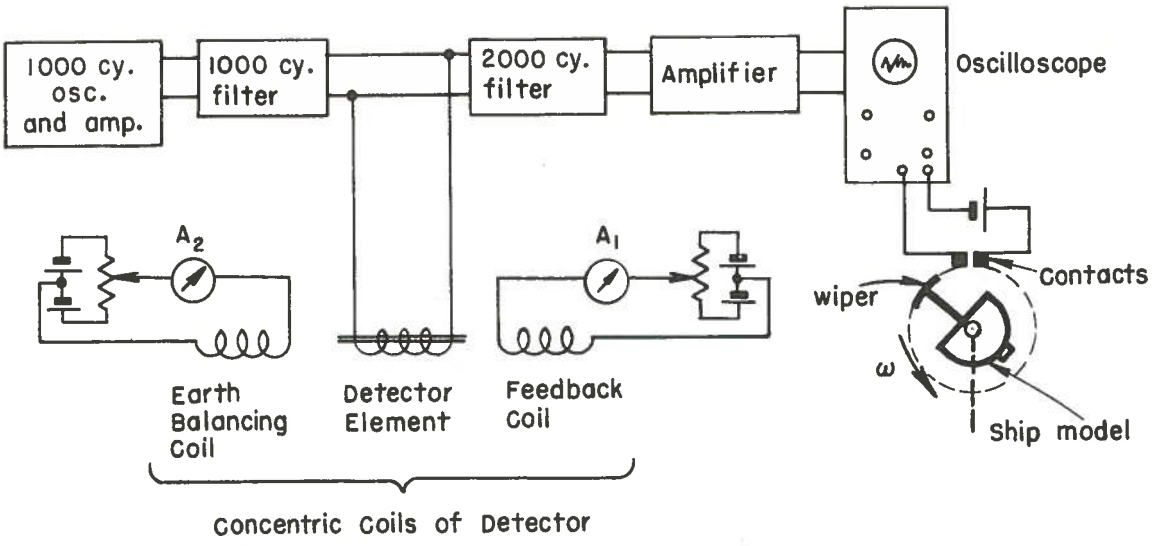

BLOCK DIAGRAM OF EDDY-CURRENT FIELD MAGNETOMETER

FIG. 18

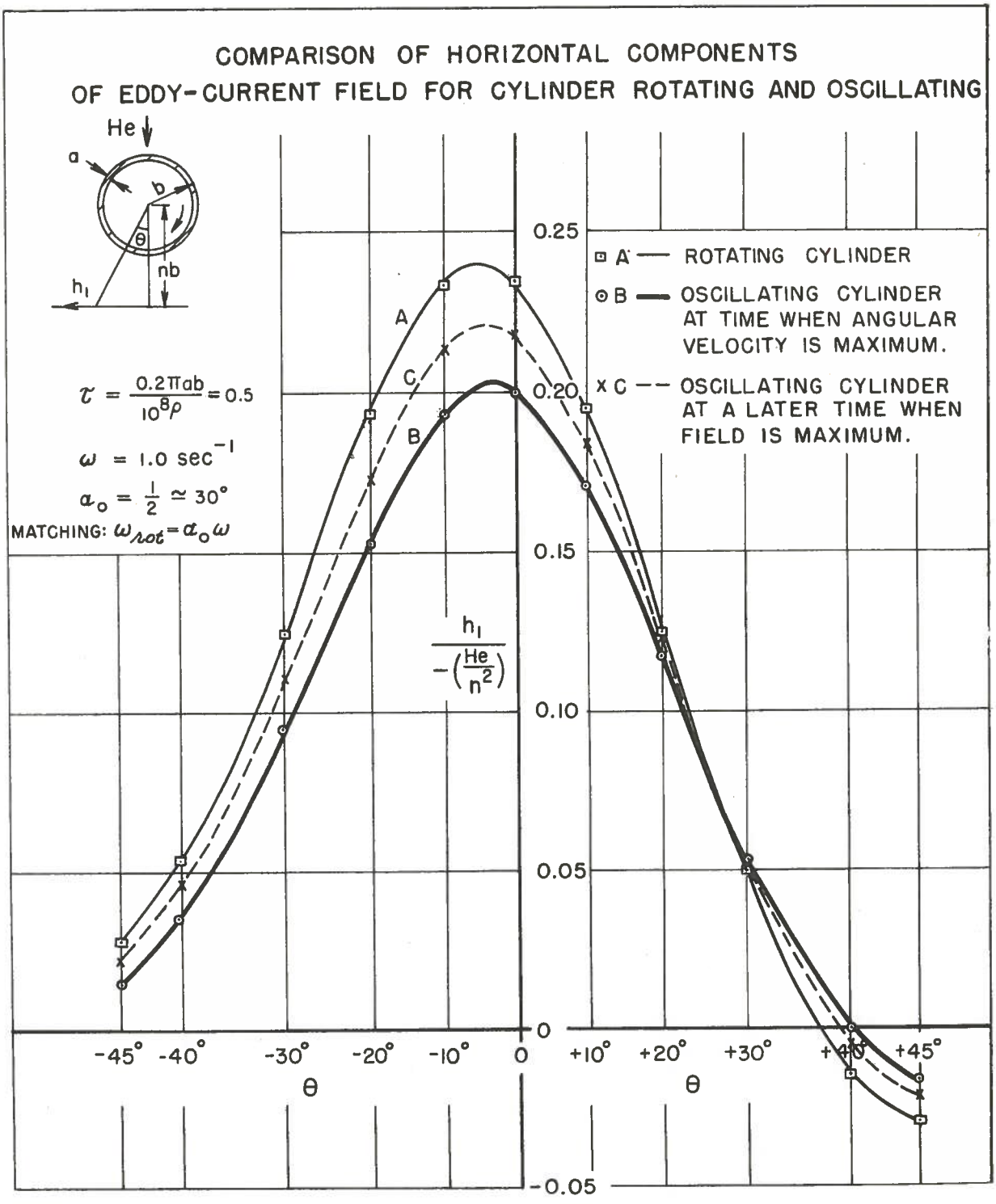

SECRET

FIG. 19

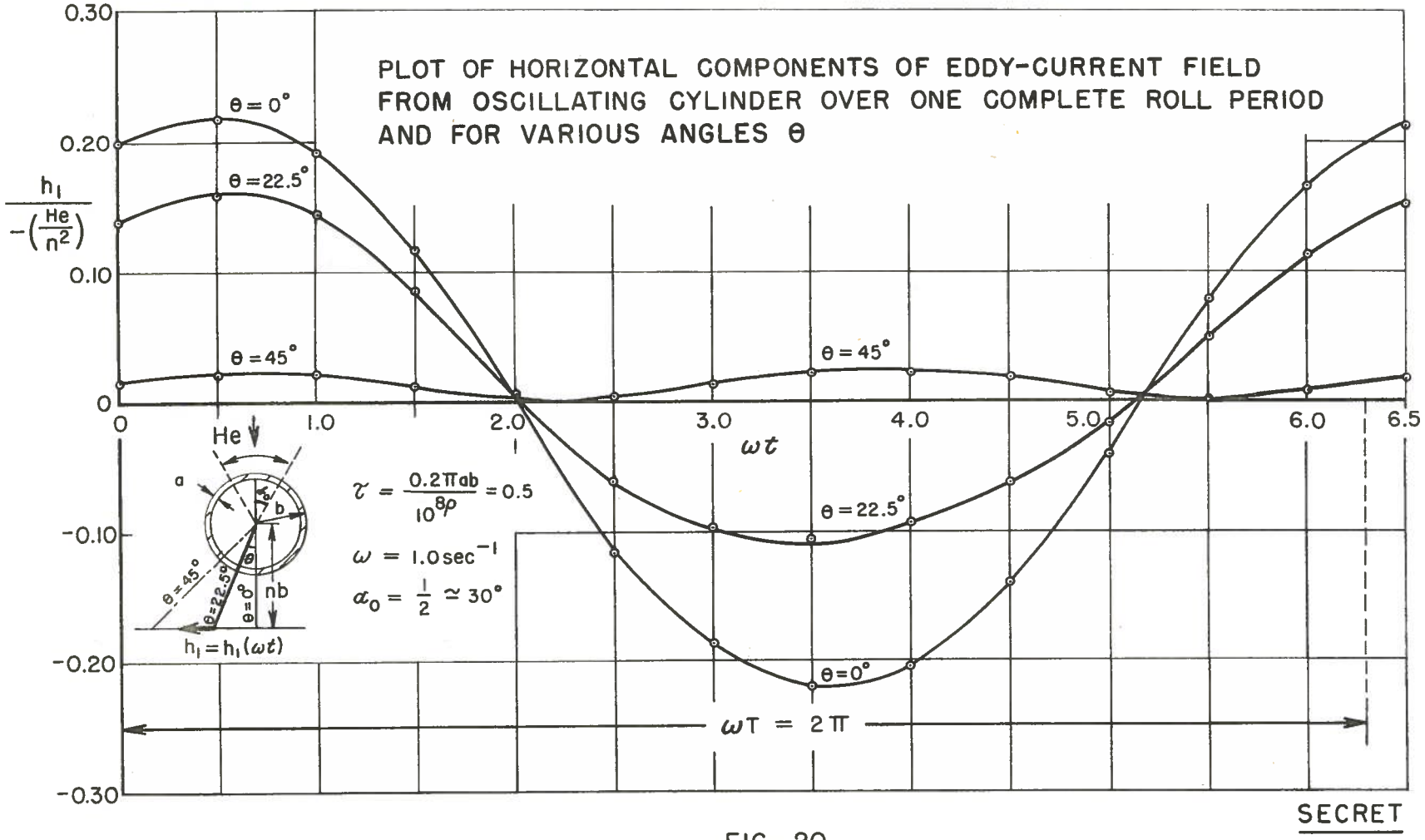
PLOT OF HORIZONTAL COMPONENTS OF EDDY-CURRENT FIELD
FROM OSCILLATING CYLINDER OVER ONE COMPLETE ROLL PERIOD
AND FOR VARIOUS ANGLES θ
$\frac{h_1}{-\left(\frac{He}{n^2}\right)}$
0.30
0.20
0.10
0
-0.10
-0.20
-0.30
θ = 0°
θ = 22.5°
θ = 45°
0
1.0
2.0
3.0
4.0
5.0
6.0
6.5
ωt
He
a
b
nb
θ
$\tau = \frac{0.2\pi ab}{10^8 \rho} = 0.5$
$\omega = 1.0 \text{ sec}^{-1}$
$\alpha_0 = \frac{1}{2} \simeq 30°$
$h_1 = h_1(\omega t)$
$\omega T = 2\pi$
SECRET

FIG. 20

SECRET

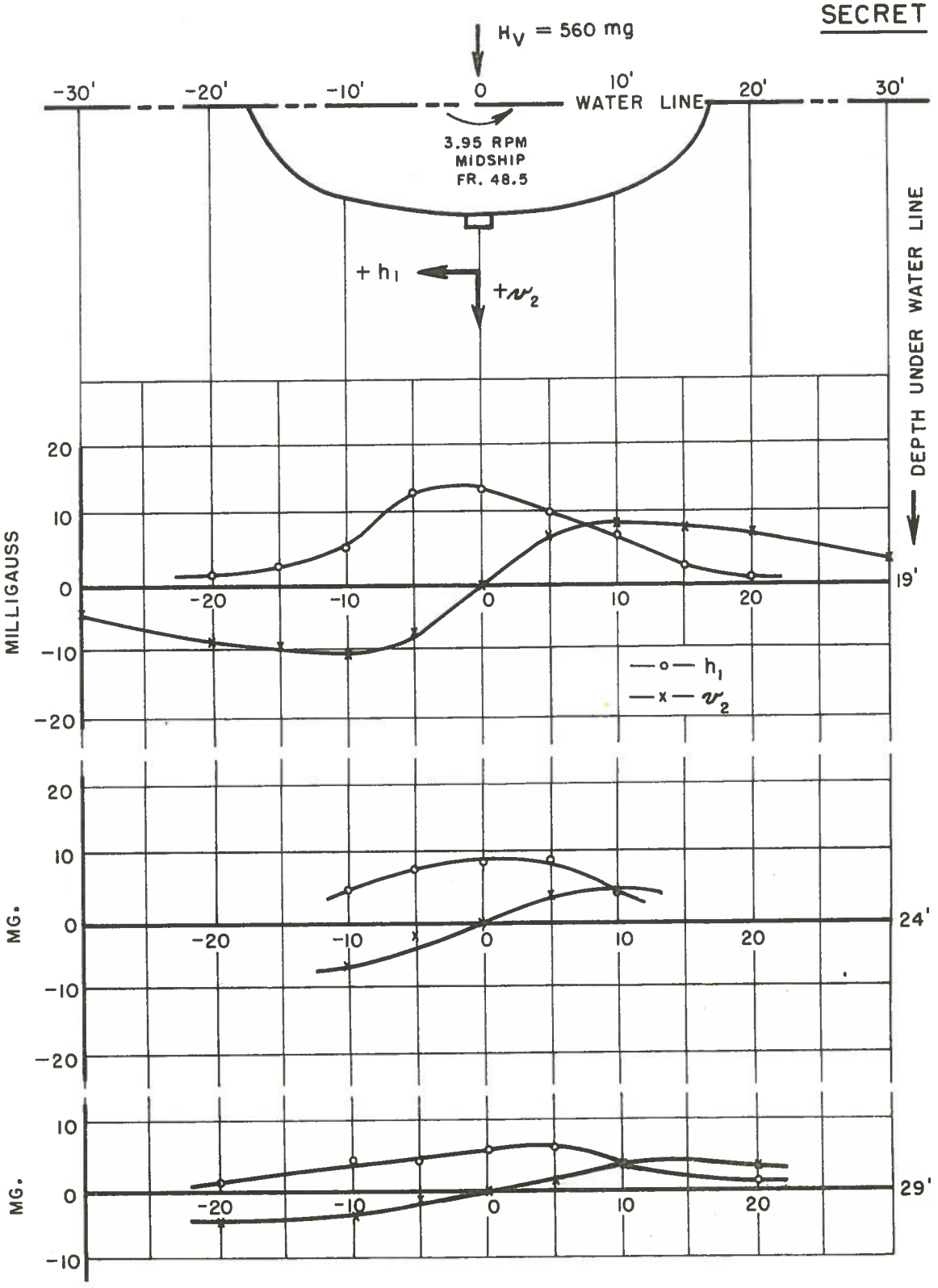

MINIMUM STRUCTURE (STAGE I)

FIG. 21

SECRET

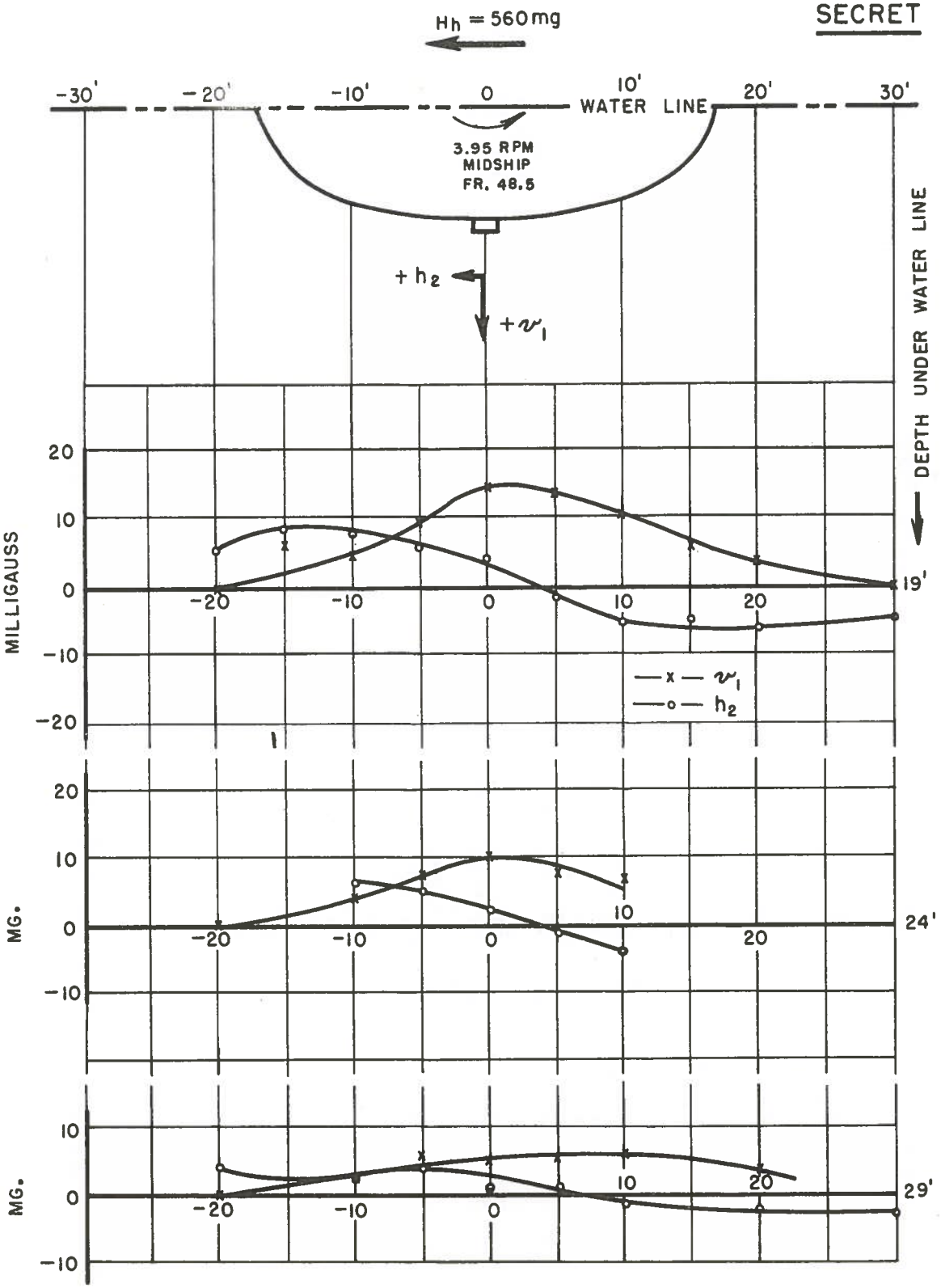

MINIMUM STRUCTURE (STAGE I)

FIG. 22

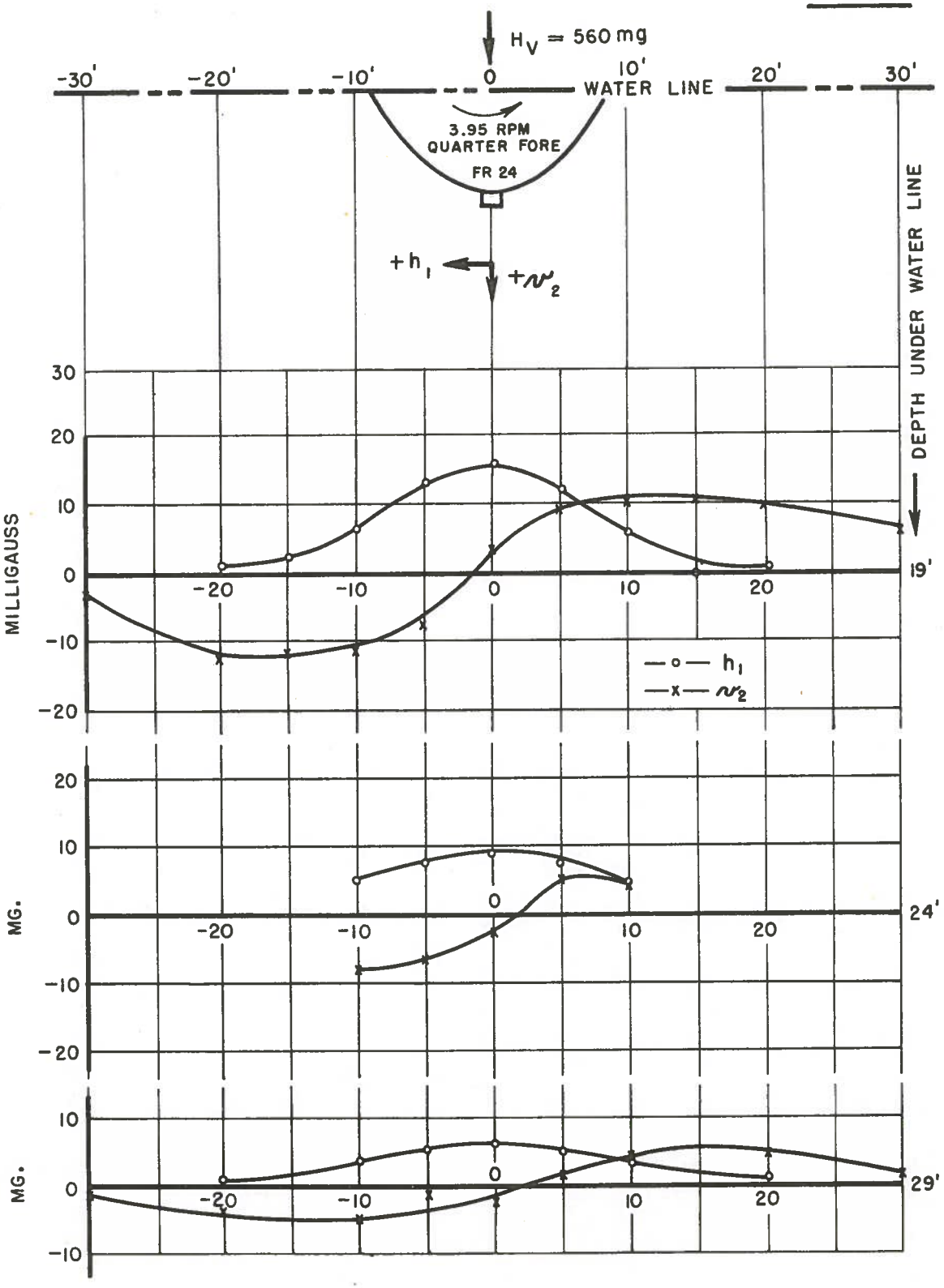

MINIMUM STRUCTURE (STAGE 1)

FIG. 23

SECRET

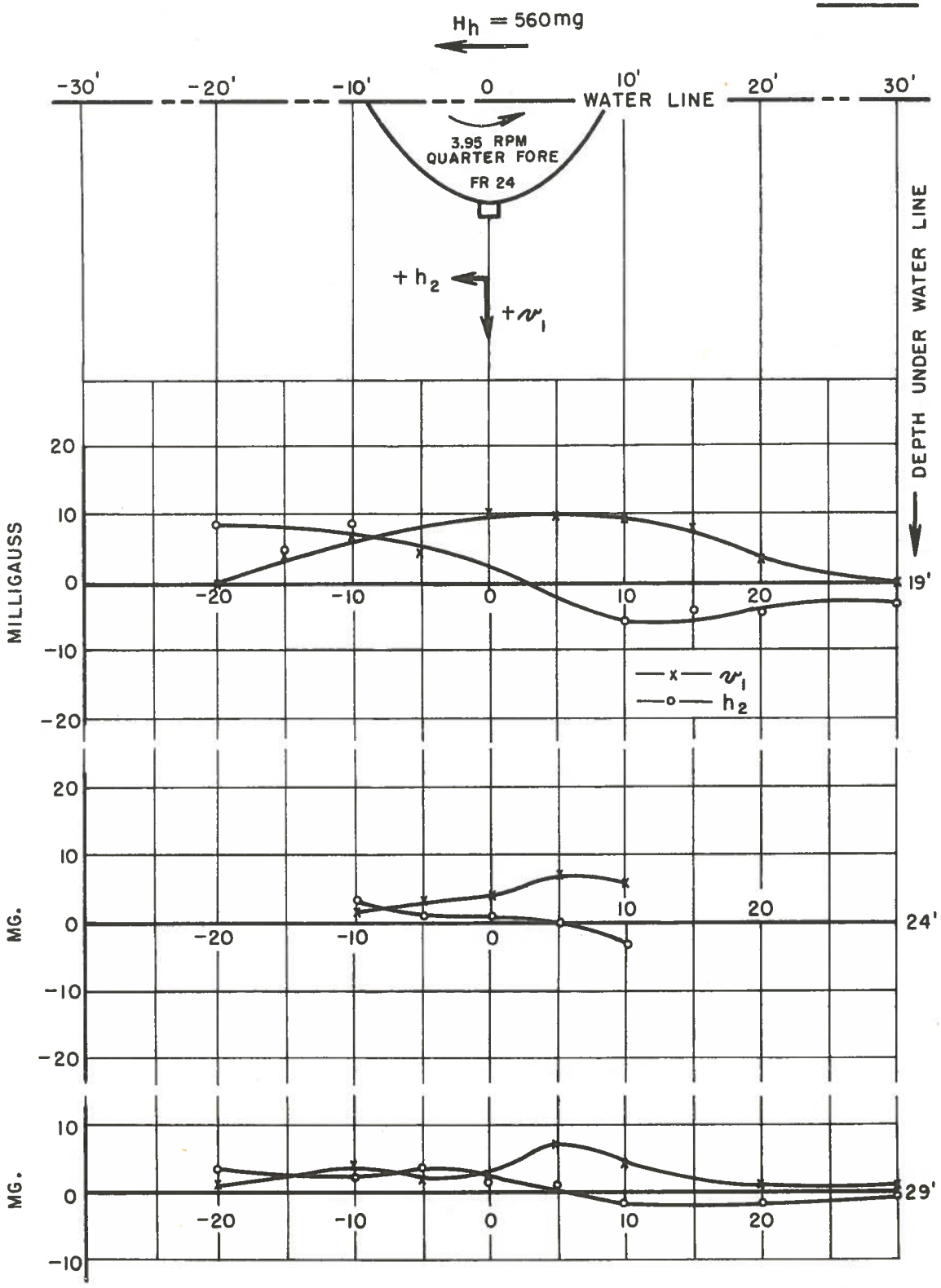

MINIMUM STRUCTURE (STAGE 1)

FIG. 24

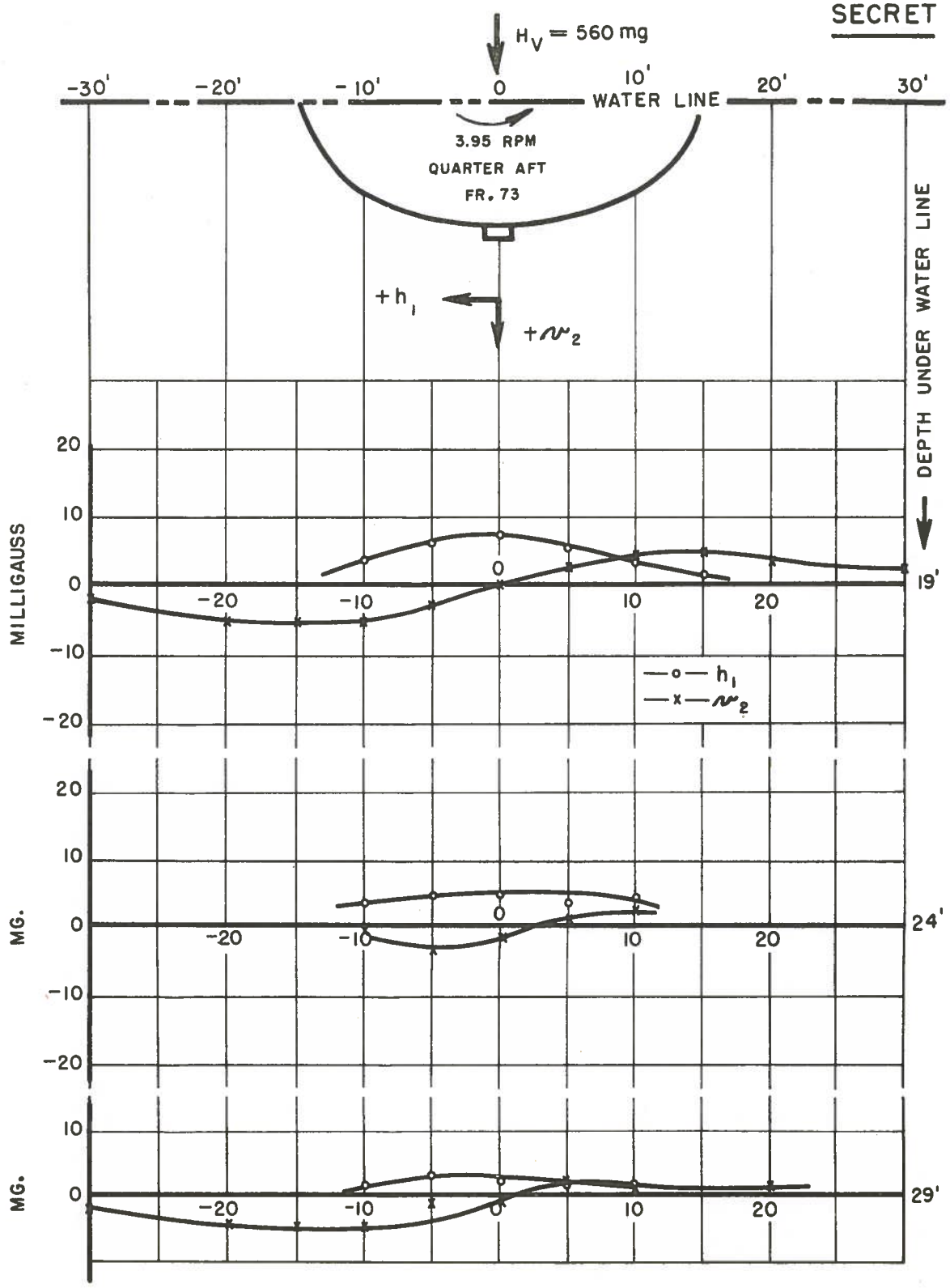

MINIMUM STRUCTURE (STAGE 1)

FIG. 25

SECRET

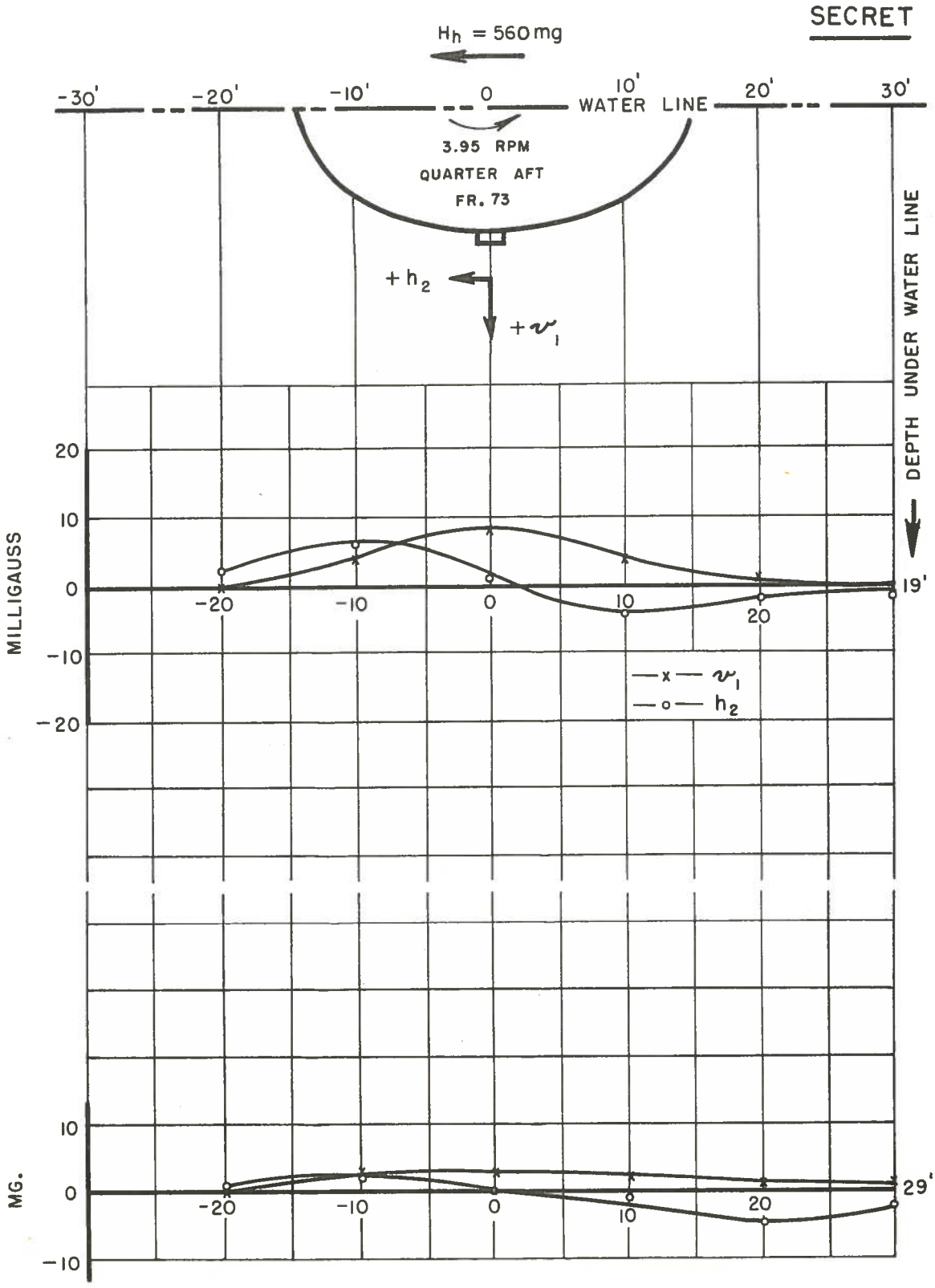

MINIMUM STRUCTURE (STAGE I)

FIG. 26

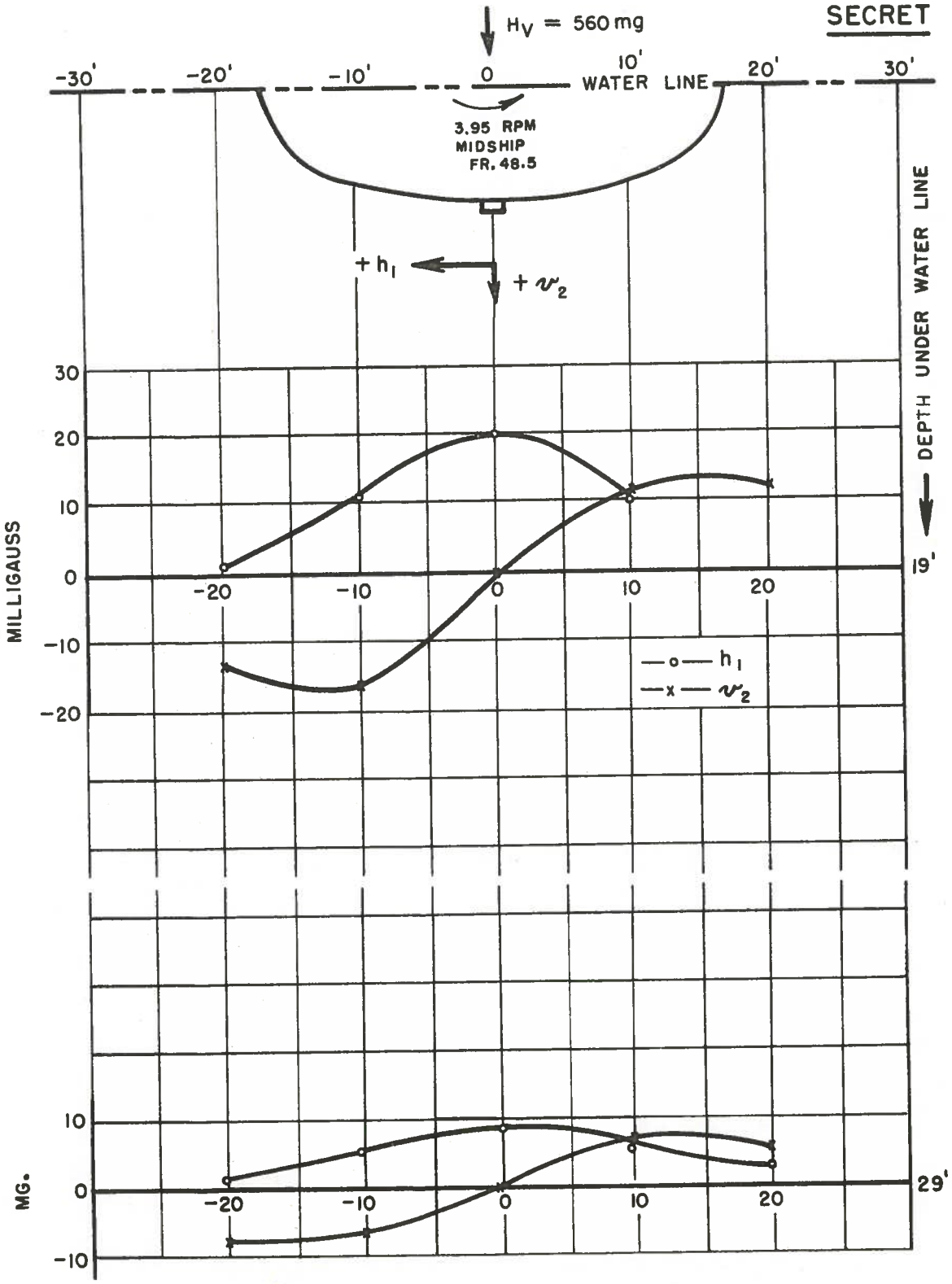

INTERMEDIATE STRUCTURE (STAGE 2)

FIG. 27

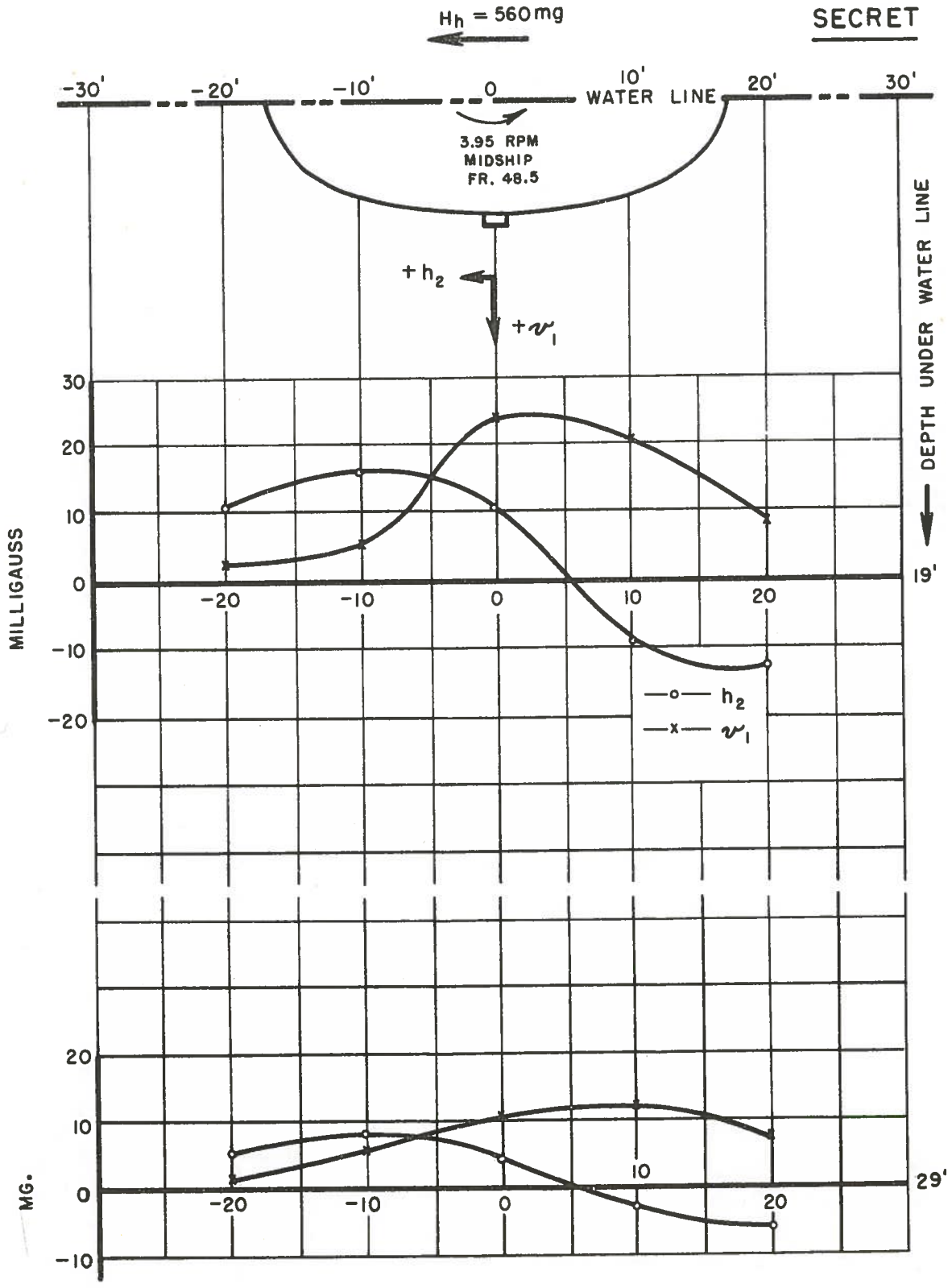

INTERMEDIATE STRUCTURE (STAGE 2)

FIG. 28

SECRET

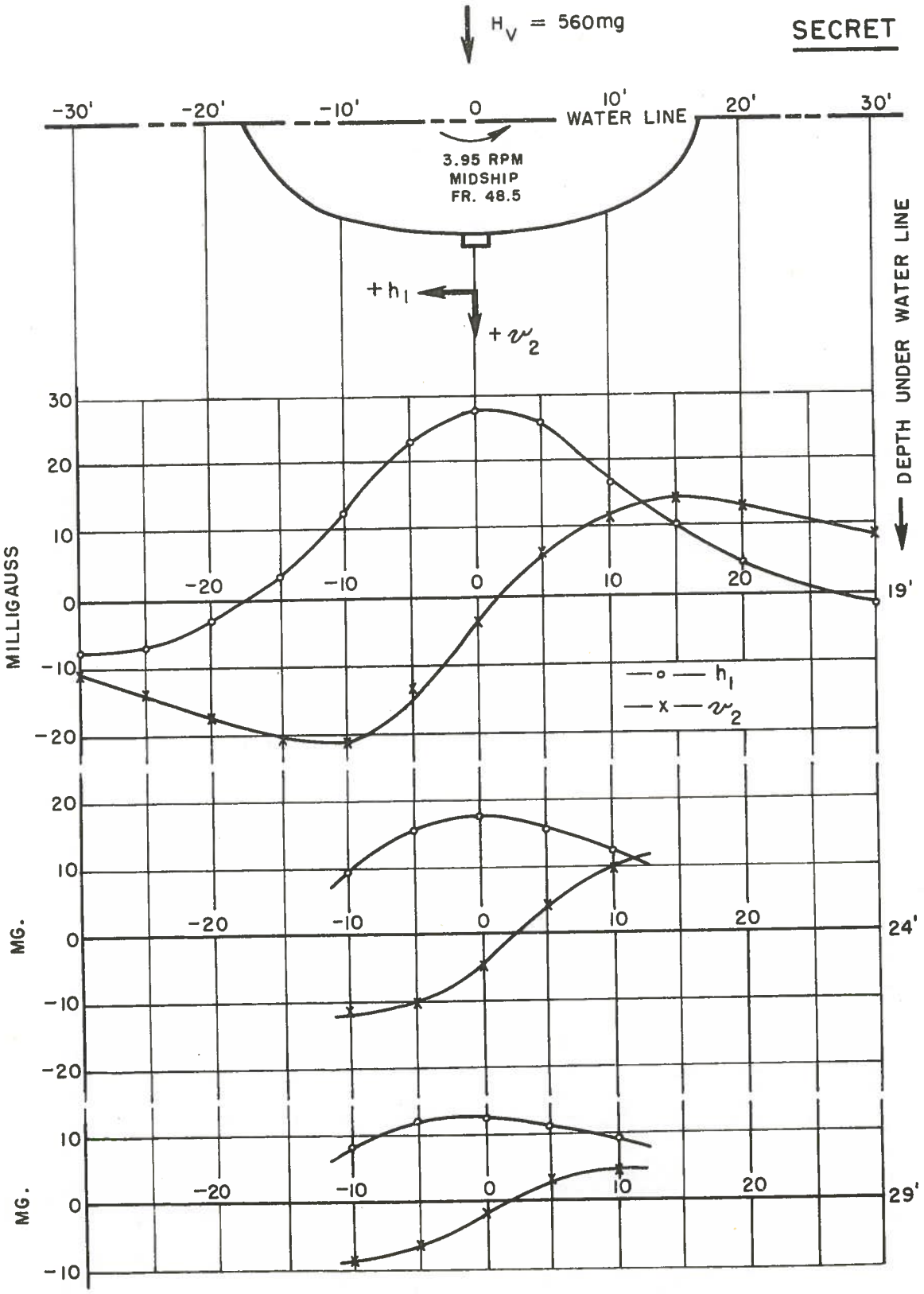

COMPLETE STRUCTURE (STAGE 3)

FIG. 29

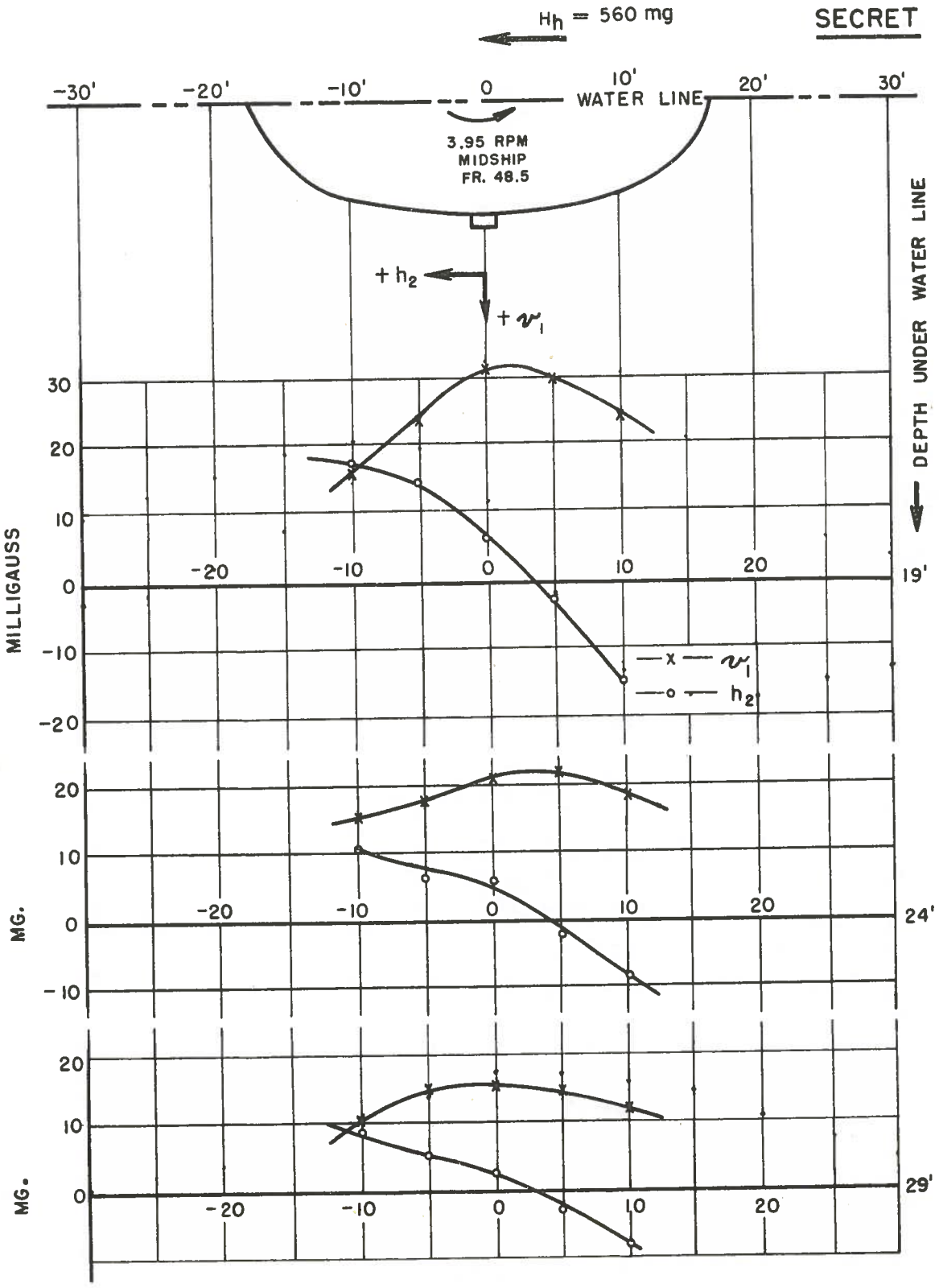

COMPLETE STRUCTURE (STAGE 3)
FIG. 30

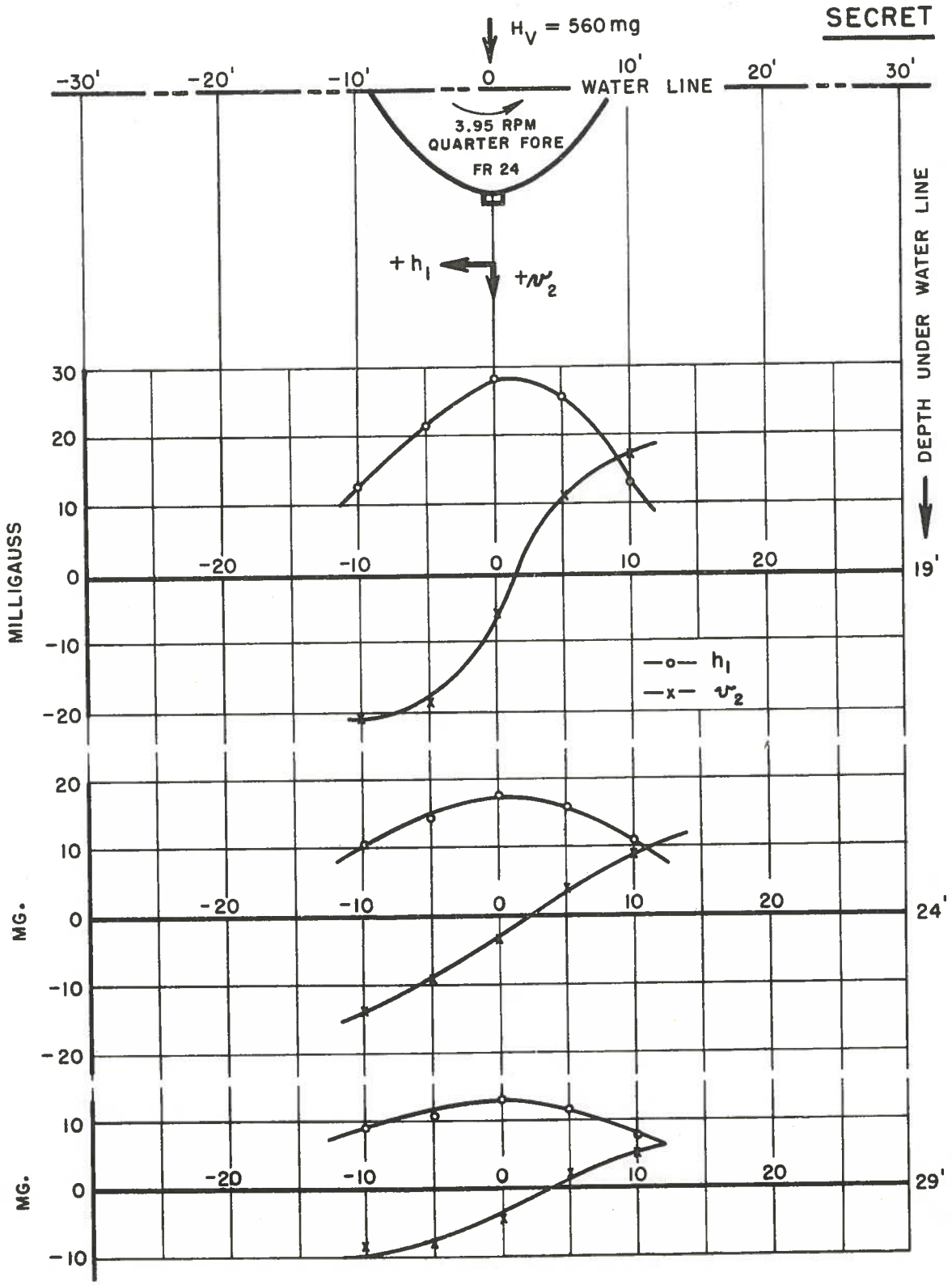

COMPLETE STRUCTURE (STAGE 3)

FIG. 31

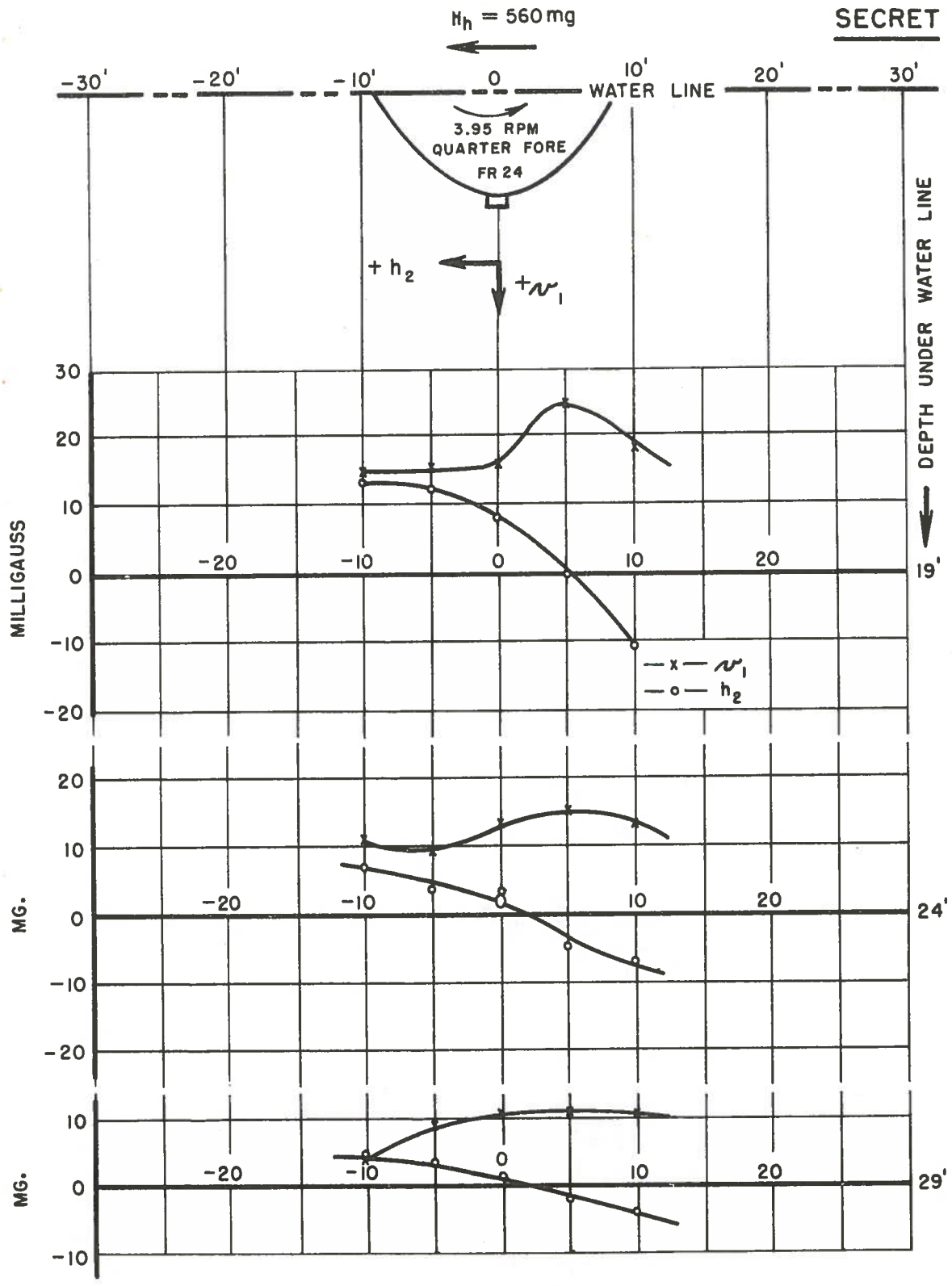

COMPLETE STRUCTURE (STAGE 3)

FIG. 32

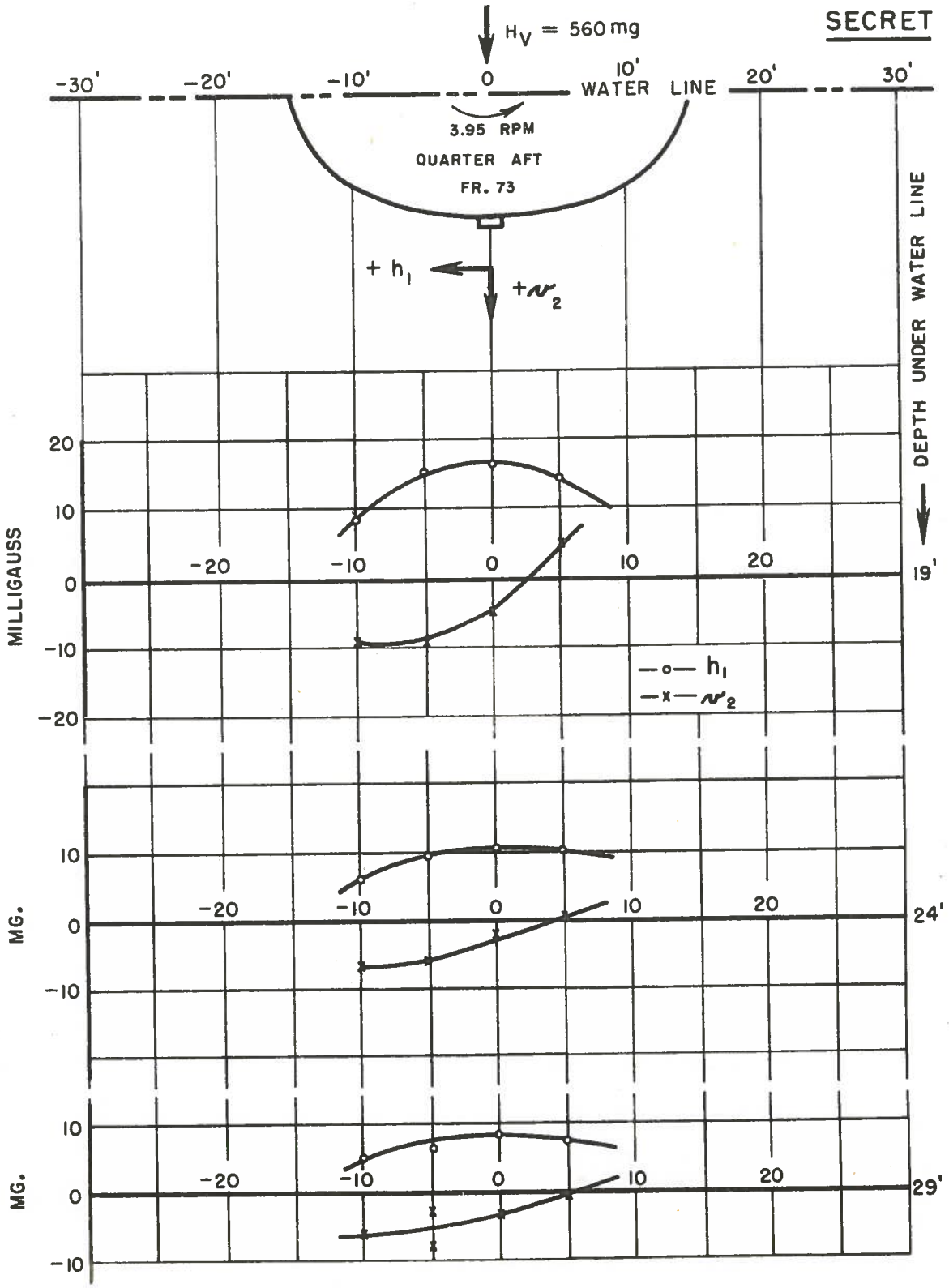

COMPLETE STRUCTURE (STAGE 3)

FIG. 33

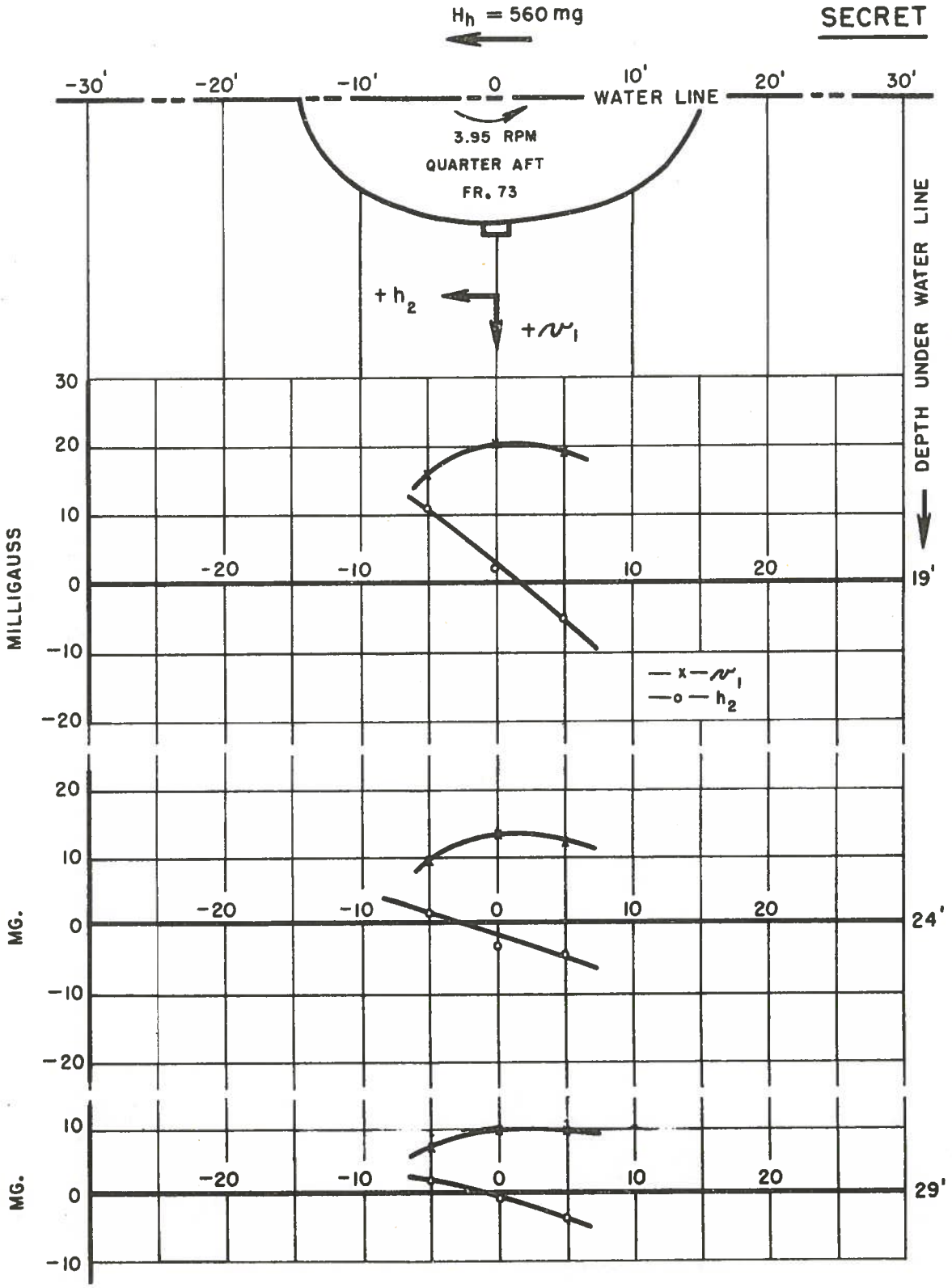

COMPLETE STRUCTURE (STAGE 3)

FIG. 34

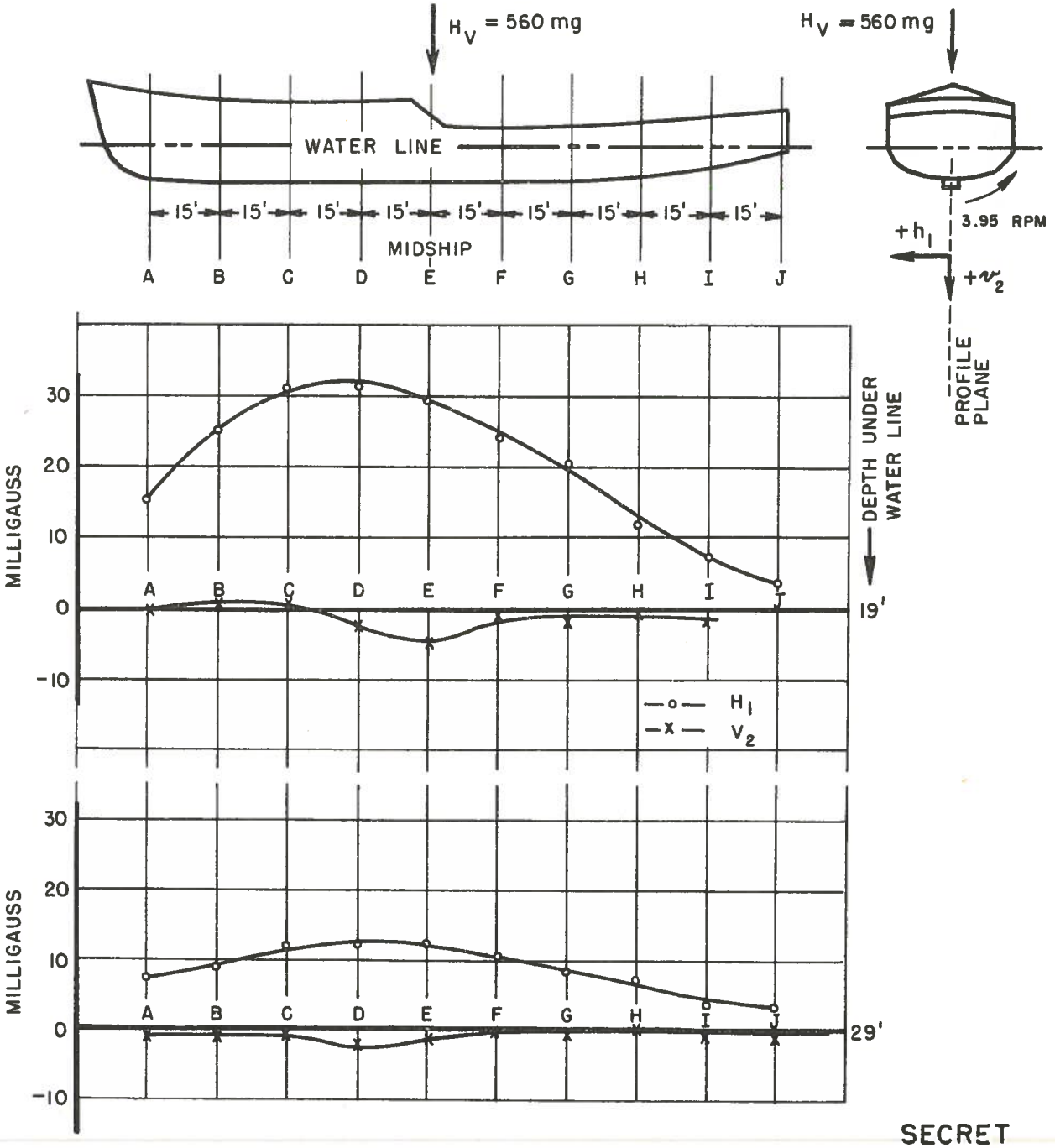

LONGITUDINAL PROFILES OF h_1 AND ν_2

COMPLETE STRUCTURE (STAGE 3)

FIG. 35

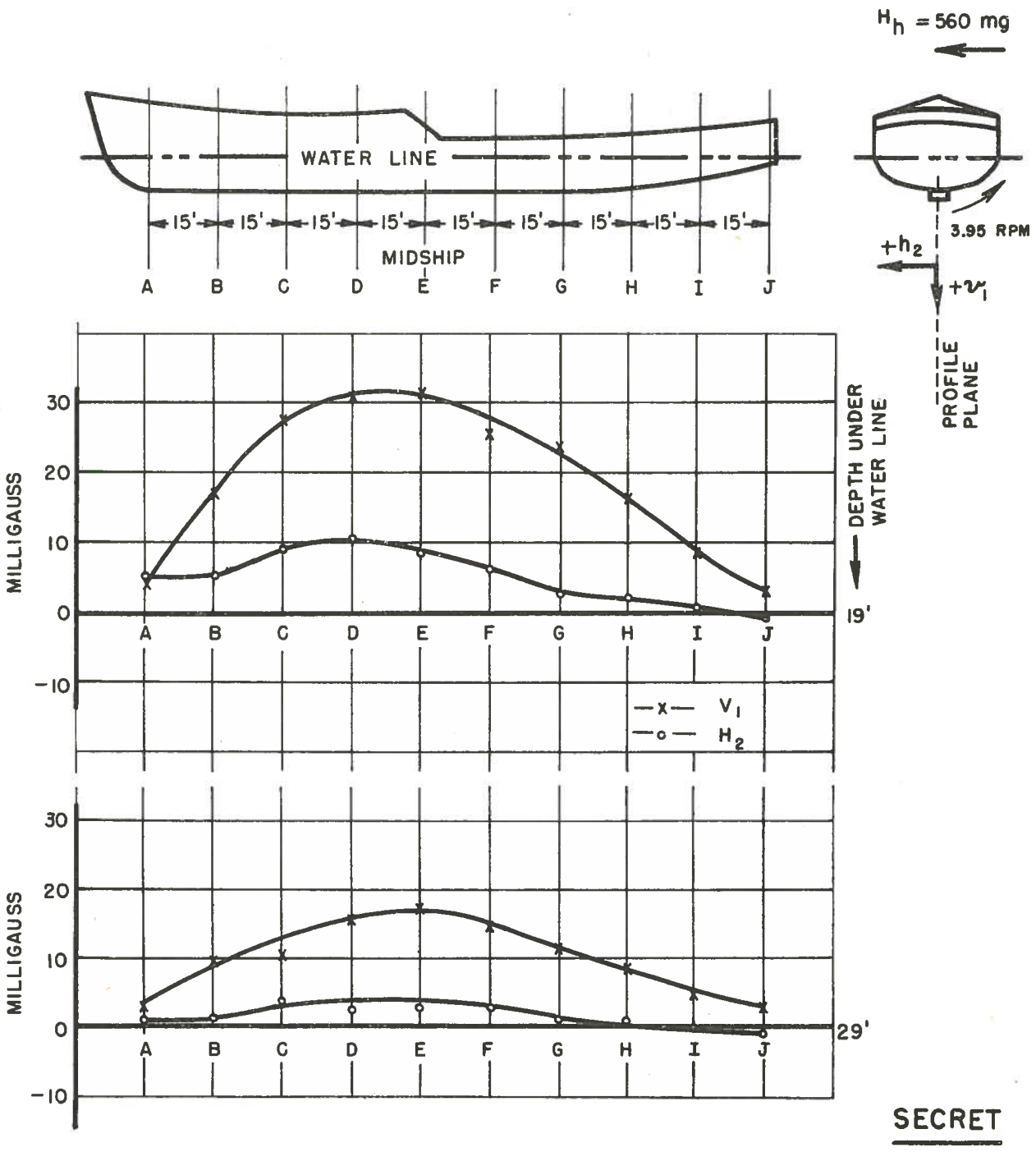

LONGITUDINAL PROFILES OF h_2 AND v_1

COMPLETE STRUCTURE (STAGE 3)

FIG. 36

SECRET

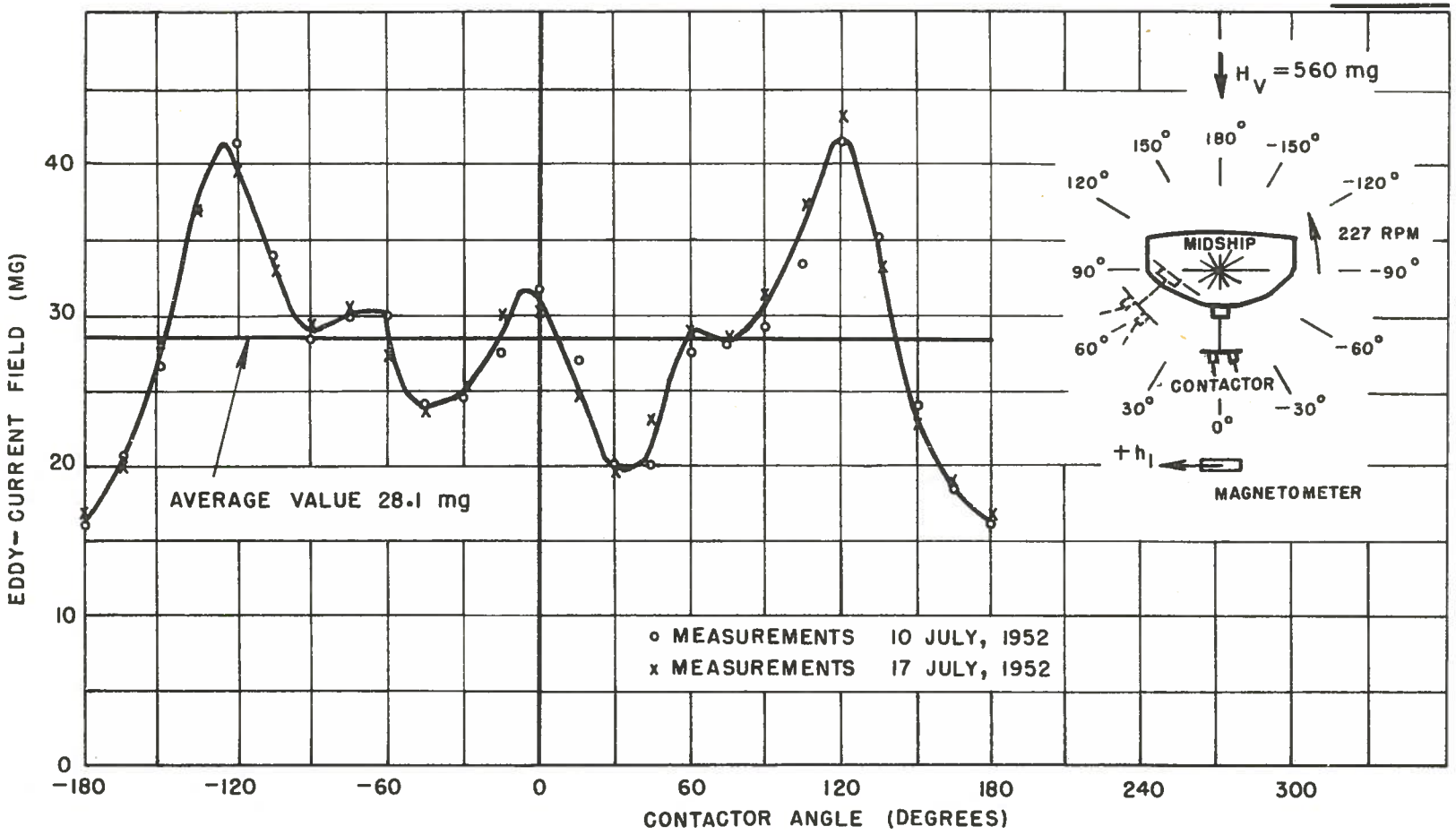

"h_l" (HORIZONTAL EDDY-CURRENT FIELD DUE TO H_V) AS A FUNCTION OF CONTACTOR ANGLE

(MIDSHIP — 19' UNDER WATER LINE — STAGE 3)

FIG. 37

SECRET

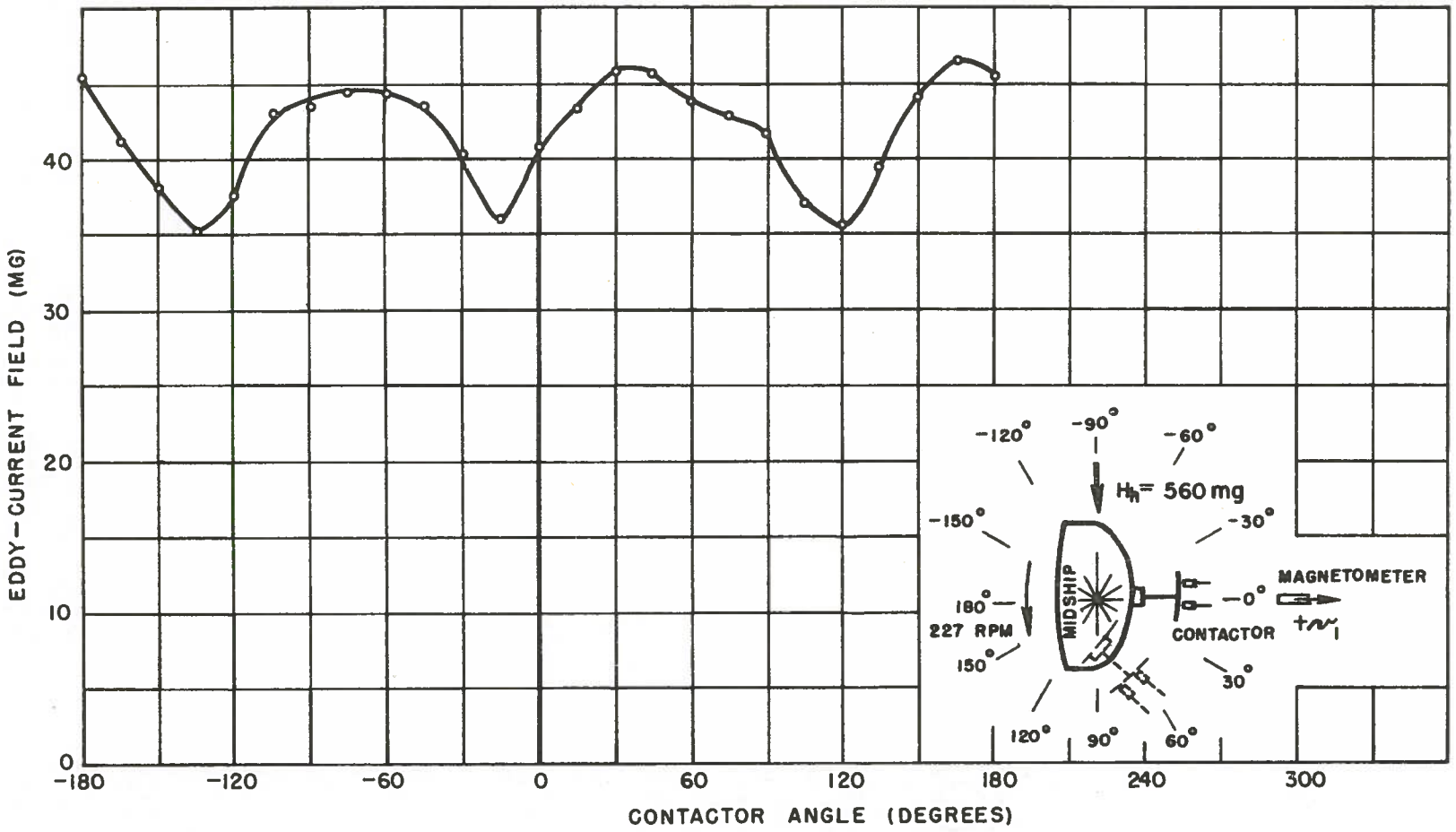

"$\mathcal{M}_1$" (VERTICAL EDDY-CURRENT FIELD DUE TO H_h) AS A FUNCTION OF CONTACTOR ANGLE

(MIDSHIP — 19' UNDER WATER LINE — STAGE 3)

FIG. 38

SECRET

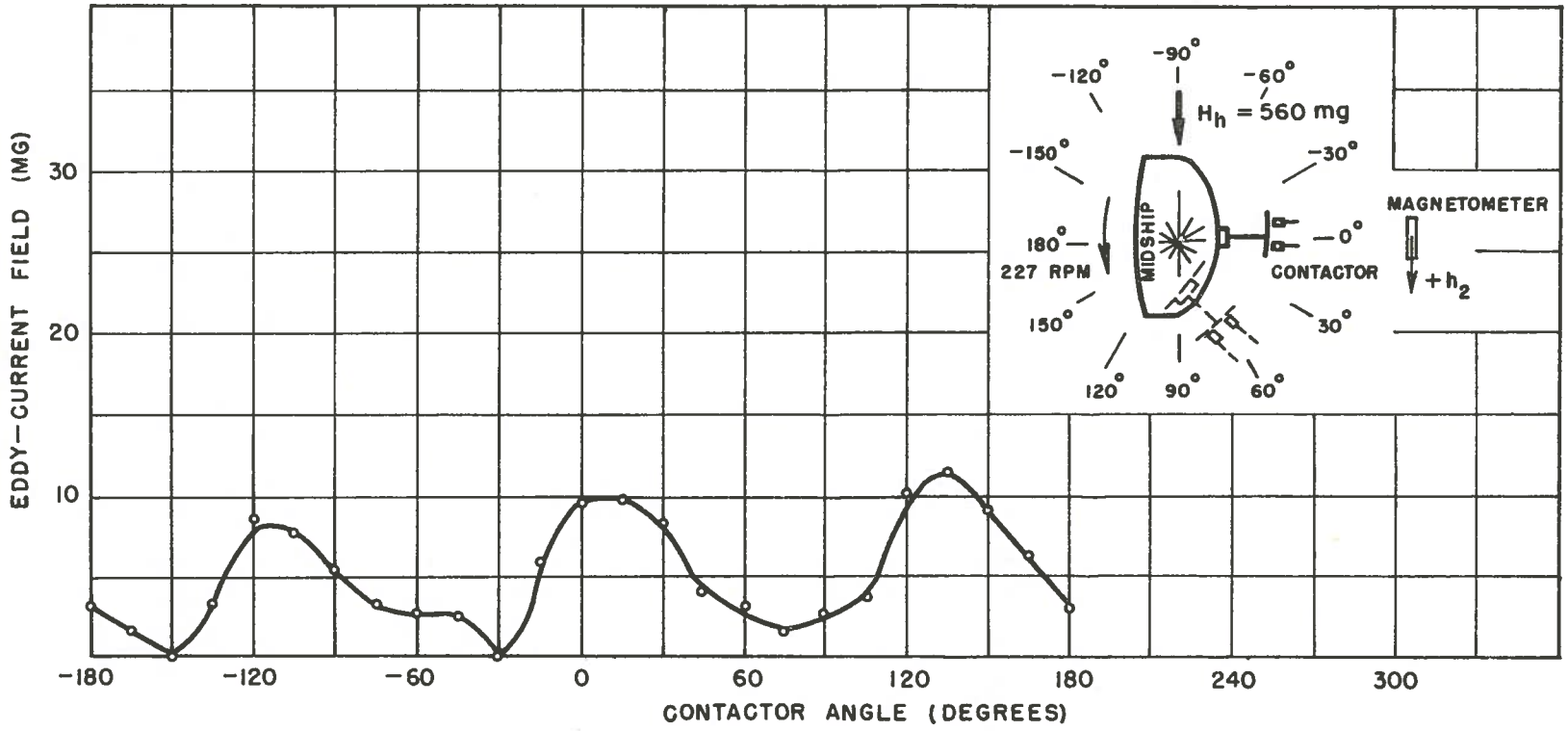

"h_2" (HORIZONTAL EDDY-CURRENT FIELD DUE TO H_h) AS A FUNCTION OF CONTACTOR ANGLE

(MIDSHIP — 19' UNDER WATER LINE — STAGE 3)

FIG. 39

SECRET

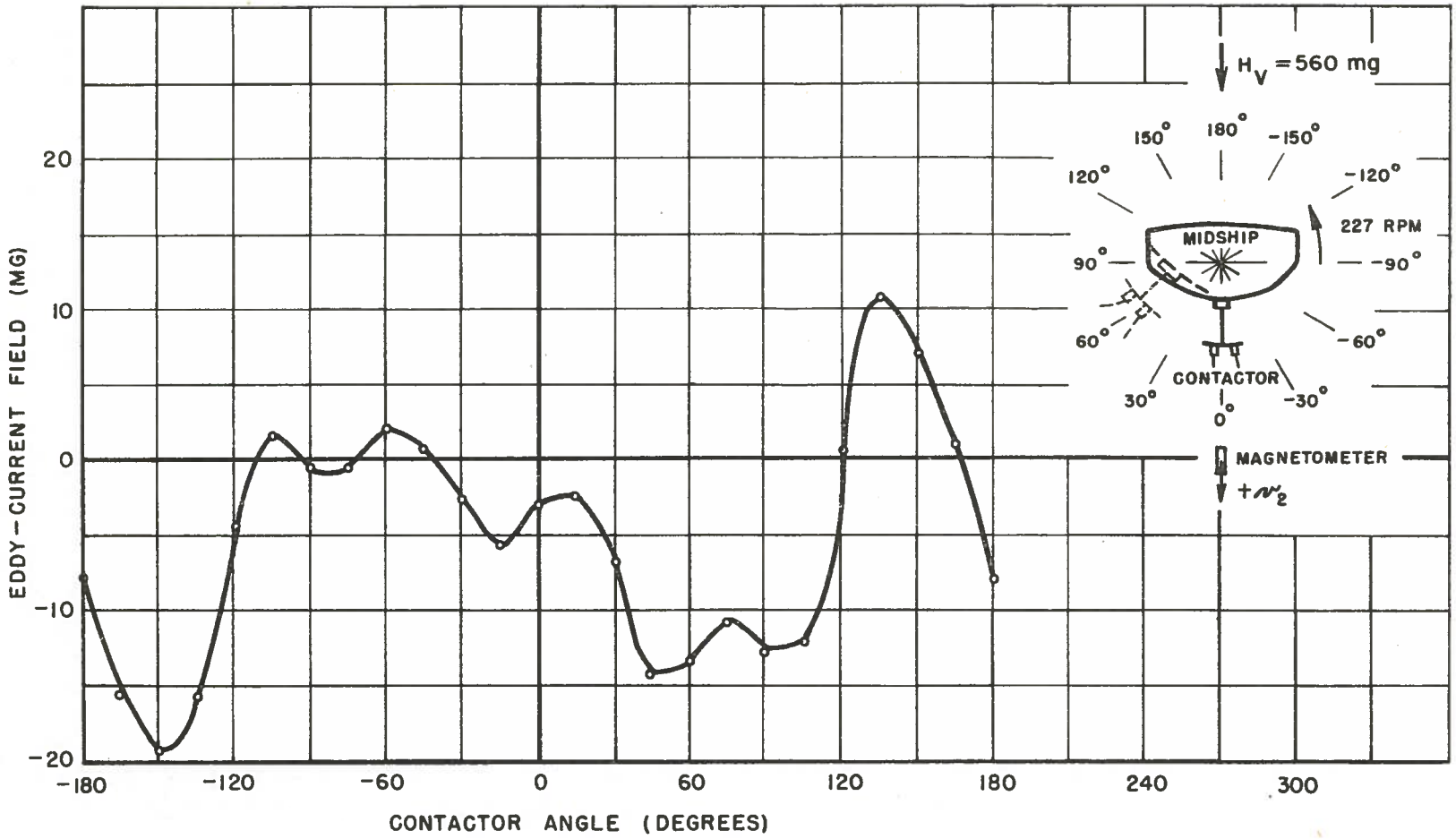

"μ_2" (VERTICAL EDDY-CURRENT FIELD DUE TO H_V) AS A FUNCTION OF CONTACTOR ANGLE

(MIDSHIP — 19' UNDER WATER LINE — STAGE 3)

FIG. 40

SECRET

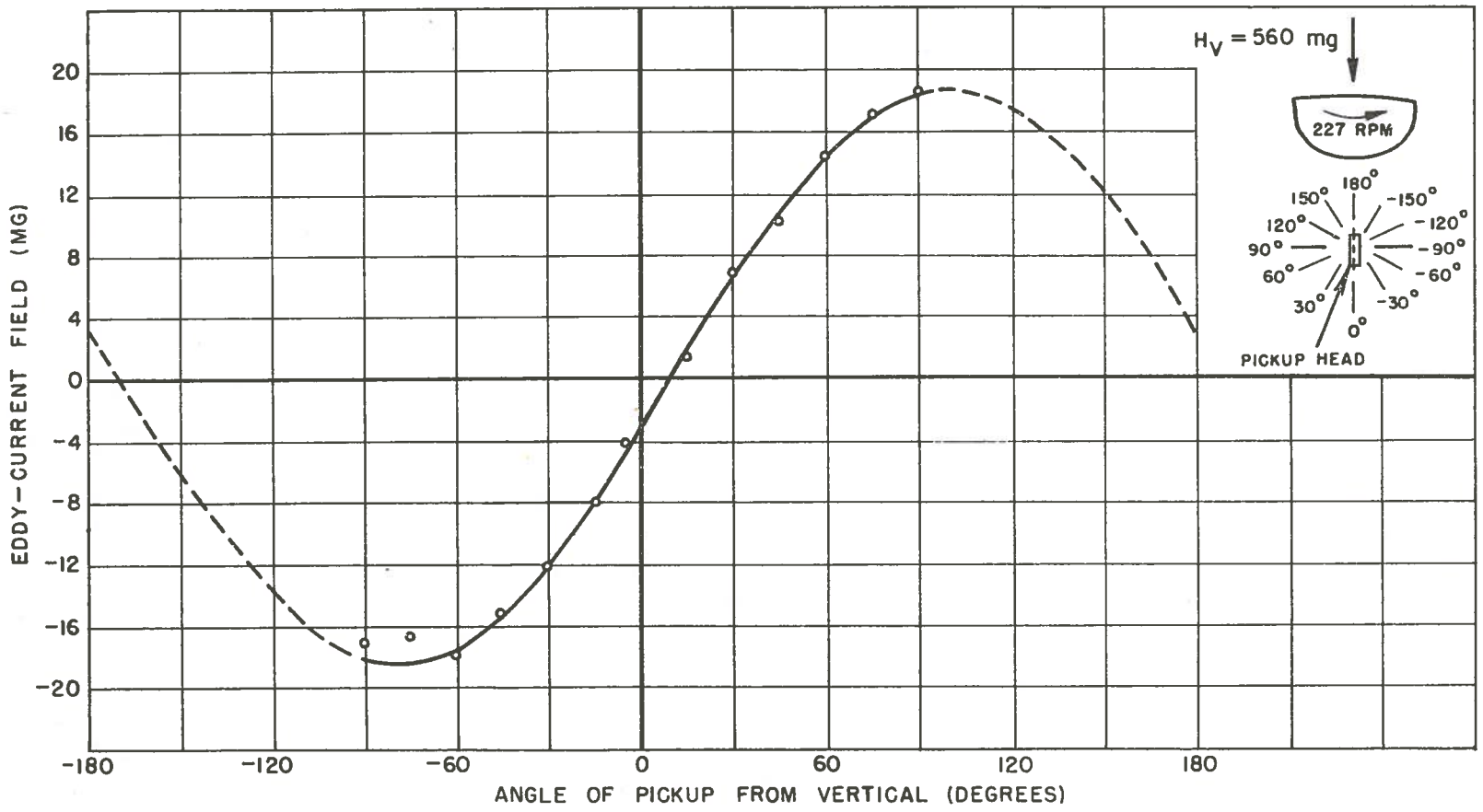

EDDY-CURRENT FIELD AS A FUNCTION OF PICKUP ANGLE

(MIDSHIP — 24' UNDER WATER LINE — STAGE 3)

FIG. 41

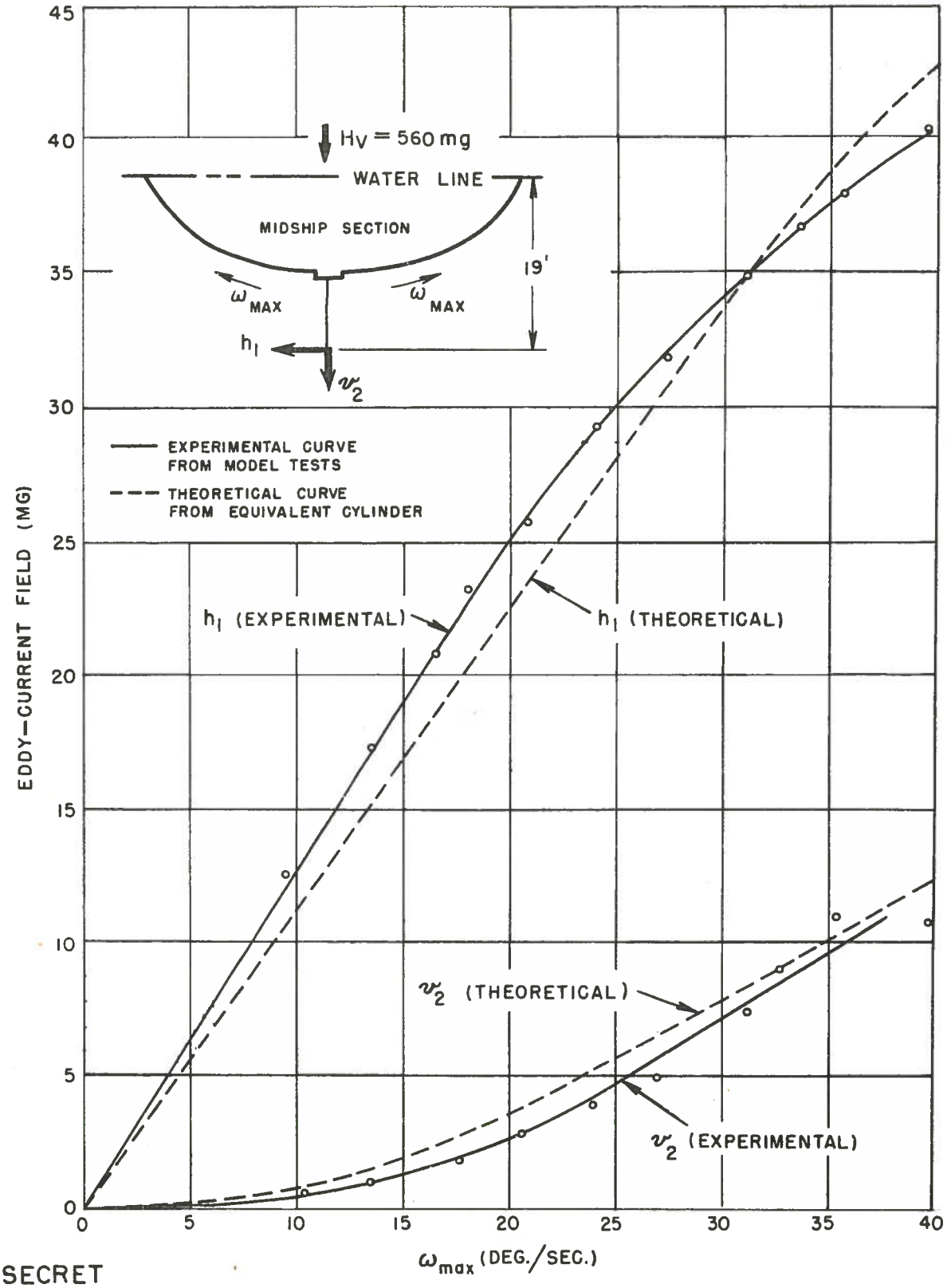

SECRET

EDDY-CURRENT FIELD COMPONENTS DUE TO H_V
VS. MAXIMUM ANGULAR VELOCITY OF ROLL

FIG. 42

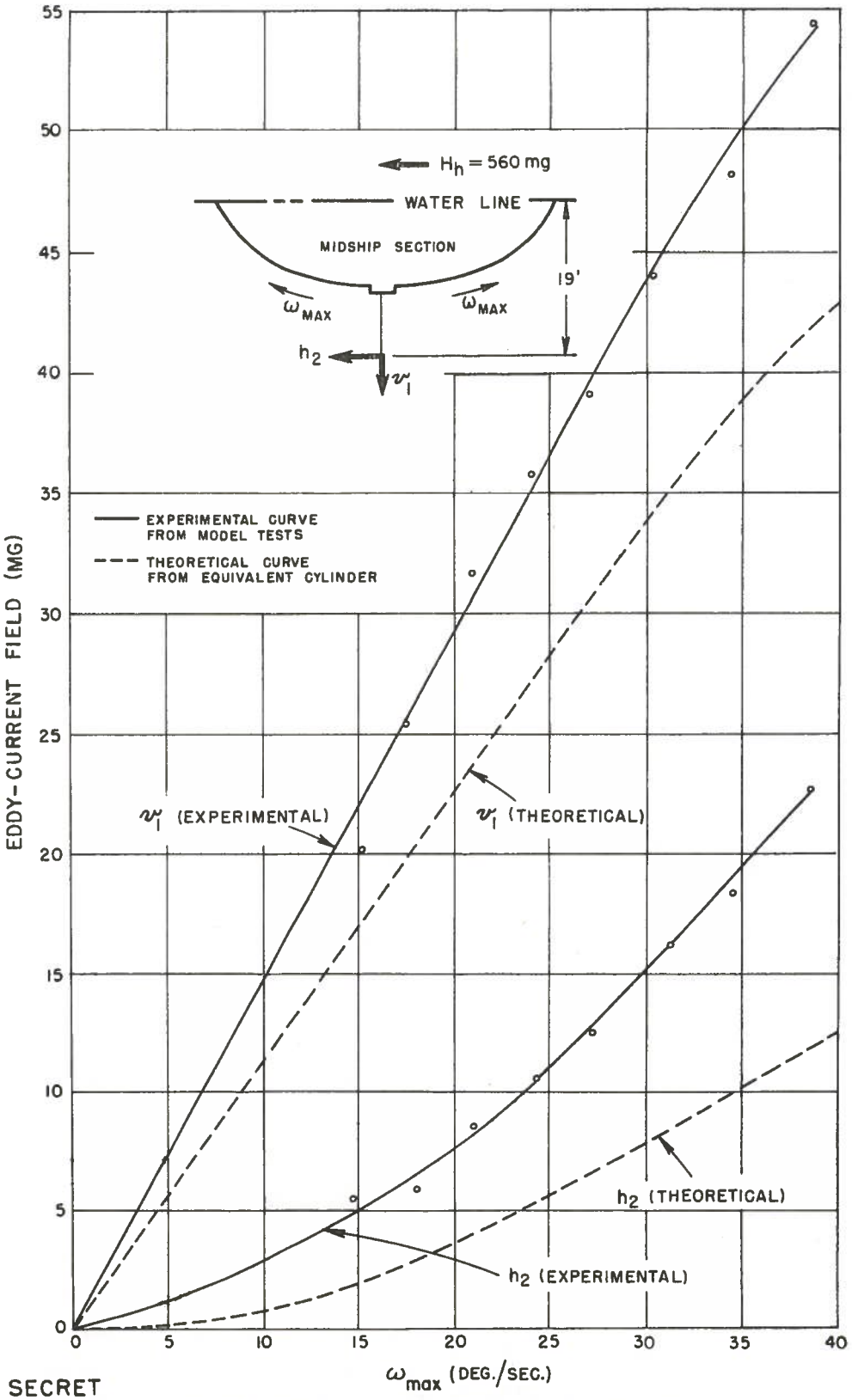

SECRET

EDDY-CURRENT FIELD COMPONENTS DUE TO H_h
VS. MAXIMUM ANGULAR VELOCITY OF ROLL

FIG. 43

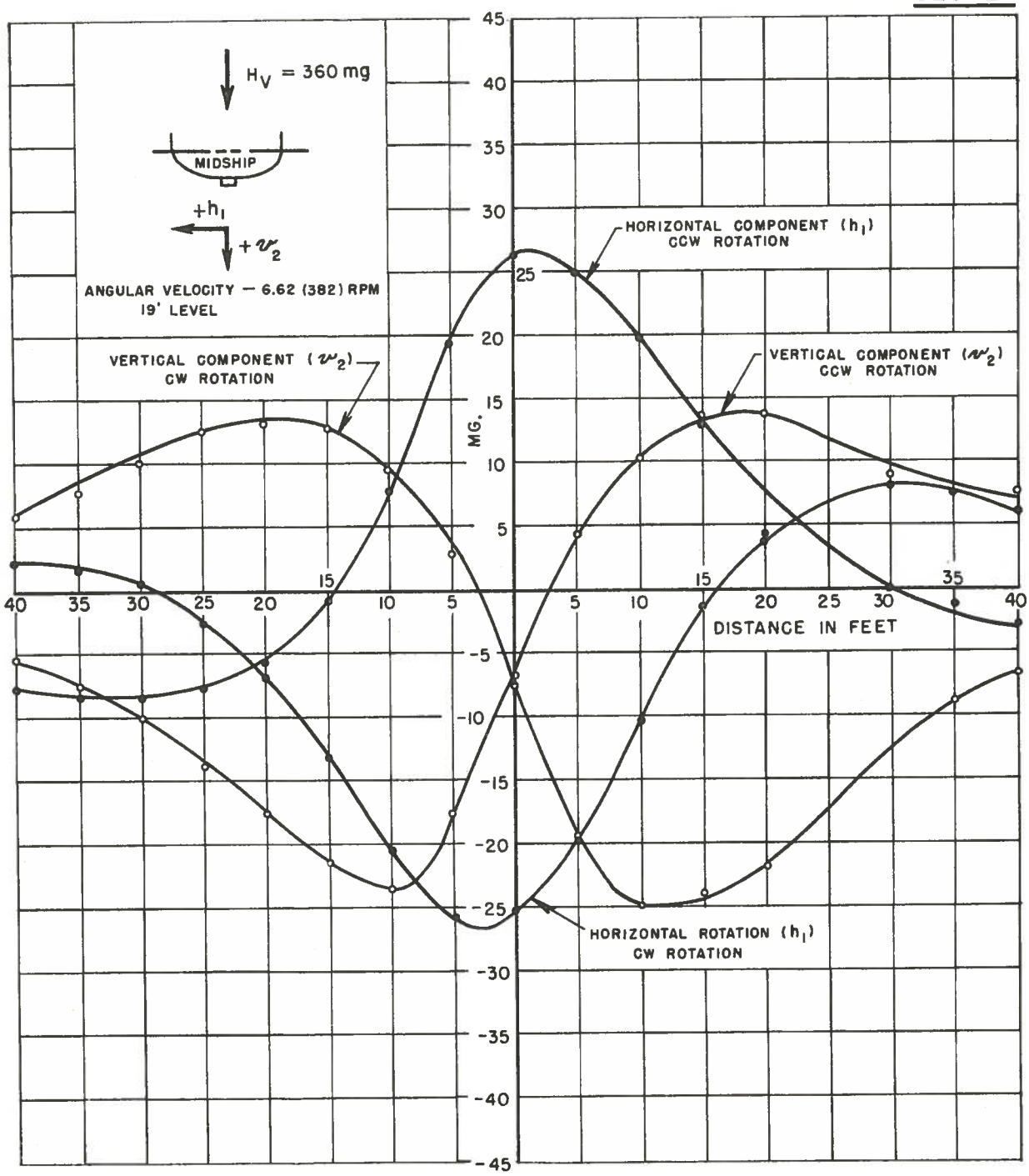

EDDY-CURRENT FIELDS DUE TO A VERTICAL EXCITING FIELD

FIG. 44

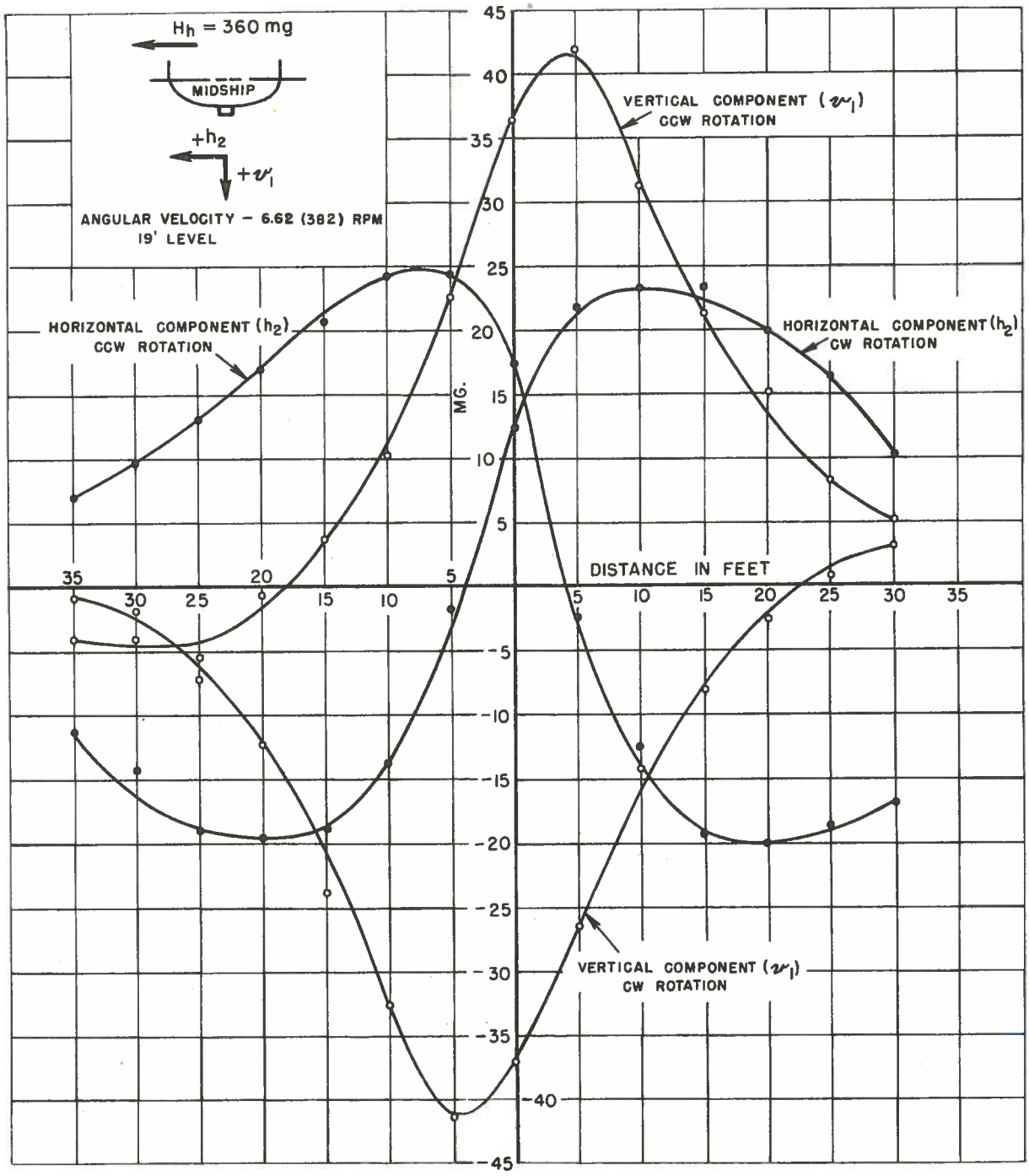

EDDY-CURRENT FIELDS DUE TO A HORIZONTAL EXCITING FIELD

FIG. 45

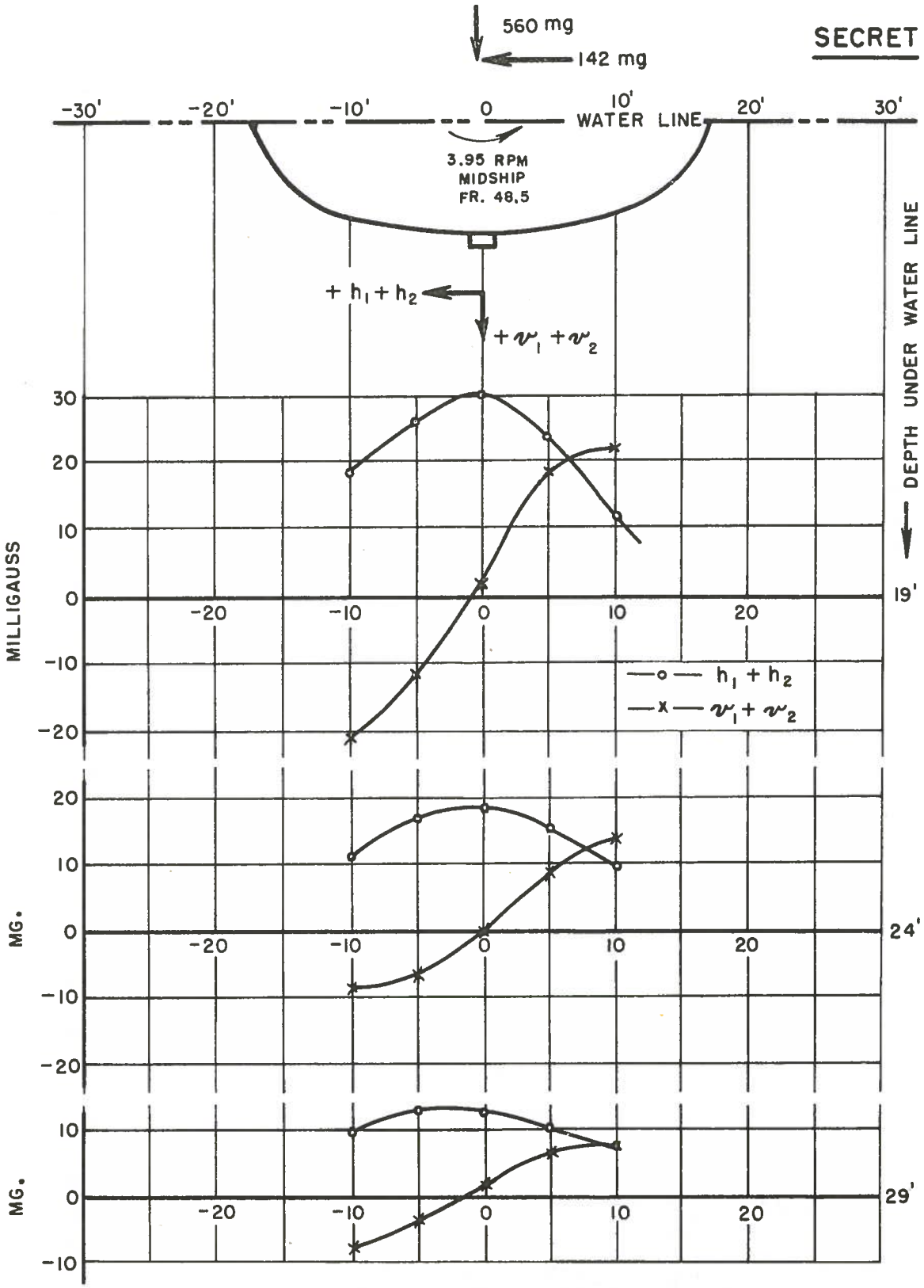

COMBINED EDDY-CURRENT FIELDS AT OTTAWA ($H_V = 560$, $H_h = 142$)
($h_1 + h_2$) AND ($\nu_1 + \nu_2$)

COMPLETE STRUCTURE (STAGE 3)

FIG. 46

SECRET

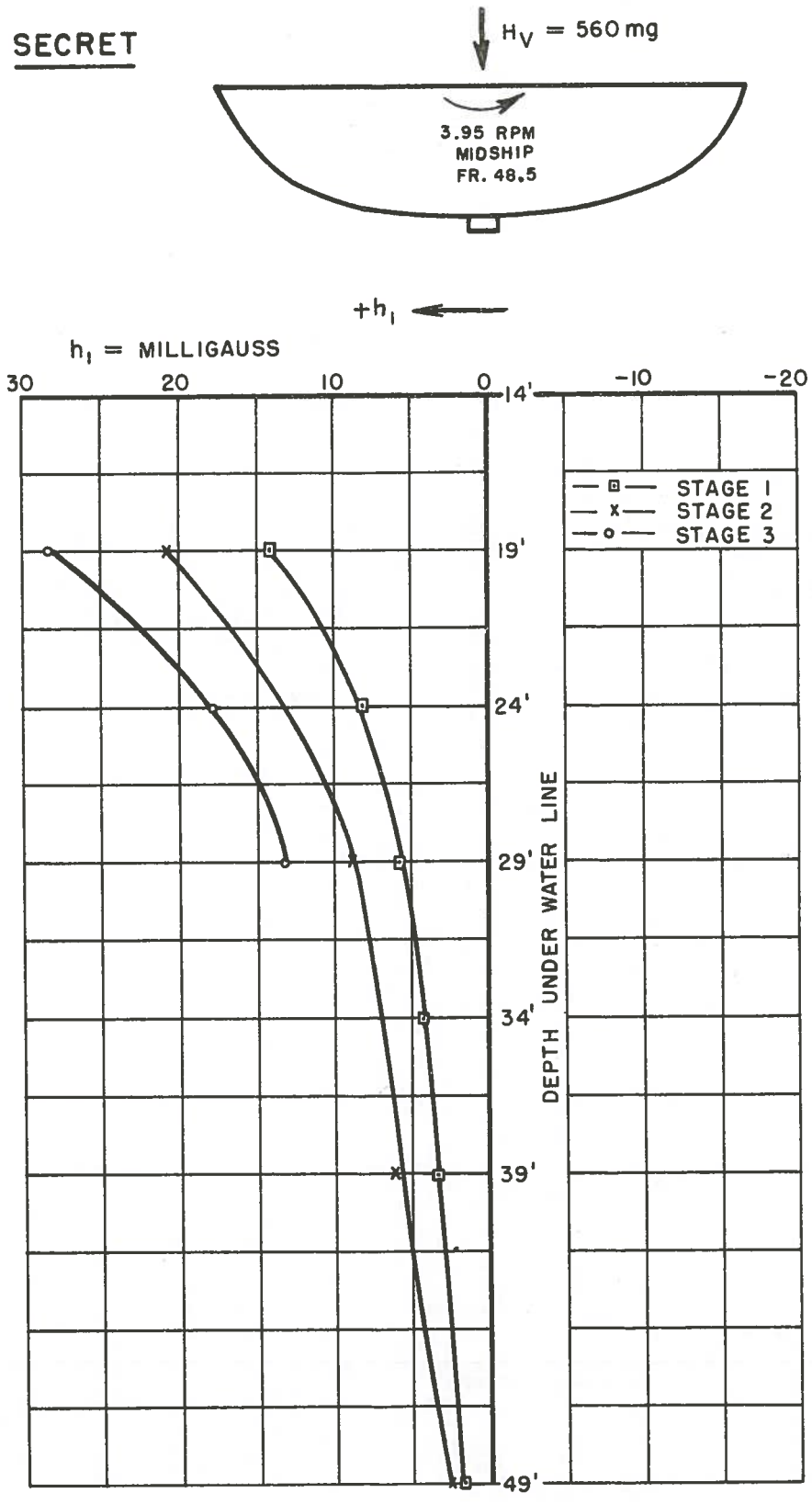

VARIATION OF EDDY-CURRENT FIELD (h_l)
WITH DEPTH UNDER WATER LINE

FIG. 47

SECRET

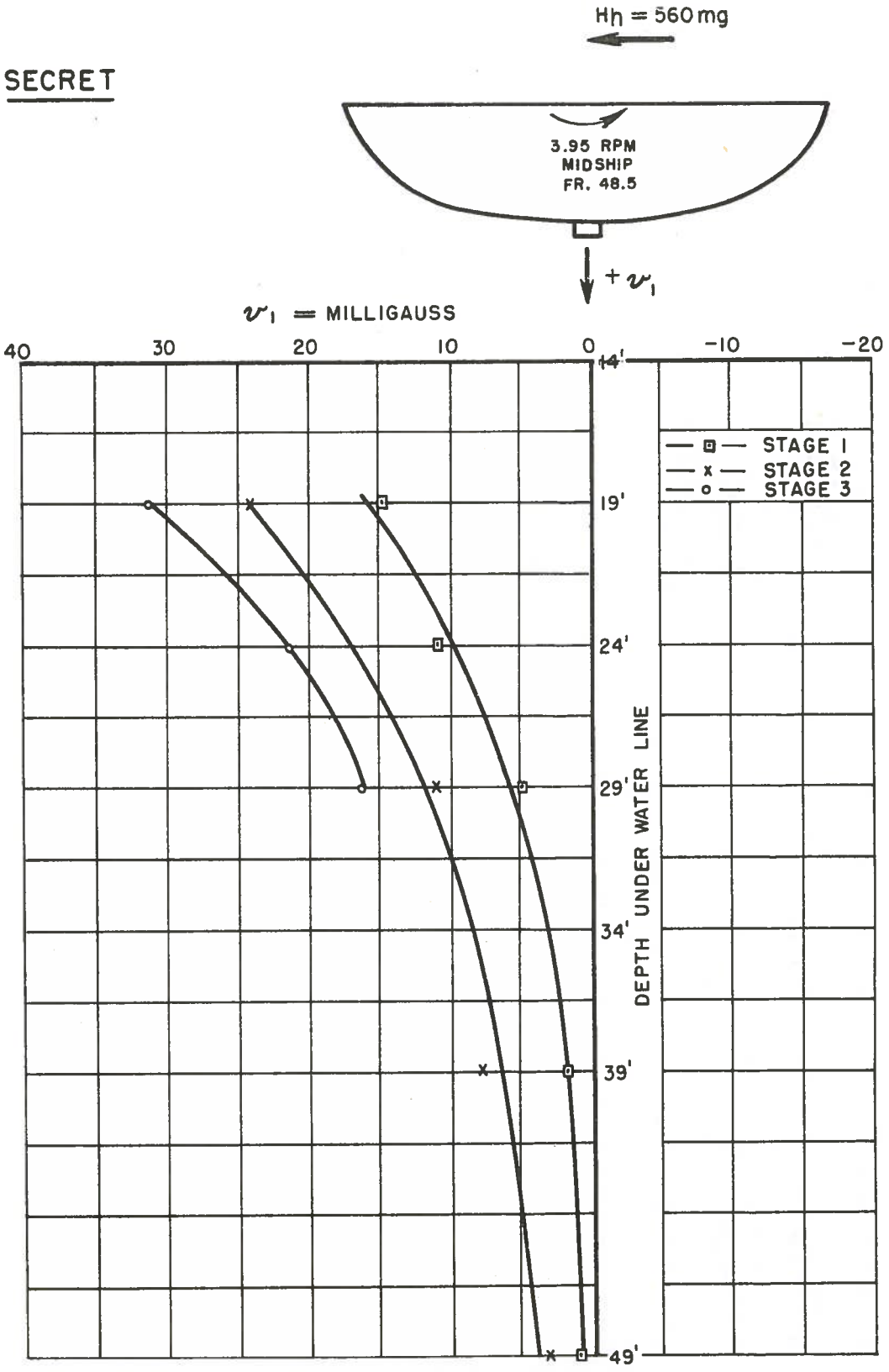

VARIATION OF EDDY-CURRENT FIELD (v_1)
WITH DEPTH UNDER WATER LINE
FIG. 48

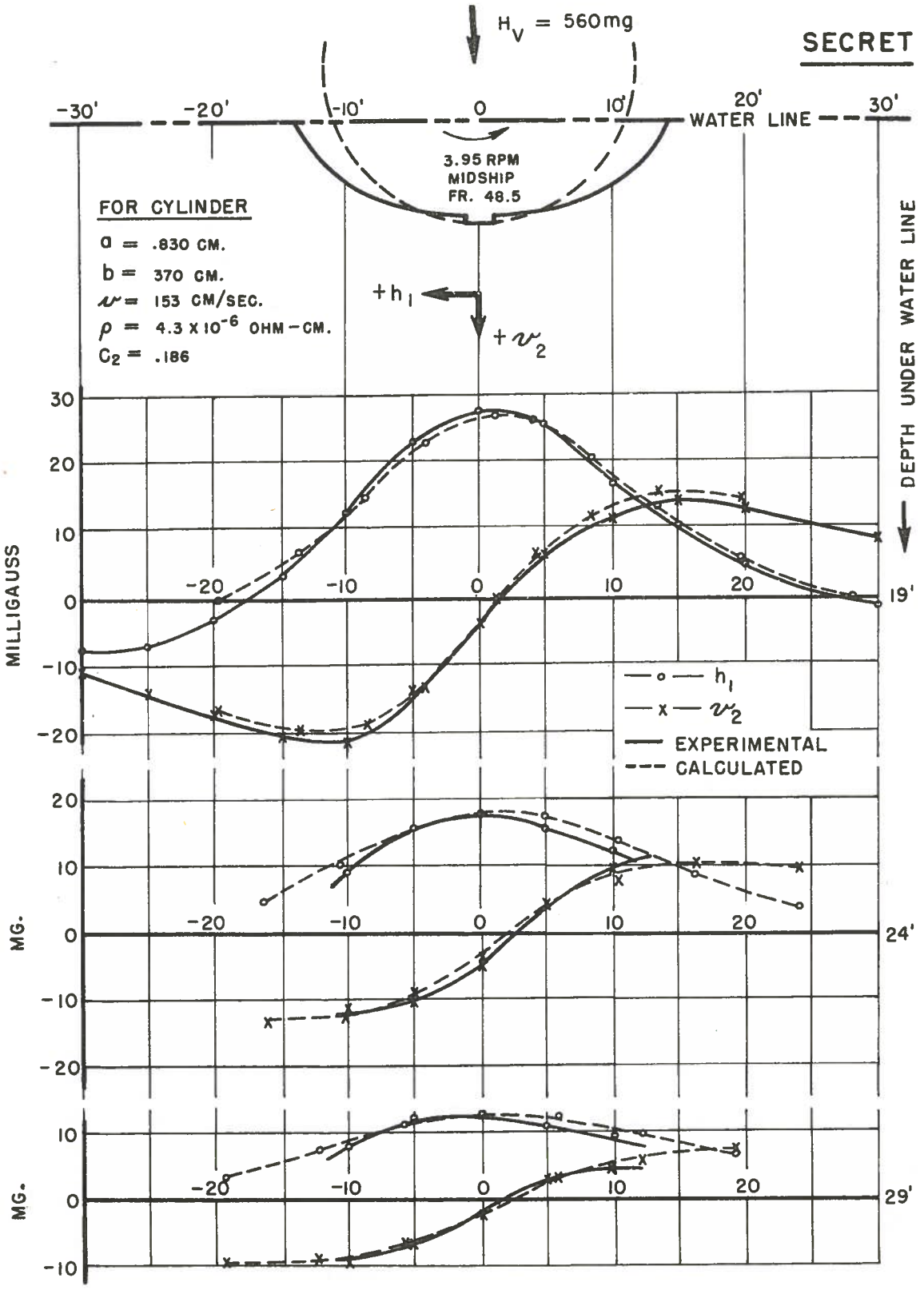

COMPLETE STRUCTURE (STAGE 3)

FIG. 49

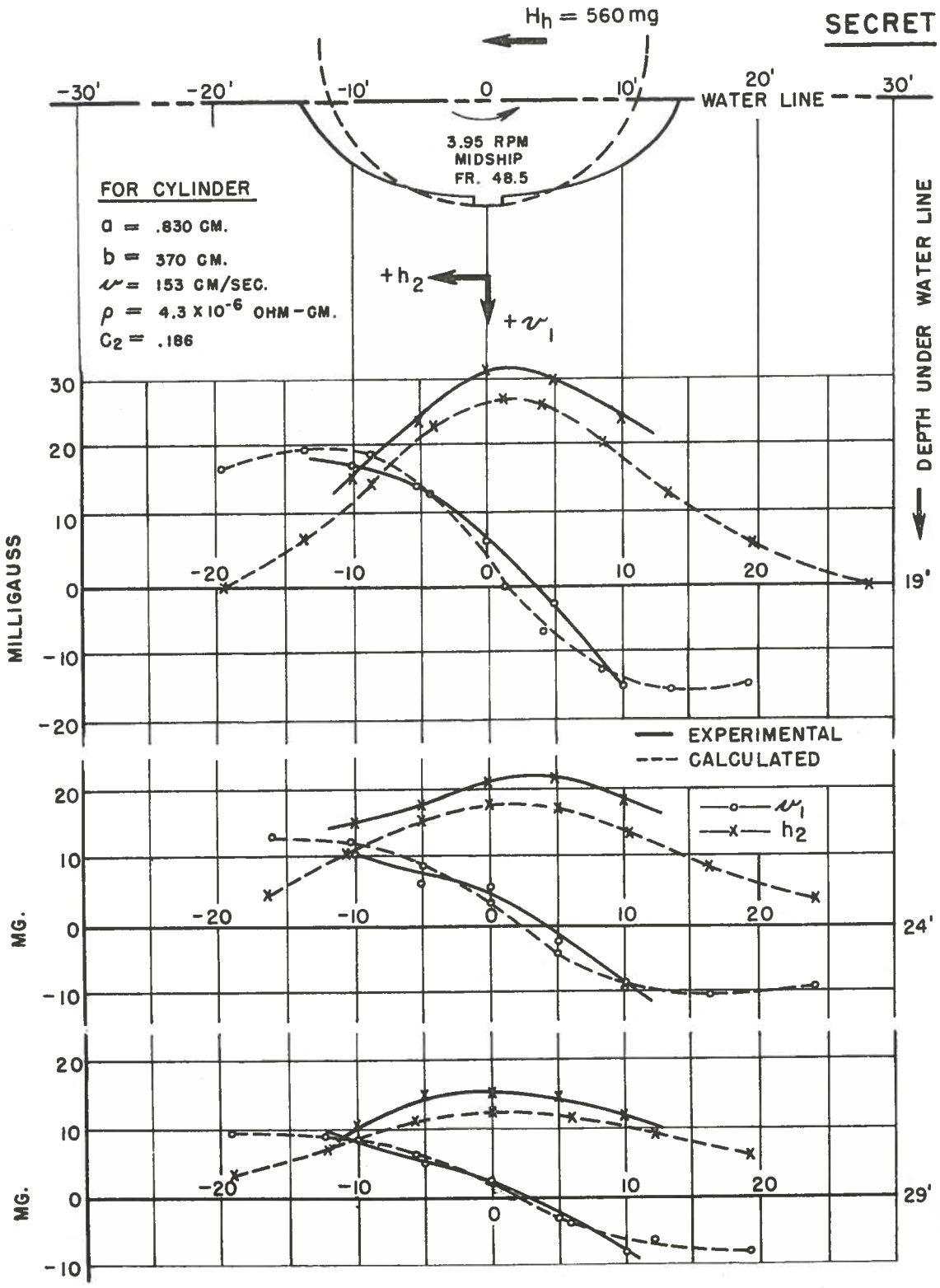

COMPLETE STRUCTURE (STAGE 3)

FIG. 50

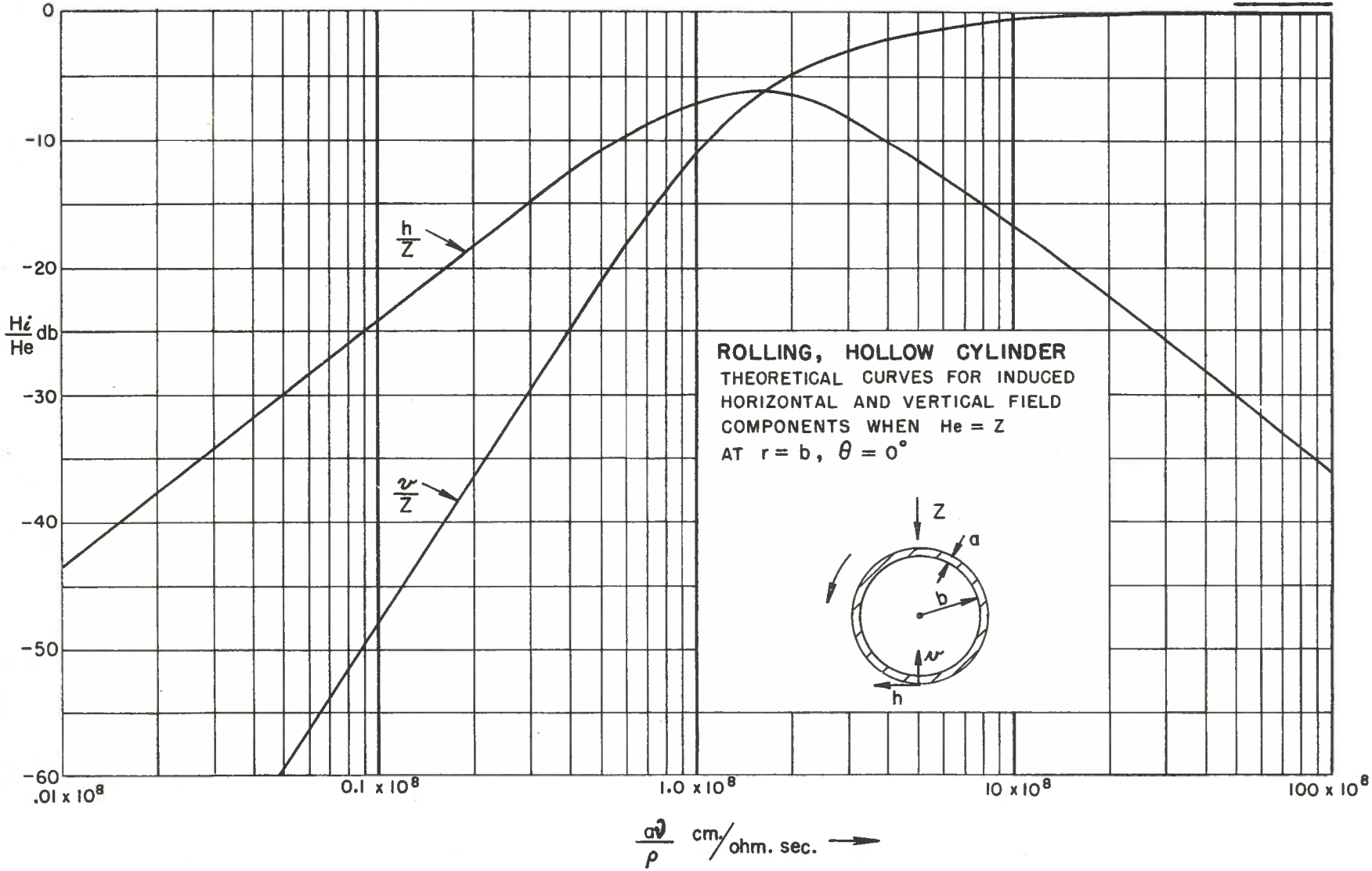
0
-10
-20
-30
-40
-50
-60
Hi/He db
h/Z
v/Z
.01 x 10^8
0.1 x 10^8
1.0 x 10^8
10 x 10^8
100 x 10^8
aν/ρ cm./ohm. sec.
ROLLING, HOLLOW CYLINDER
THEORETICAL CURVES FOR INDUCED HORIZONTAL AND VERTICAL FIELD COMPONENTS WHEN He = Z AT r = b, θ = 0°
Z
a
b
v
h

FIG. 51

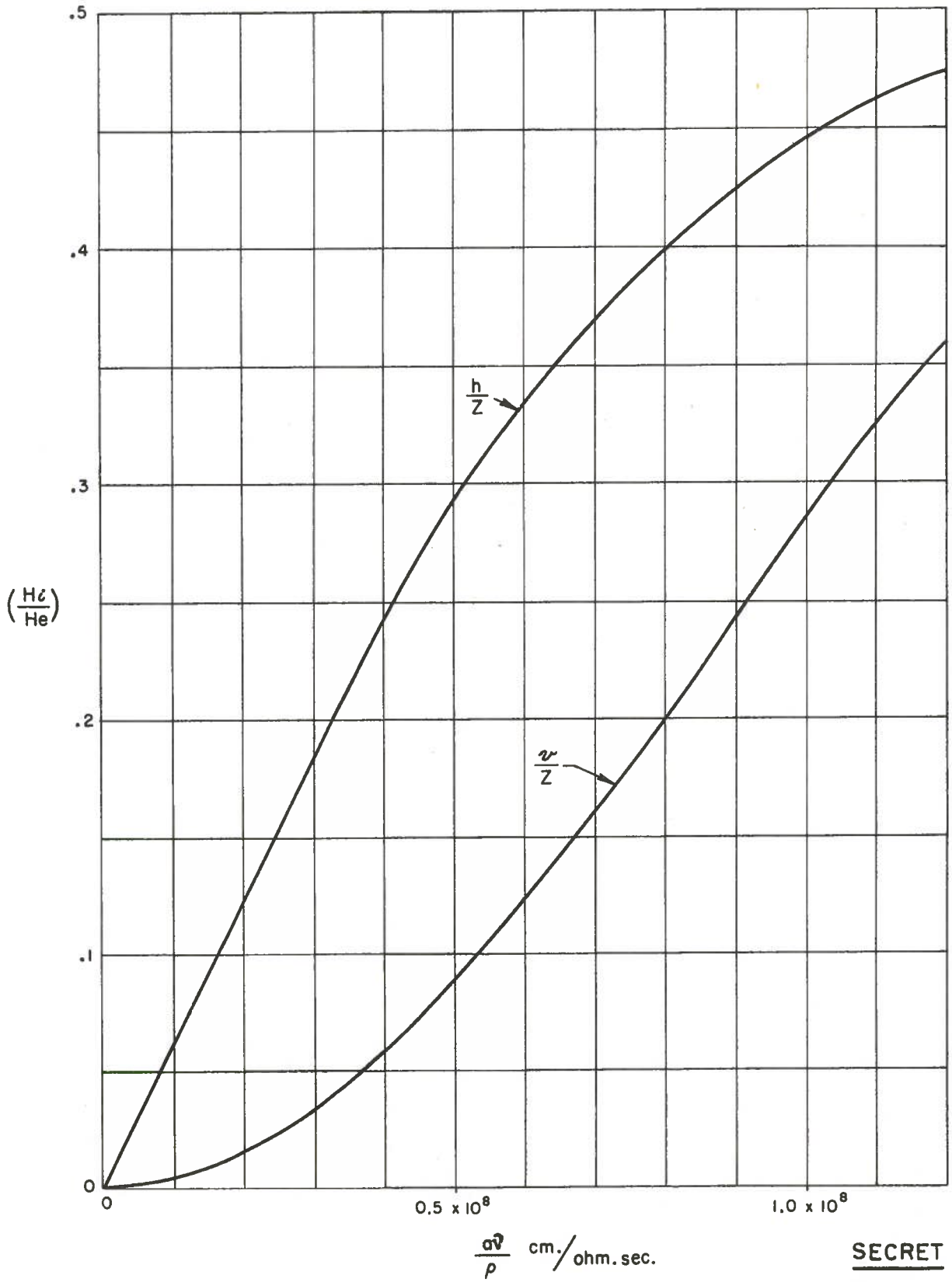

SECRET

FIG. 52

SECRET

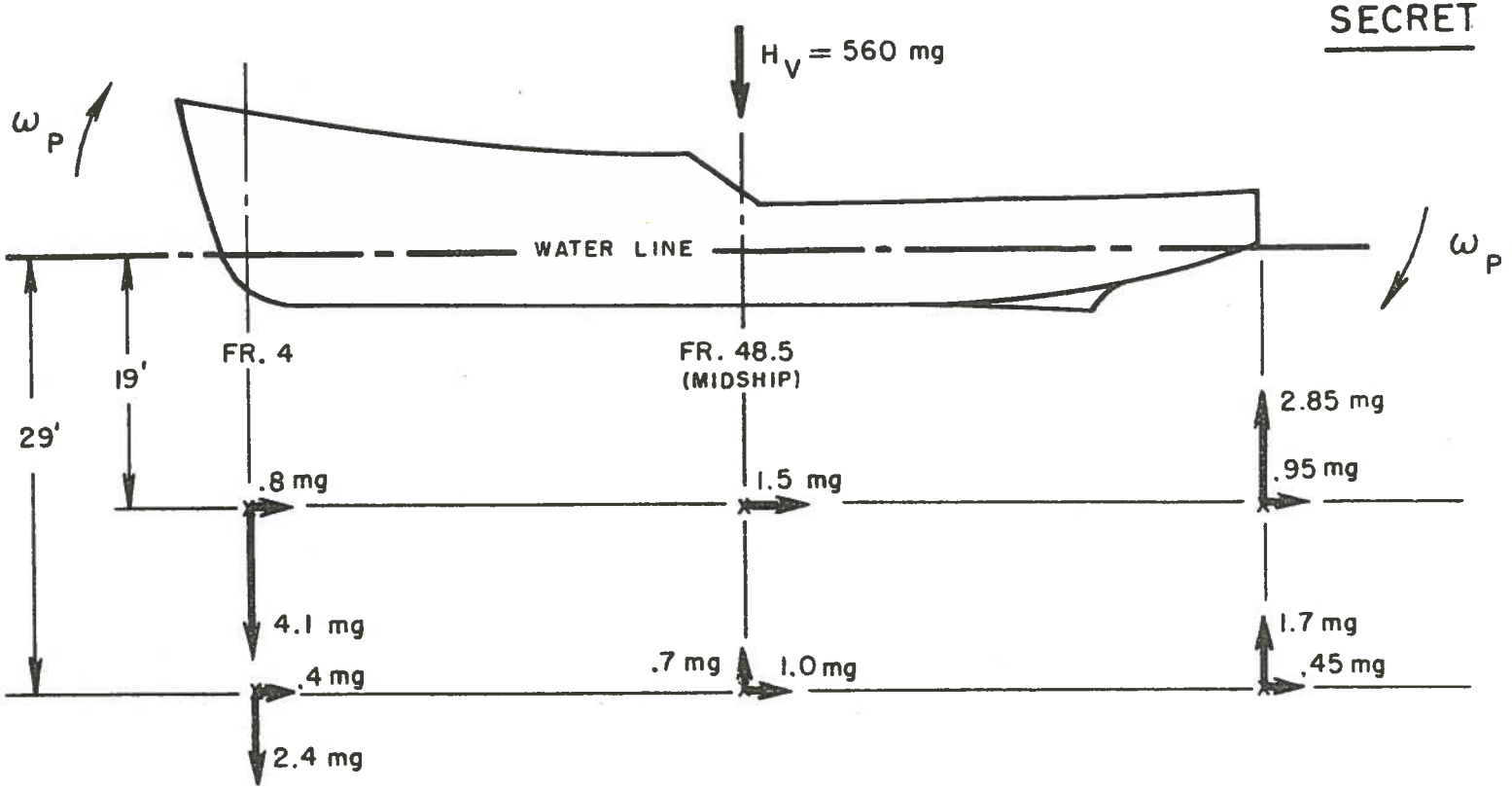

ESTIMATE OF
EDDY-CURRENT FIELD DUE TO PITCHING OF VERTICAL TRANSVERSE CIRCUITS
PITCH OF ±8° WITH 4.5 SEC. PERIOD

FIG. 53

APPENDIX I

Derivation of the Equation of the Flux Lines Created by a Thin, Hollow Cylinder Rotating in a Uniform Magnetic Field

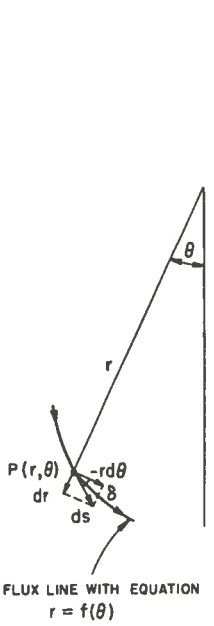

FIG. A

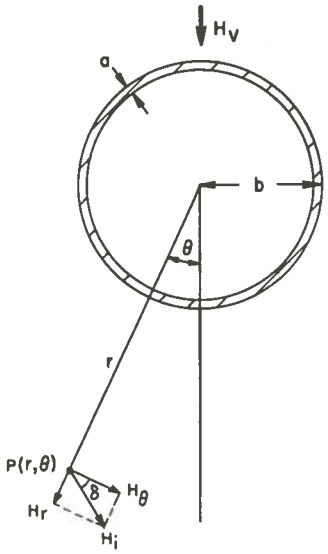

FIG. B

In the two-dimensional case, the equation of the flux lines created by a rotating cylinder will be of the form $r = f(\theta)$. In Fig. A, the point $P(r,\theta)$ lies on a magnetic flux line in the polar plane. A small displacement $\vec{ds}$, tangent to the flux line at the point P, has radial and tangential components of displacement dr and $-rd\theta$. If δ is the angle between the tangent to the flux curve and the negative tangential direction as shown, then δ is given by

$$\tan \delta = \frac{dr}{-rd\theta} .$$

In Fig. B, the magnetic field $\vec{Hi}(r,\theta)$, created by a thin cylinder of radius b rotating in a constant exciting field H_v, is shown at the point P. From Equation (1), page 3, this field is, in terms of its positive and negative tangential components, given by

$$H_r = H_v \frac{C_2}{\sqrt{1 + C_2^2}} \frac{b^2}{r^2} \sin(\theta - \phi) ,$$

$$H_\theta = H_v \frac{C_2}{\sqrt{1 + C_2^2}} \frac{b^2}{r^2} \cos(\theta - \phi) , \text{ provided } r > b.$$

By definition, the field $\vec{Hi}(r,\theta)$ is tangent to the flux line at the point P. Thus from Fig. B, the angle δ defined before is given by

$$\tan \delta = \frac{H_r}{H_\theta} ,$$

and using the field equations above it follows that

$$\tan \delta = \tan(\theta - \phi) .$$

Equating the two values of tan δ it follows that

$$\frac{dr}{-rd\theta} = \tan(\theta - \phi) .$$

Integration of both sides of this equation gives

$$r = C \cos(\theta - \phi) ,$$

where C is an integration constant. This is the equation of a family of circles all passing through the center of the cylinder and having their centers on a common line which makes an angle ϕ with the direction of the exciting field H_v. Since the field equations hold only for $r > b$, the condition $c > b$ must be satisfied. In other words, the above equation of the magnetic flux lines holds only for points external to the cylinder. The integration constant C may be written as

$$C = nb,$$

where n is any positive number greater than unity. The equation for the magnetic flux lines external to the cylinder is thus

$$r' = nb \cos(\theta - \phi) \quad n > 1 .$$

APPENDIX II

DERIVATION OF THE EQUATIONS FOR THE HORIZONTAL AND VERTICAL COMPONENTS OF THE EDDY-CURRENT FIELD AT POINTS EXTERNAL TO THE ROTATING CYLINDER

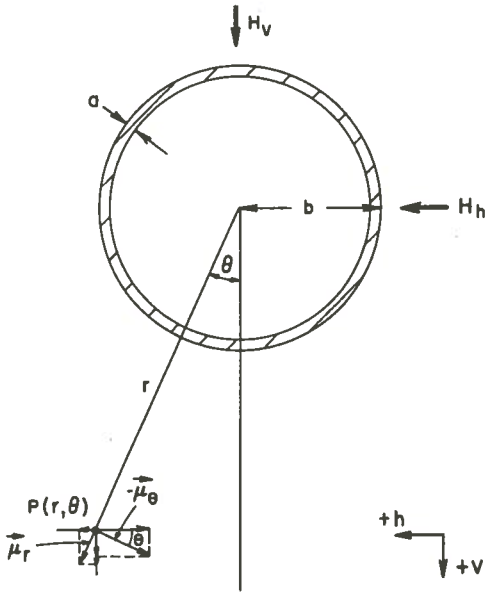

1. Equations of Component Due to Exciting Field Component H_v

From Eq. (1), the radial and tangential components of the field at the point (r, θ) outside the cylinder are as follows:

$$H_r = H_v \frac{C_2}{\sqrt{1 + C_2^2}} \frac{b^2}{r^2} \sin(\theta - \phi)$$

$$H_\theta = H_v \frac{C_2}{\sqrt{1 + C_2^2}} \frac{b^2}{r^2} \cos(\theta - \phi) .$$

Let the depth from the center of the cylinder to a horizontal plane under the cylinder be "nb", where $n > 1$.

Then let

$$K = \frac{1}{n^2} \frac{C_2}{\sqrt{1 + C_2^2}} .$$

Substitution gives:

$$H_r = H_v K\left(\frac{nb}{r}\right)^2 \sin(\theta - \phi)$$

$$= H_v K \cos^2\theta \sin(\theta - \phi), \text{ and}$$

$$H_\theta = H_v K\left(\frac{nb}{r}\right)^2 \cos(\theta - \phi) = H_v K \cos^2\theta \cos(\theta - \phi).$$

Let the horizontal component due to H_v be called h_1 (this is the principal component under the keel due to H_v) and the vertical component due to H_v be called v_2. The components in the +h and the +v directions defined by the above diagram are found to be as follows:

$$h_1 = KH_v\cos^2\theta \sin(\theta - \phi) \sin\theta - KH_v\cos^2\theta \cos(\theta - \phi) \cos\theta = -KH_v\cos^2\theta \cos(2\theta - \phi)$$

$$v_2 = KH_v\cos^2\theta \sin(\theta - \phi) \cos\theta + KH_v\cos^2\theta \cos(\theta - \phi) \sin\theta = KH_v\cos^2\theta \sin(2\theta - \phi).$$

2. Equations of Components Due to Exciting Field Component H_h

Let the vertical component due to H_h be called v_1 (this is the principal component under the keel due to H_h) and the horizontal component due to H_v be called h_2. It can easily be shown that

$$v_1 = -KH_h\cos^2\theta \cos(2\theta - \phi),$$

$$h_2 = -KH_h\cos^2\theta \sin(2\theta - \phi).$$

3. Determination of the Zeros, Maxima and Minima of the Functions $\cos^2\theta \sin(2\theta - \phi)$ and $\cos^2\theta \cos(2\theta - \phi)$

Determination of zeros of $\cos^2\theta \sin(2\theta - \phi)$:

Let $\cos^2\theta \sin(2\theta - \phi) = 0$

$\therefore$ Zeros occur when $\theta = \pm 90°$, $\theta = \frac{\phi}{2}$.

Determination of maxima and minima of $\cos^2\theta \sin(2\theta - \phi)$:

Let $\frac{d}{d\theta}[\cos^2\theta \sin(2\theta - \phi)] = 0$

$$\frac{d}{d\theta}\left[\tfrac{1}{2}\sin(2\theta - \phi) + \tfrac{1}{4}\sin(4\theta - \phi) + \tfrac{1}{4}\sin(-\phi)\right] = 0$$

$$\cos(2\theta - \phi) = -\cos(4\theta - \phi)$$

$$\cos 2\theta \cos\phi + \sin 2\theta \sin\phi = -[\cos 4\theta \cos\phi + \sin 4\theta \sin\phi]$$

$$\cos\phi[\cos 2\theta + \tan\phi \sin 2\theta] = -\cos\phi\,[\cos 4\theta + \tan\phi \sin 4\theta]$$

$$\cos 2\theta + \cos 4\theta = -\tan\phi[\sin 2\theta + \sin 4\theta]$$

$$2\cos 3\theta \cos\theta = -2\tan\phi[\sin 3\theta \cos\theta]$$

$$\tan 3\theta = -\operatorname{cct}\phi = \tan(90° + \phi) = \tan(-90° + \phi)$$

$\therefore$ Maxima and minima occur when $\theta = \frac{\phi}{3} \pm 30°$.

Determination of zeros of $\cos^2\theta \cos(2\theta - \phi)$:

Let $\cos^2\theta \cos(2\theta - \phi) = 0$.

Zeros occur when $\theta = \pm 90°$, $\theta = \frac{\phi}{2} \pm 45°$.

Determination of maxima and minima of $\cos^2\theta \cos(2\theta - \phi)$:

Let $\frac{d}{d\theta}[\cos^2\theta \cos(2\theta - \phi)] = 0$

$$\frac{d}{d\theta}\left[\tfrac{1}{2}\cos(2\theta - \phi) + \tfrac{1}{4}\cos(4\theta - \phi) + \tfrac{1}{4}\cos(-\phi)\right] = 0$$

$$\sin(2\theta - \phi) = -\sin(4\theta - \phi)$$

$$\sin 2\theta \cos\phi - \cos 2\theta \sin\phi = -[\sin 4\theta \cos\phi - \cos 4\theta \sin\phi]$$

$$\sin 2\theta - \tan\phi \cos 2\theta = -[\sin 4\theta - \tan\phi \cos 4\theta]$$

$$\sin 2\theta + \sin 4\theta = \tan\phi \cos[2\theta + \cos 4\theta]$$

$$2\sin 3\theta \cos\theta = 2 \tan\phi \cos 3\theta \cos\theta$$

$$\tan 3\theta = \tan\phi = \tan 180° + \phi = \tan -180° + \phi$$

$\therefore$ Maxima and minima occur when $\theta = \frac{\phi}{3}$, $\theta = \frac{\phi}{3} \pm 60°$.

The zeros, maxima and minima of the functions are summarized in Table I of the text.

APPENDIX III

REPRESENTATION OF THE SHIP BY AN EQUIVALENT CYLINDER

At midship, where end effects are not great, an attempt may be made to represent the ship by an infinitely long, thin, hollow, conducting cylinder. The method of obtaining the dimensions of such a cylinder will now be described. From this cylinder an estimate of the space phase lag and time constant of the field induced by the rolling ship may be made. The field distributions obtained from such a cylinder may be compared with the field distributions from the ship.

Determination of b (radius of the equivalent cylinder)

The basis for obtaining the radius of the equivalent cylinder is to equate the cross-sectional area of the ship at midship to the area of the cylinder. The areas of two frames in the region of midship, namely Frames 40 and 57, were measured on the plans of the ship by means of a planimeter and an average value for the area taken. Multiplying this measured area by the scale of the drawing gave an average value for the area of the actual ship at midship of 434,000 cm^2. By equating this value to the cross-sectional area of a thin cylinder, πb^2, a value for b of 370 cm is obtained.

Determination of a (wall thickness of the equivalent cylinder)

The basis for obtaining the wall thickness of the equivalent cylinder was to redistribute the total cross-sectional area of all longitudinal aluminum members at midship uniformly about the walls of the cylinder, as suggested by scaling relations developed in Section II. The cross-sectional areas of all longitudinal members at Frames 40 and 57 were summed and a average for the two frames taken. The value obtained was 1940 cm^2. To make a uniform redistribution of this area of metal about the walls of a cylinder, use was made of the relation

$$2\pi ra = 1940 \text{ cm}^2,$$

where r = 370 cm. From this relation, the value for the wall thickness a is found to be 0.83 cm.

Estimate of the phase lag of the induced field

From the theory of a thin, hollow, conducting cylinder rotating with constant angular velocity in a uniform magnetic field, the angle ϕ is given by

$$\phi = \tan^{-1} \frac{0.2\pi av}{10^8 \rho},$$

where a = thickness of cylinder wall in cm., v = tangential velocity of cylinder in cm/sec, and ρ = resistivity of the metal in ohm-cm.

For the equivalent cylinder of the ship, a = 0.83 cm. and $\rho = 4.3 \times 10^{-6}$ ohm-cm. The velocity may be calculated from the relation

$$v = \frac{2\pi}{T} \theta_{max} b , \qquad (2)$$

where T = period of roll of ship in seconds, θ_{max} = maximum angle of roll of ship in radians, and b = radius of equivalent cylinder in centimeters. Under maximum conditions, T = 8 seconds, $\theta_{max} = 30°$, and for b = 370 cm, the value obtained for the velocity v, is v = 153 cm/sec.

Substituting these values in Equation (1), an estimate of the phase angle is: = 10°.

Estimate of the time constant of the induced field

The time constant τ of the induced field is related closely to Equation (1), and is given by

$$\omega\tau = \frac{0.2\pi av}{10^8\rho} .$$

Since $\omega = \frac{v}{r}$, it follows that

$$\tau = \frac{0.2\pi ab}{10^8\rho} .$$

Using the same values for a, b, and ρ as before, an estimate of the time constant τ, is $\tau = 0.5$ seconds.

Note that the time constant τ may also be written

$$\tau = \frac{1}{10^9} \frac{2\pi ba}{\ell} = \frac{1}{10^9} \frac{\text{cross-sectional area of metal}}{\text{resistivity of metal}} .$$

Horizontal and Vertical Field Components Induced by a Vertical Exciting Field

As derived in Appendix II, the horizontal and vertical field components, h_1 and v_2, induced by a vertical exciting field are given by

$$h_1 = -\frac{H_v}{n^2} \frac{C_2}{\sqrt{1 + C_2^2}} \cos^2\theta \cos(2\theta - \phi),$$

and

$$v_2 = \frac{H_v}{n^2} \frac{C_2}{\sqrt{1 + C_2^2}} \cos^2\theta \sin(2\theta - \phi),$$

where H_v = vertical exciting field, n = number of cylinder radii the level under consideration is below the center of the cylinder, θ = angle the

radius vector makes with H_v, $\phi = \tan^{-1} C_2$, and where C_2 is given by

$$C_2 = \frac{0.2\pi av}{10^8 \rho} .$$

Using the cylinder dimensions already found, the constant C_2 is calculated to be $C_2 = 0.184$. The phase angle ϕ is given as before, $\phi = 10°$. For H_v = 560 mg. the above equations become

$$h_1 = -\frac{102}{n^2} \cos^2\theta \cos(2\theta - 10°)$$

and

$$v_2 = +\frac{102}{n^2} \cos^2\theta \sin(2\theta - 10°) .$$

These functions are plotted for various levels (i.e., various n values) and are shown as the dotted curves in Figs. 49 and 50. A comparison with the fields obtained from the model under the same conditions is shown. The assumption has been made that the bottom of the cylinder coincides with the keel of the ship. The following diagram illustrates the case for the 19-foot level.

SHIP

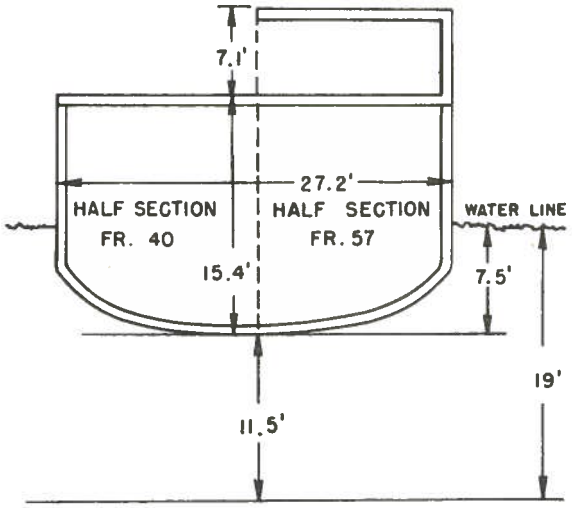

EQUIVALENT CYLINDER

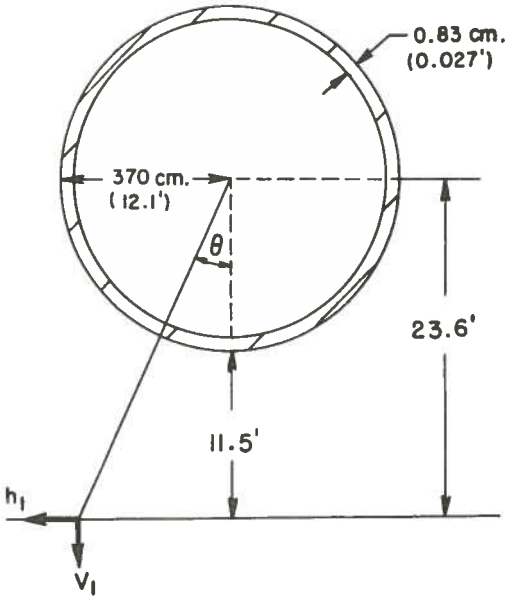

n FOR THE 19' LEVEL

$$n = \frac{23.6}{12.1} = 1.95$$

$$n^2 = 3.80$$

For the 19-foot level the field components become

$$h_1 = -26.7 \cos^2\theta \cos(2\theta - 10°),$$

$$v_2 = +26.7 \cos^2\theta \sin(2\theta - 10°) .$$

These functions are plotted by assigning different values to θ .

APPENDIX IV

CALCULATION OF THE EXTERNAL MAGNETIC FIELD PRODUCED BY AN INFINITELY-LONG, NON-MAGNETIC, CONDUCTING, HOLLOW CYLINDER OSCILLATING IN A UNIFORM MAGNETIC FIELD

INTRODUCTION:

An exact calculation of the magnetic field produced by the rolling of a ship in the earth's magnetic field is an extremely difficult and tedious task. The introduction of certain approximations makes the calculation a much less formidable one.

In the past, two methods of calculation have been developed based upon these simplifying assumptions. The first method[4] neglects the inductance of the conducting members of the ship's structure and takes only their resistance into account. The eddy currents generated are calculated by relaxation methods. These currents are assumed to be exactly in phase with the rolling motion of the ship.

The second method approximates the ship by a hollow cylinder of suitable dimensions, but takes the inductance of the ship into account. In a previous work[2] the field produced by such a cylinder continuously rotating with an angular velocity equal to the peak attained by the ship during a sinusoidal oscillation was calculated.

The calculation presented in this appendix is for a hollow cylinder oscillating in a simusoidal manner. The results derived are compared with those previously obtained for the same cylinder undergoing continuous rotation. This comparison shows significant differences between the two calculations. The fields produced by rotation and oscillation are the same only if the inductance of the cylinder is negligible.

Outline of Method of Derivation

Consider an infinitely-long, non-magnetic, conducting, thin cylinder of radius b and wall thickness a, performing sinusoidal oscillations about the z axis in a uniform magnetic field H_e transverse to this axis. A cross-section of the cylinder, the material of which has a resistivity ρ, is shown in Fig. 1 of this appendix. The mechanical oscillation of the cylinder is given by

$$\left.\begin{aligned} \alpha &= \alpha_o \sin \frac{2\pi}{T_\alpha} t \\ &= \alpha_o \sin \omega t \end{aligned}\right\} \quad \text{where } \omega = \frac{2\pi}{T_\alpha} \qquad (1)$$

where α = roll angle (rad) at time t (sec.), α_o = maximum angle of roll (rad), T_α = period of roll (sec.). It is required to calculate the

magnetic field at P (r, θ) due to the eddy currents set up in the cylinder wall as a function of r, θ, and t, where $r > b$.

Let a set of rectangular co-ordinate axes, x-y-z , be fixed with respect to the cylinder. Fig. 2 of this appendix shows this co-ordinate system on the cylinder at time t. An observer at the origin of this co-ordinate system, O, is not conscious of the motion of the cylinder, but sees two time-varying fields applied to the cylinder, H_1 along the x axis and H_2 along the y axis where H_1 and H_2 are given by

$$\left.\begin{aligned} H_1 &= H_e \sin \alpha = H_e \sin \left\{ \alpha_o \sin \omega t \right\} \\ H_2 &= H_e \cos \alpha = H_e \cos \left\{ \alpha_o \sin \omega t \right\} \end{aligned}\right\} \qquad (2)$$

For amplitudes of roll not too great these reduce to a good approximation to

$$\left.\begin{aligned} H_1 &= H_e \ \alpha_o \sin \omega t \\ H_2 &= H_e \left\{ 1 - \frac{\alpha_o^2}{4} \right\} + H_e \ \frac{\alpha_o^2}{4} \cos 2\omega t \end{aligned}\right\} \qquad (3)$$

Thus to the observer at O the cylinder is stationary, and two alternating fields of single and double frequency are applied to the cylinder, 90° out of phase in time and in space.

These fields excite eddy currents in the cylinder walls, and since the cylinder is infinitely long these currents all flow parallel to the z axis. The magnetic field they produce external to the cylinder will be a two-dimensional one.

The case for the external field produced by a stationary cylinder in an alternating field has been worked out by Smythe[9] . This result together with the Superposition Theorem may be used to determine the external field due to the two alternating fields H_1 and H_2 . The field at a fixed point external to a moving cylinder may then be found by a transformation of co-ordinate systems.

EXTERNAL FIELD DUE TO EDDY CURRENTS INDUCED IN CYLINDER BY AN ALTERNATING MAGNETIC FIELD

The solution for this part of the problem was obtained by modifying a treatment by Smythe found in "Static and Dynamic Electricity" pp. 411 - 413. In a cylindrical co-ordinate system (r, θ', z) the vector potential $\vec{A}'$ of the alternating exciting field expressed in circular harmonics is given by

$$\vec{A}' = \vec{\mu_z} \sum_n (C_n r^n + D_m r^{-n}) (M_n \cos n\theta' + N_n \sin n\theta') \ e^{j\omega t} \left\{ \begin{matrix} \text{real part} \\ \text{or} \\ \text{imaginary part} \end{matrix} \right\} \qquad (4)$$

The vector potential $\vec{A}$ of the external field due to the eddy currents flowing in the walls of the cylinder is given by

$$\vec{A} = \vec{\mu}_z \sum_n r^{-n} \frac{K}{\sqrt{n^2 + K^2}} (C_n b^{2n} + D_n)(M_n \cos n\theta' + N_n \sin n\theta') \begin{Bmatrix} + \\ \text{or} \\ - \end{Bmatrix} \begin{Bmatrix} \sin(\omega t - \delta_n) \\ \text{or} \\ \cos(\omega t - \delta_n) \end{Bmatrix} \quad (5)$$

where $K = \frac{0.2\pi ab\omega}{10^8 \rho}$, and $\delta_n = \tan^{-1} \frac{K}{n}$. The constants C_n, D_n, M_n, N_n are determined by boundary conditions.

EXTERNAL FIELD DUE TO SUPERPOSITION OF TWO ALTERNATING FIELDS OF SINGLE AND DOUBLE FREQUENCY APPLIED TO CYLINDER

Equations (4) and (5) may be applied successively to find the external field due to the exciting fields $H_1(t)$ and $H_2(t)$ given by Equations (3). To find their combined effect use is made of the Superposition Theorem.

First consider the field $H_1 = \alpha_o H_e \sin \omega t$ applied to the cylinder as shown in Fig. 3. At $P'(r,\theta')$ this exciting field expressed in radial and tangential components is given by

$$\vec{H}_i(\theta') = -\alpha_o H_e \sin \omega t \left[\vec{\mu}_r \sin \theta' + \vec{\mu}_\theta \cos \theta' \right] \quad (6)$$

The associated vector potential at (r,θ') is then

$$\vec{A}_1' = \vec{\mu}_z \alpha_o H_e \sin \omega t \; r \cos \theta' \; . \quad (7)$$

This is easily verified by taking the curl of Equation (7) which should equal Equation (6). Determination of the constants in Equation (5) is now possible by comparing Equations (4) and (7). This yields the following values for the constants: $M = 1, D_n = 0, C_n M_n = \alpha_o H_e$, $N_n = 0$. Since $\sin \omega t = \varepsilon^{j\omega t}$ (imaginary part) the cosine time function is chosen in Equation (5). Equation (5) now takes the form

$$\vec{A}_1 = -\vec{\mu}_z \alpha_o H_e \frac{K}{\sqrt{1 + K^2}} b^2 \cos(\omega t - \delta) \frac{\cos \theta'}{r} \; , \quad (8)$$

where $K = \frac{0.2\pi ab}{10^8 \rho} \omega$ and $\delta = \tan^{-1} K$.

Next consider the field $H_2 = H_e \left\{ 1 - \frac{\alpha_o^2}{4} \right\} + H_e \frac{\alpha_o^2}{4} \cos 2\omega t$

applied to the cylinder shown in Fig. 4 of this appendix. At $P'(r,\theta')$ this exciting field expressed in radial and tangential components is given by

$$H_2(\theta') = \left[H_e\left\{1 - \frac{a_o^2}{4}\right\} + H_e \frac{a_o^2}{4} \cos 2\omega t\right]\left[\vec{\mu}_r \cos\theta' - \vec{\mu}_\theta \sin\theta'\right]. \quad (9)$$

The associated vector potential at (r,θ') is then

$$\vec{A}_2 = \vec{\mu}_z \frac{a_o^2}{4} H_e \cos 2\omega t \; r \sin\theta' + \vec{\mu}_z \left\{1 - \frac{a_o^2}{4}\right\} H_e \; r \sin\theta' , \quad (10)$$

which again may be easily verified. The second term of Equation (10) is invariant in time and will induce no eddy currents. Comparison of the first term of Equation (10) with Equation (4) yields the following values for the constants: $n = 1$, $D_n = 0$, $M_n = 0$, $C_n N_n = \frac{a_o^2}{4} H_e$.

Since $\cos 2\omega t = e^{j2\omega t}$ (real part) the sine time function is chosen in Equation (5). Equation (5) now takes the form

$$\vec{A}_2 = \vec{\mu}_z \frac{a_o^2}{4} H_e \frac{2K}{\sqrt{1 + 4K^2}} b^2 \sin(2\omega t - \delta') \frac{\sin\theta'}{r} , \quad (11)$$

where

$$K = \frac{0.2\pi ab}{10^8 \rho} \omega \text{ and } \delta' = \tan^{-1} 2K .$$

By the Superposition Theorem the total vector potential at the point $P'(r, \theta')$ is

$$\vec{A}_1 + \vec{A}_2 = \vec{\mu}_z \left[-a_o H_e \frac{K}{\sqrt{1 + K^2}} b^2 \cos(\omega t - \delta)\frac{\cos\theta'}{r} + \frac{a_o^2}{4} H_e \frac{2K}{\sqrt{1 + 4K^2}} b \sin(2\omega t - \delta')\frac{\sin\theta'}{r}\right]$$

The magnetic field $\vec{H}_i(r, \theta', t)$ due to the eddy currents is

$$\vec{H}_i = \nabla \times (\vec{A}_1 + \vec{A}_2) = \frac{1}{r} \begin{vmatrix} \vec{\mu}_r & r\vec{\mu}_\theta & \vec{\mu}_z \\ \frac{\partial}{\partial r} & \frac{\partial}{\partial \theta} & \frac{\partial}{\partial z} \\ 0 & 0 & \begin{matrix} -a_o H_e \frac{K}{\sqrt{1+K^2}} b^2 \cos(\omega t - \delta) \frac{\cos\theta'}{r} \\ + \frac{a_o^2}{4} H_e \frac{2K}{\sqrt{1+4K^2}} b^2 \sin(2\omega t - \delta') \frac{\sin\theta'}{r} \end{matrix} \end{vmatrix}$$

$$= H_e \frac{b^2}{r^2} \vec{\mu}_r \left[\frac{a_o K}{\sqrt{1+K^2}} \cos(\omega t - \delta) \sin\theta' + \frac{a_o^2}{4} \frac{2K}{\sqrt{1+4K^2}} \sin(2\omega t - \delta') \cos\theta'\right]$$

$$- H_e \frac{b^2}{r^2} \vec{\mu}_\theta \left[a_o \frac{K}{\sqrt{1+K^2}} \cos(\omega t - \delta) \cos\theta' - \frac{a_o^2}{4} \frac{2K}{\sqrt{1+4K^2}} \sin(2\omega t - \delta') \sin\theta'\right] \quad (13)$$

TRANSFORMATION OF CO-ORDINATE SYSTEMS

Equation (13) gives the external field due to the eddy currents in the cylinder wall at a point in the x - y - z co-ordinate system fixed on the cylinder. An observer outside this system sees the cylinder performing a rolling motion about its longitudinal axis. The induced field at any time seen by this observer external to the oscillating cylinder may be found by a transformation of co-ordinate systems.

In Fig. 5 of this appendix, the observer is at $P(r, \theta)$ which is a fixed point with respect to horizontal and vertical axes through the center of the cylinder, but is not a fixed point with respect to the x - y - z co-ordinate system. In order that Equation (13) may always give the field at (r,θ) it is necessary that the angle θ' vary continuously with time. With reference to Fig. 5 the necessary transformation is

$$\begin{aligned} \theta' &= \theta - \alpha \\ &= \theta - \alpha_o \sin \omega t. \end{aligned} \tag{14}$$

Substituting this relation into Equation (13), and again making use of the approximation for small angles α, i.e., $\sin \alpha = \alpha$ and $\cos \alpha = 1 - \frac{\alpha^2}{2!}$ (used previously in obtaining Equations (3)) it may be shown that the induced field outside the oscillating cylinder is given by

$$\vec{H}_i(r,\theta,t) = H_e \frac{b^2}{r^2} \left\{ \vec{\mu}_r \left[F_1(t) \sin\theta + F_2(t) \cos\theta \right] - \vec{\mu}_\theta \left[F_1(t) \cos\theta - F_2(t) \sin\theta \right] \right\}$$

where

$$\begin{aligned} F_1(t) &= \frac{K}{\sqrt{1+K^2}} \alpha_o \cos(\omega t - \delta) - \frac{\alpha_o^3}{2} \frac{K}{\sqrt{1+K^2}} \cos(\omega t - \delta) \sin^2 \omega t \\ &\quad + \frac{2K}{\sqrt{1+4K^2}} \frac{\alpha_o^3}{4} \sin(2\omega t - \delta') \sin \omega t \end{aligned} \tag{15}$$

$$\begin{aligned} F_2(t) &= \frac{2K}{\sqrt{1+4K^2}} \frac{\alpha_o^2}{4} \sin(2\omega t - \delta') - \frac{2K}{\sqrt{1+4K^2}} \frac{\alpha_o^4}{8} \sin(2\omega t - \delta') \sin^2 \omega t \\ &\quad - \frac{K}{\sqrt{1+K^2}} \alpha_o^2 \cos(\omega t - \delta') \sin \omega t. \end{aligned}$$

COMPARISON OF RESULTS FOR CYLINDER WHEN OSCILLATING AND WHEN ROTATING

Equation (15) gives the induced field outside the cylinder when it is oscillating in a sinusoidal manner with a period T_α. At the instant $t = \frac{2n\pi}{\omega}$, the cylinder is moving across the exciting field H_e with maximum angular velocity. Substitution of $t = \frac{2n\pi}{\omega}$, $K = 0.5$, $\alpha_o = \frac{1}{2}$

into Equations (16) determines values for F_1 and F_2. The value chosen for K is approximately that for the equivalent cylinder obtained previously. A plot of Equations (15) versus the angle θ for these values of F_1 and F_2 gives curve B, Fig. 19. Curve A, Fig. 19 was plotted for the cylinder when continuously rotating at the maximum angular velocity attained by the cylinder when oscillating. It is seen that the horizontal field (plotted on a normalized scale) obtained by rotating the cylinder is higher and the space phase shift more pronounced than when the cylinder is oscillating*. Curve C is the maximum field produced by the oscillating cylinder. This occurs at a later time given approximately by $t = \frac{2n\pi + \delta}{\omega}$. In the region of $\theta = 0°$ the field of the cylinder lags the angular velocity of the cylinder approximately by the angle δ. This effect is shown in Fig. 20 which is a plot of the field of the oscillating cylinder versus time over one complete roll period. At $\theta = 0°$ the effect of the second harmonic is negligible and the curve is essentially a sine wave. At $\theta = 22.5°$ the phase shift in time is greater than the angle δ. This, and the fact that the curve shows considerable distortion, is due to the increased importance of the effect of the second harmonic exciting field at this angle θ. At $\theta = 45°$ the field lags the angular velocity essentially by the angle δ. Furthermore, the field now pulsates with twice the frequency of roll and is unidirectional. This is because the field at this angle θ is induced entirely by the second harmonic exciting field and always acts in such a direction as to oppose this exciting field. These effects may also be seen by using the flux line distributions derived in Appendix I.

* Note: Admittedly the value of $\alpha_o = \frac{1}{2} (\simeq 30°)$ is somewhat high for the small angle approximation used in this treatment. Inclusion of the next term for the expansion of sin α introduces the third harmonic.

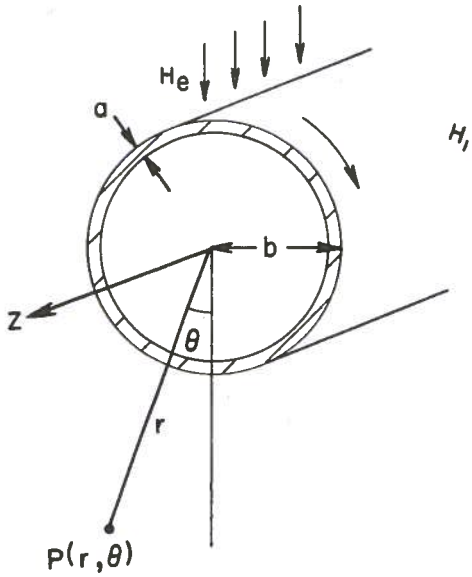

FIG. 1

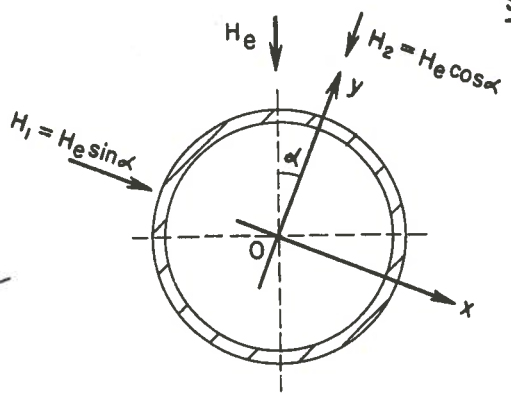

Z axis out of paper

FIG. 2

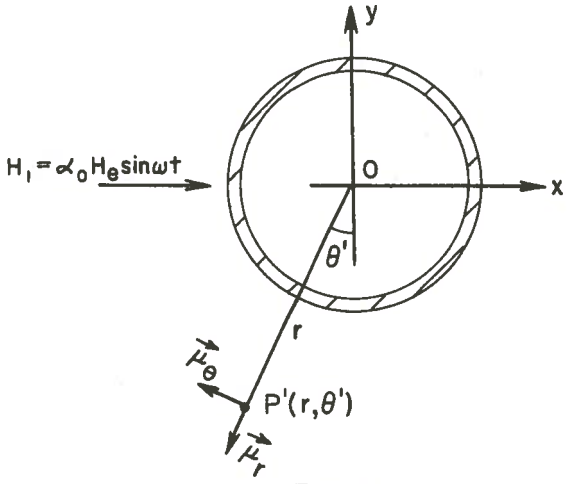

FIG. 3

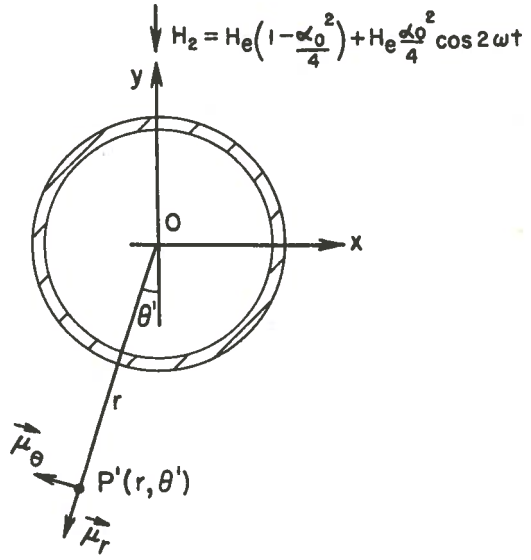

FIG. 4

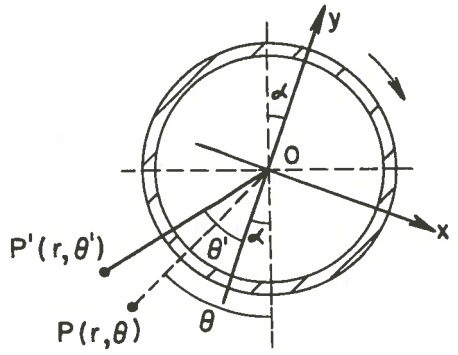

FIG. 5

APPENDIX V

Conversion of Model Test Results for Comparison with Full-Scale Results

The conditions under which the full-scale ship measurements were made are described in detail in ERA-231 [3] .

Model test results were converted to equivalent conditions of ship tests by use of the following formulae:

$$h_1' = h_1 \times \frac{H_v'}{H_v} \times \left(\frac{d}{d^1}\right)^2 \times \frac{h_1(\omega')}{h_1(\omega)}$$

$$h_2' = h_2 \frac{H_h'}{H_h} \times \left(\frac{d}{d^1}\right)^2 \frac{h_2(\omega')}{h_2(\omega)} ,$$

where the primed symbols refer to ship test conditions and unprimed symbols refer to unconverted model test conditions. In the formulae the first factor on the right is the field obtained under the conditions of the model tests; the second factor accounts for the different exciting fields used in the model and ship tests; the third factor is an inverse-square depth conversion, and the fourth factor is an angular velocity conversion obtained from the curves of Figs. 40 and 41.

The following sample calculation illustrates the method used to obtain the values given in Table IV. The ship test results given in Table IV were taken for an angular velocity of the ship of ω = 4.9 deg/sec at a depth of d = 25' under the waterline at midship, for an exciting field of H_v' = 542 mg., H_h' = 113 mg. They show a horizontal eddy current field component of 4.1 mg. The model test results were taken at an angular velocity of ω = 23.6 deg/sec (maximum of a ± 30°, 8-sec roll), at a depth corresponding to d = 24' under the water line on the ship scale and for separate exciting fields of H_v = 560 mg and H_h = 560 mg. From Fig. 27 the horizontal component due to H_v = 560 mg is, h_1 = 18 mg. From Fig. 28 the horizontal component due to H_h = 560 mg is h_2 = 6 mg. The angular velocity conversion obtained from Figs. 40 and 41 is $H(\omega')$ = 6.2 mg, $h_1(\omega)$ = 28.8 mg, $h_2(\omega')$ = 1.2 mg, $h_2(\omega)$ = 10 mg. Conversion of these model test results to equivalent conditions of the ship tests may now be obtained by substitution into the

above equations and adding the results as follows:

$$h_1' = 18 \times \frac{542}{560} \times \left(\frac{24}{25}\right)^2 \times \frac{6.2}{28.8} = 3.5 \text{ mg.}$$

$$h_2' = 6 \times \frac{113}{560} \times \left(\frac{24}{25}\right)^2 \times \frac{1.2}{10} = 0.1 \text{ mg.}$$

Therefore $h_1' + h_2' = 3.6$ mg.